Investigation of protein signalling pathways activated by sonoporation in cancer

Silje Maria Sundøy

This thesis is submitted in partial fulfilment of the requirements for the degree of Master in
Medical Biology – Biomedical Sciences

Department of Biomedicine /Klinisk Institutt 2
University of Bergen
[Semester 2, 2018]

Acknowledgements

This Master of Biomedical Sciences was performed at the Faculty of Medicine at the Department of Biomedicine at the University of Bergen in the period June 2017 to June 2018

Firstly, I would like to express my gratitude to my main supervisor Emmet Mc Cormack and thank him for this great opportunity to excel in the field of Biomedicine and for valuable advice, especially during presentations. I never learned so much in such a short period of time as the past year, and that is partly due to the high quality of work performed by everyone in this lab pushing me to want to succeed.

I also want to sincerely thank my co–supervisor, Ragnhild Haugse, who has followed me closely and endured endless repetition of questions. She has handled my stress with grace and helped tremendously when I got lost in signalling pathways and experimental plans! And, although he is not titled my supervisor, Spiros Kotopoulis has also been a great help and been very patient explaining physics and "sciencing" in great detail. In addition to my supervisors, he contributed significantly to the advisement on how this thesis should be well written. I am very grateful for all your help!

Assistance provided by Ida Karlsen and Mireia Mayoral Safont concerning all lab technical and western blot questions was greatly appreciated

I would also like to thank Gorka Ruiz de Garibay, and Pascal, both of whom have been a great help in mastering western blots. Elisa Ulvøen Thodesen, as well as Tormod Karlsen Bjånes, have been greatly helpful teaching me how to handle Petakas and the sonicators

Another very important person in the lab I need to thank is May Eriksen, my fellow student. We have shared frustrations and her moral support has been priceless!

Finally, I need to thank my family for their support through this process. Support by believing in me and by accepting that during the past two years they have barely seen or spoken to me since all my time was spent in the lab. A special thanks to my sister Siv Anita, especially the past few weeks. She has kept the house tidy, been very considerate when I needed space to write and made sure I ate fresh vegetables!

Bergen, 2018

Silje Maria Sundøy

Table of Contents

Acknowledgements **2**

Abbreviations **6**

Summary **8**

1.0 Introduction **10**

1.1 Cancer *10*

1.1.2 PDAC characteristics *11*

1.1.3 Current treatments and limitations *11*

1.2 Background Sonoporation 1.2.1 Ultrasound 12

1.2.2 Microbubbles 12

1.2.3 The mechanisms of sonoporation 13

1.2.5 Intracellular effects of sonoporation 15

1.2.6 Previous research 16

1.2.7 Choice of signalling pathways 17

1.2.7.1 Unfolded protein response 17

1.2.7.2 MAPK pathway 18

1.2.7.3 JAK/STAT pathway 20

1.2.7.4 PI3K-mTOR pathway 20

1.2.7.5 Rho/ROCK pathway 21

1.3 Preclinical results *22*

1.4 Clinical trials *23*

1.5 Choice of cell lines *24*

1.6 Ultrasound treatment of cell culture *24*

1.6.1 Challenges 24

1.5.3 Adherent cells 24

1.6.4 Cell detachment in Petaka 25

1.7 Western Blot *26*

2.0 Aims **28**

3.0 Materials and Methods **29**

3.1.1 Cell culturing *29*

3.1.2 Cell passaging *29*

3.1.2 Cryopreservation and thawing of cells *30*

3.2 Antibodies *30*

3.2.1 Positive controls and antibodies 30

3.3 Viability assays *31*

3.3.1. Trypan Blue apoptotic cell stain 31

3.3.1.2hoechst 33342 apoptotic stain 31

3.3.1.3 WST–1 metabolic assay 31

3.3.2 Viability optimisation MOLM-13 32

3.3.2.1hoechst 33342 32

3.3.2.2 WST-1 33

3.3.3 Viability optimisation MIA PaCa-2 33

3.3.3.1 WST-1 - Cell number and incubation time for MIA PaCa-2 33

3.3.3.2 Viability test of MIA PaCa-2 in Petakas 33

3.5 Ultrasound treatment of cells in vitro *34*

3.5.1 MOLM–13 ... 34
3.5.2 Cell culture before experiments ... 35
3.5.3 Ultrasound and microbubble treatment ... 35
3.5.4 MIA PaCa–2 ... 36
3.5.5 Cell culture before experiments ... 36
3.5.6 Protocol for seeding adherent cells in Petaka ... 37
3.5.7 Protocol for detachment of adherent cells in Petaka ... 37
3.6 *In vitro* optimisation ... 37
3.6.1 Optimisation of cell lysis ... 37
3.6.2 Optimisation of growth rate for MIA PaCa–2 in Petaka ... 37
3.6.3 Optimisation of cell detachment ... 38
3.6.3.1 Optimisation of timing of cell detachment with cold 1× trypsin and 10× trypsin ... 38
3.6.3.2 Optimisation of cell detachment–western blot ... 39
3.6.3.3 Optimisation of cell detachment with 10× trypsin –Viability and western blot ... 40
3.6.4 Optimisation of incubation time following sonoporation ... 40
3.6.5. Optimisation of western blot ... 40
3.6.6 Ultrasound and microbubble treatment of MIA PaCa–2 ... 41
3.7 Western blot ... 42
3.7.1 Protein extraction ... 42
3.7.2 Protein quantification and sample preparation ... 43
3.7.3 Sample reparation MOLM–13 ... 43
3.7.4 Sample preparation pancreatic cell lines ... 43
3.7.5 Gel electrophoresis ... 43
3.7.8 Electrophoretic transfer of proteins ... 44
3.7.9 Immunostaining ... 45

4.0 Results ... **46**
4.1 Results MOLM–13 ... 46
4.1.1 Optimisation of WST–1 for MOLM–13 ... 46
4.1.2 Viability – trypan blue and Hoechst staining of sonoporated MOLM–13 ... 47
4.1.3 Western Blot analysis MOLM–13 ... 49
4.2 Results Pancreatic cell lines ... 50
4.2.1 Optimisation of cell lysis ... 50
4.2.2 Viability optimisation MIA PaCa-2 ... 51
4.2.2.1 WST-1 - Cell number and incubation time for MIA PaCa-2 ... 51
4.2.2.2 Viability test of MIA PaCa-2 in Petakas ... 52
4.2.4 Optimisation of growth rate for MIA PaCa–2 in Petaka ... 53
4.2.5 Optimisation of timing of cell detachment with cold 1× trypsin and 10× trypsin ... 55
4.2.6 Optimisation of cell detachment–western blot ... 55
4.2.7 Optimisation of cell detachment with 10× trypsin –Viability ... 56
4.2.8 Optimisation of cell detachment with 10× trypsin– Western blot ... 57
4.2.9 Optimisation of western blotting ... 58
4.2.10 Optimisation of incubation time following sonoporation ... 59
4.3 Sonoporation of MIA PaCa–2 cells ... 60
4.3.1 Viability sonoporated MIA PaCa–2 ... 60
4.3.2 Western blot sonoporated MIA PaCa–2 ... 62

5.0 Discussion ... **63**
5.1 Choice of signalling pathways ... 63
5.2 MOLM–13 ... 64
5.2.1 Trypan blue ... 64
5.2.2hoechst 33342 ... 64
5.2.3 WST–1 assay ... 65
5.2.4 Sonoporated MOLM-13 – Western blot and viability ... 66

5.2.4.1 MAPK pathway ... 66
5.2.4.2 UPR pathway ... 68
5.2.4.3 PI3K–mTOR pathway ... 68
5.2.4.4 JAK/STAT pathway ... 69
5.2.5 Concluding remarks MOLM–13 ... 69
5.3 Pancreatic cell lines ... 69
5.3.1 Ultrasound treatment of cells – challenges ... 69
5.3.2 Optimisation of cell lysis ... 70
5.3.3 WST–1 – Optimisation of cell number seeded and incubation time – MIA PaCa–2 ... 70
5.3.4 Optimisation of viability assays ... 71
5.3.5 Optimisation of growth rate ... 72
5.3.6 Optimisation of timing of cell detachment with cold 1× trypsin ... 73
5.3.7 Optimisation of cell detachment with cold 1× trypsin – western blot ... 74
5.3.8 Optimisation of cell detachment with cold 10× trypsin ... 74
5.3.8.1 Optimisation of cell detachment with cold 10× trypsin – viability ... 75
5.3.8.2 Optimisation of cell detachment with cold 10× trypsin –western blot ... 75
5.3.9 Optimisation of western blotting ... 76
5.3.10 Optimisation of incubation time following sonoporation ... 76
5.3.11 Sonoporated MIA PaCa–2 – viability ... 77
5.3.12 Sonoporated MIA PaCa–2 – western blot ... 78
5.3.12.1 MAPK pathway ... 78
5.3.12.3 JAK-STAT pathway ... 79
5.3.12.4 PI3K–mTOR pathway ... 79
5.3.12.5 Rho-ROCK pathway ... 80
6.0 Concluding remarks and future directions ... **80**
7.0 Bibliography ... **82**
8.0 Appendixes ... **88**
Appendix A Antibodies ... 88
Appendix B Positive controls ... 89
Appendix D Ponceau images from western blots ... 90

Abbreviations

5% CO_2, 37˚C	Humidified atmosphere with 5% CO_2 at 37˚C
Ab	Antibody
AGD–CS	Automatic Gas Diffusion Control System
Akt	Also known as Protein Kinase B (PKB)
ATF6	Activating transcription factor 6
DMEM	Dulbecco's Modified Eagle Medium
DMSO	Dimethyl Sulfoxide
DO	Dissolved Oxygen
dsDNA	double–stranded DNA
eIF2α	eukaryotic Initiation Factor 2 α subunit
ERK 1/2	Extracellular signal–Regulated Kinase 1/2 (MAPK)
G+nP	Gemcitabine combined with nab–paclitaxel
HIF	Hypoxia–inducible factor
IRE1	Inositol–requiring enzyme 1
mAb	Monoclonal antibody
MAPK	Mitogen Activated Protein Kinase
MBs	Microbubbles
MLC2	Myosin Light Chain 2
mmHg	Millimeter of mercury
MQ–H_2O	Ultra–purified water filtered by Milli Q Type1 Ultrapure Water System
MYPT1	Myosin–binding subunit of myosin phosphatase 1
NAD(P)H	Nicotinamide adenine dinucleotide phosphate
NFkB	Nuclear Factor κ B
OS	Overall Survival
p38	p38 (MAPK)
pAb	Polyclonal antibody
PAR2	G protein–coupled receptor protease–activator receptor 2
PBS	Phosphate Buffered Saline
PDAC	Pancreatic Ductal Adenocarcinoma
PDGF	Platelet–derived growth factor

PERK	PKR–like ER kinase
PFS	Progression Free Survival
Phospho–	Phosphorylated
PKC	Protein kinase C
PS	Performance Status
PTM	Post–Translational Modifications
RH	Relative Humidity
RPMI	Roswell Park Memorial Institute
RT	Room Temperature
S6	S6 Ribosomal Protein
SAPK/JNK	Stress–Activated Protein Kinase/Jun–amino–terminal Kinase (MAPK)
SDS–PAGE	Sodium Dodecyl Sulphate– Polyacrylamide Gel Electrophoresis
STAT3	Signal Transducers and Activators of Transcription 3
TBS	Tris Buffered Saline
TBS–T	Tris Buffered Saline–Tween
TIFP	Tumour Interstitial Fluid Pressure
TME	Tumour Micro Environment
TNFα	Tumour necrosis factor α
Trypsin	Trypsin–EDTA
US	Ultrasound
UV	Ultraviolet light
WB	Western blot

Summary

Pancreatic ductal adenocarcinoma (PDAC) is one of the most lethal cancers worldwide. patients with a metastatic PDAC only survive 3 – 5 months if left untreated and less than 25% of diagnosed patients are eligible for surgery. Radiation and chemo–therapy, improves survival by only a few months to live. Overall, the one–year survival is 20%, while the five–year survival rate is a mere 5 – 7%. The poor prognosis of PDAC is predominantly due to the asymptomatic nature of the tumour in early stages. The PDAC tumour is known be severely hypoxic and desmoplastic making it particularly hard to treat. In spite of limited success in increased survival with the chemotherapy, the outcome is still not satisfactory. Clearly, there is a dire need for better and more efficient treatment options. Ultrasound (US) mediated cancer therapy with microbubbles, or sonoporation, is currently one of the emerging cancer treatments.

The primary aim of this project is to elucidate the pathways activated by sonoporation in pancreatic cell lines by analysing post–translational modifications (*i.e.*, phosphorylation). The long–term goal is to identify biomarkers for sonoporation that can be used to optimise sonoporation therapy. The pathways investigated were the Mitogen Activated Kinases (MAPKs) ERK 1/2, p38 and SAPK/JNK; the unfolded protein response (UPR) protein eIF2α; and the JAK/STAT pathway protein STAT3. Furthermore, ribosomal protein S6 of the PI3K-mTOR pathway was investigated, in addition to MLC and MYPT1, which are regulators in the Rho/ROCK pathway.

More specific aims were to:

- Iinvestigate of protein signalling pathways activated by sonoporation in the AML cell line MOLM–13
- develop methodology for *in vitro* optimisation of sonoporation
- investigate the influence of sonoporation on cell viability
- investigate protein signalling pathways activated by sonoporation in the pancreatic cell lines MIA PaCa–2, PANC-1 and BxPC-3

Cells were treated using bespoke US treatment chambers designed for suspension or adherent cells. Adherent cells were treated in the bioreactor Petaka G3 LOT. Following sonoporation, cell viability was assessed using trypan blue (live/dead cell exclusion assay), Hoechst 33342

(apoptotic assay) and WST-1 (metabolic assay). Furthermore, phosphorylation status of selected signalling proteins in sonoporated cells were analysed by western blot. For pancreatic cell lines methodology was optimised, including viability assays, growth rate in Petakas, cell detachment, incubation time post sonoporation before protein extraction and, finally, western blotting was optimised by inducing phosphorylation to test the antibodies in aforementioned cell lines.

Sonoporation–induced cell signalling was successfully detected using MOLM-13. Results showed that enzymatic cell detachment with pre-heated trypsin can influence cell signalling. Sonoporation of MIA PaCa-2 cells showed that the cells' viability was affected at the higher US intensities without microbubbles, shown as decreased metabolic activity (WST–1), suggesting that US alone affects cell viability. Trypan blue showed a relative increase of trypan blue stained cells at low US intensity. Hoechst 33342 analysis showed a trend of decreasing number of dead cells with and without microbubbles with increasing US intensity, indicating that high US and microbubbles affects cell viability. In western blot analysis of the MAPKs, no phosphorylation of p38 or JNK was detected, however, there was an increasing phosphorylation of ERK 1/2. eIF2α, and STAT3 were phosphorylated in all samples, suggesting they are constitutively active in MIA PaCa-2. S6 was phosphorylated at the higher US intensities with microbubbles. MLC, was phosphorylated at the highest US intensity with microbubbles, while MYPT1 was not phosphorylated.

Methodology for in vitro optimisation of sonoporation was developed. Using this methodology, we have identified several pathways activated by sonoporation that may have potential as biomarkers for PDAC that can be used to optimise sonoporation therapy. It was also found that higher US intensities and microbubbles may have an effect of cell viability, depending on the US intensity. However, these are preliminary results which needs to be confirmed.

1.0 Introduction

1.1 Cancer

Cancer is the second leading cause of death worldwide, responsible for 8.8 million deaths in 2015 (2). The most common causes of cancer death are cancers of lung, liver, colorectal, stomach and breast (2). In 2012 an estimated 14.1 million new cancer cases occurred and the burden of cancer is expected to increase to 23.6 million new cases each year by 2030 (3). Although incidence of other cancers is higher, pancreatic ductal adenocarcinoma (PDAC) is currently one of the most lethal cancers worldwide. Patients with locally advanced PDAC have a median survival of 6 –10 months, and patients with a metastatic PDAC only survive 3 – 5 months if left untreated. Less than 25% of diagnosed patients are eligible for surgery, which gives the patient the best chance of survival. That leaves radiation and chemo–therapy, which, at best, provides the patient with a few additional months to live. (4). Only 20% of PDAC patients survive one year after initial diagnosis, while the five–year survival rate is a mere 5 – 7% (5). Furthermore, survival rates for pancreatic cancer has not changed during the

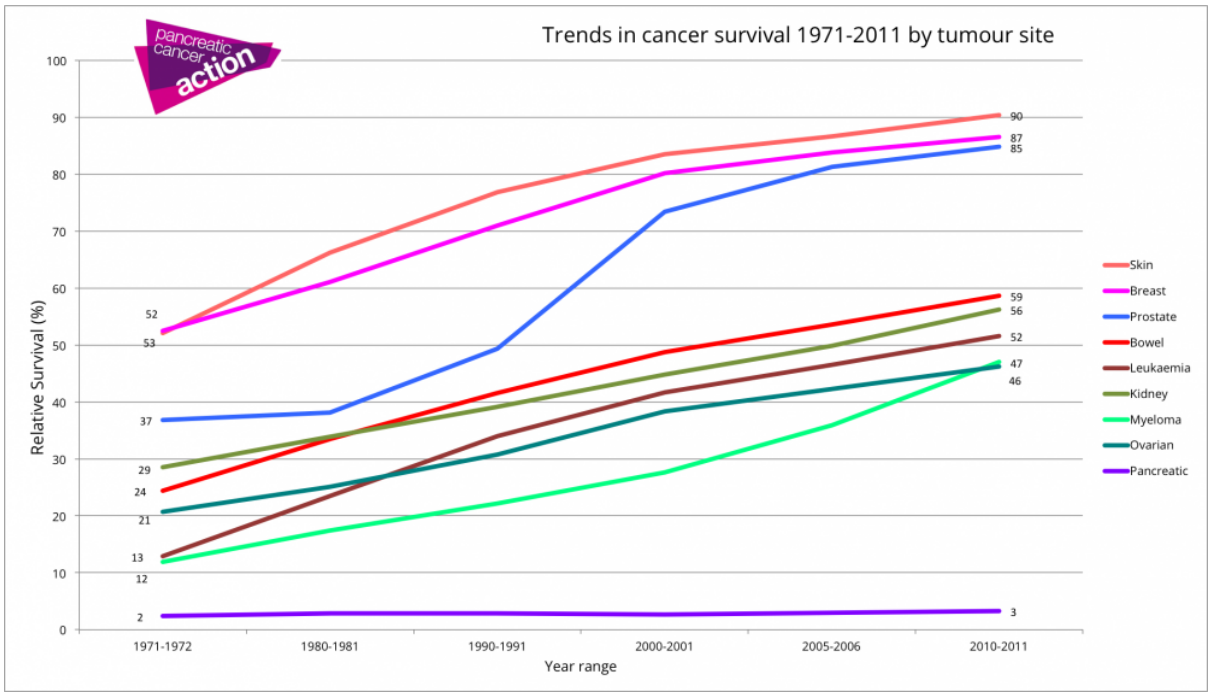

Figure 1: Trends cancer survival rates as a function of time (6). Pancreatic cancer has the lowest survival of all 21 common cancers, reflected in the minor increase in survival from 2% in 1971 to 3% in 2011). Survival rates for other common cancers have increased by up to 37%.

past five decades, while for other common cancers it has increased significantly (7) (**Figure 1**). In the UK the survival rates for pancreatic cancer has only shown an increase of 1%, from 2% in 1971 to 3% in 2011. In contrast, the survival rates for other cancer have increased by up to 37% (6) (**Figure 1**).

1.1.2 PDAC characteristics

The poor prognosis of PDAC is predominantly due to the asymptomatic nature of the tumour in early stages. Typically, by the time the tumour is discovered it has encased major vessels surrounding it and metastasized (5). Tumours grow rapidly, compared to non–cancerous cells, and when the tumour grows beyond 1 – 2 mm in diameter the majority of cells are too far away from the regular vasculature to take advantage of the oxygenated blood, resulting in a severely hypoxic tumour micro environment (TME) (8). The hypoxic TME triggers hypoxia–inducible factor (HIF), which initiate angiogenesis, and a number of growth factors. Chronic inflammation is sustained in the tumour by many factors, including cytokines, growth factors, which are produced in excess, leading to the irregular growth of tumour vasculature. The irregularity of the tumour vasculature contributes to the highly hypoxic TME (9). Furthermore, increased permeability of tumour neovasculature, caused by loss of cellular junction integrity and increased production of VEGF, and the lack of tumour lymphatic system, in addition to chronic inflammation all contribute to accumulation of fluid in the interstitium, resulting in increased tumour interstitial fluid pressure (TIFP). Another factor contributing to the build–up of fluids in the interstitium is a decreased hydrostatic pressure in the tumour vasculature, as well as elevated osmotic pressure in the interstitium, which results in stagnant blood flow. The increased tumour blood viscosity further aggravates perfusion (10). Perfusion is also repressed by pressure from the fibrous extracellular matrix (ECM) protein collagen, which is overexpressed in tumours (11, 12). Tumour heterogeneity of genetic mutations, plasticity, elevated TIFP and extreme desmoplasia lowers the efficacy of drug delivery may and render PDAC tumours resistant to chemotherapeutics, leading to poor response to treatment (4, 5, 13). KRAS gene mutations, which are found in 80% of PDAC patients, not only contributes to the promotion of tumour development and progression by stimulating growth factor receptors to initiate malignant transformation of pancreatic ductal epithelial cells, but also obstructs delivery of traditional chemotherapy (13).

1.1.3 Current treatments and limitations

From 1997 until 2011 Gemcitabine was the standard first–line chemotherapeutic treatment for metastatic PDAC (14). In 2011 the FOLFIRINOX regimen (5–fluorouracil, oxaliplatin, irinotecan, and leucovorin) proved superior to Gemcitabine in terms of overall survival (OS) with an OS of 6.8 months versus 11.1 months for FOLFIRINOX versus Gemcitabine treated patients, respectively (15). In spite of adverse effects of the FOLFIRINOX treatment it

emerged as the new standard chemotherapy for metastatic PDAC (14). Gemcitabine has been combined with other cytotoxic drugs, such as irinotecan, capecitabine, 5–fluorouracil, cisplatin, oxaliplatin and capecitabine without any significant survival advantages, compared to Gemcitabine alone (14). However, nab–paclitaxel, an albumin–bound nanoparticle linked with paclitaxel, combined with Gemcitabine has proven to have a synergistic effect (16-18). The combination treatment nab–paclitaxel plus Gemcitabine is currently the first–line treatment of metastatic pancreatic cancer (19). Treatment with FOLFIRINOX and the combination therapy Gemcitabine plus nap–paclitaxel has had limited success increasing survival in patients, however, the outcome is still not satisfactory (14, 16-19). Clearly, there is a dire need for better and more efficient treatment options. Ultrasound (US), used for clinical imaging for half a century, is considered safe to use in humans, and microbubbles (MBs) has been used as a contrast agent to enhance the signal–to–noise ratio of the vasculature (4, 20). US mediated cancer therapy with MBs, or sonoporation, is currently one of the emerging treatments (21).

1.2 Background Sonoporation

1.2.1 Ultrasound

US has been used for imaging purposes clinically for over 50 years and is considered a safe imaging modality and has for the past 30 years been used as a diagnostic tool to detect PDAC (4). Stabilised gas MBs are used as a contrast agent for diagnostic US imaging to enhance the signal–to–noise ratio of the vasculature, resulting in better images of tissue perfusion (4). The US can be aimed at a specific area, such as a tumour, with millimetre precision, which is an advantage when targeting diseased tissues during therapy (22). The US intensities used in diagnostic US range between 17 mW/cm^2, for treatment of the eye, to 720 mW/cm^2 used for peripheral vessels (23).

1.2.2 Microbubbles

The commercially available MBs are typically gas–filled (perfluorocarbon) bubbles stabilized by a monolayer phospholipid shell, approximately 2 – 10 μm in size (24). The hydrophilic head of the phospholipid face the water (outside) and the hydrophobic tail face the gas inside the MBs (25) (**Figure 2**). Clinically approved MBs include Optison (GE Healthcare, Little Chalfont, England) which has a cross–linked serum albumin shell filled with octafluoropropane gas, and Sonazoid (GE Global Healthcare, Little Chalfont, United

Kingdom) and SonoVue® (Bracco, Italy) both consisting of a phospholipid monolayer, filled with perfluorobutane and sulphurhexafluoride gas, respectively (26).

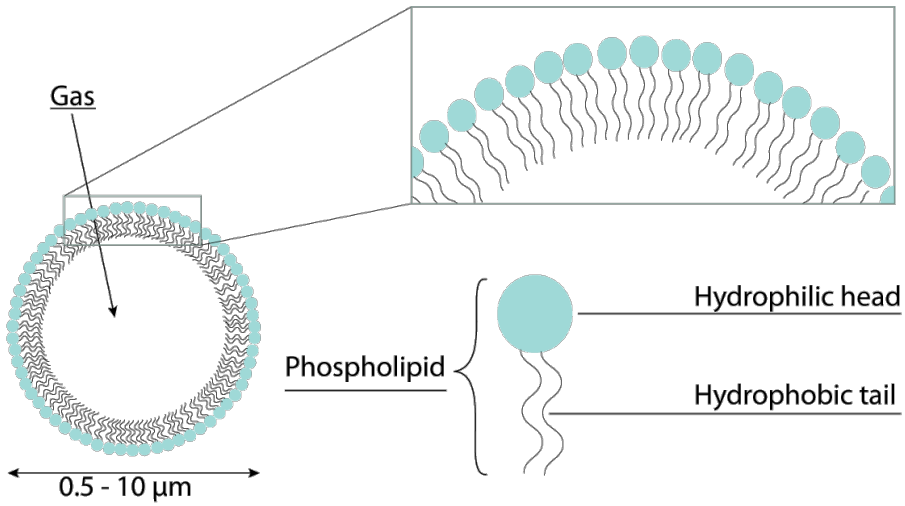

Figure 2: Typical microbubble composition. The gas filled microbubbles consists of a monolayer of phospholipids. The MB size range from 0.5 – 10 µm. The hydrophilic heads face outwards towards the water, while the hydrophobic tails face in towards the gas.

1.2.3 The mechanisms of sonoporation

When exposed to US, MBs volumetrically oscillate, creating stable or inertial cavitation (**Figure 3**). Low intensity US (LIUS) causes stable cavitation, which is a result of stable, symmetrical oscillation of the MBs. During stable cavitation the compression and expansion (rarefaction) of the MBs are inversely proportional to the US pressure (**Figure 3B**). Conversely, when the MBs are exposed to high intensity US (HIUS), inertial cavitation occurs. A lengthening of the expansion phase enlarges the MBs, eventually resulting in implosion (27) (**Figure 3C**). The MBs generate their own ultrasonic pulse when the US wave hits the MBs scattering the incoming US (24). When the MBs are in close vicinity of cells as they are exposed to US the cells experience sheer stress, which may induce a wide range of mechanical and biological effects in addition to creating pores (27) (**Figure 3D–H**). The oscillating MBs interact with the plasma membrane in many ways (**Figure 3**). A stable cavitating MB push and pull the plasma membrane during the expansion and compression phase, respectively, creating transient pores when in close vicinity of the cell (27) (**Figure 3D**).

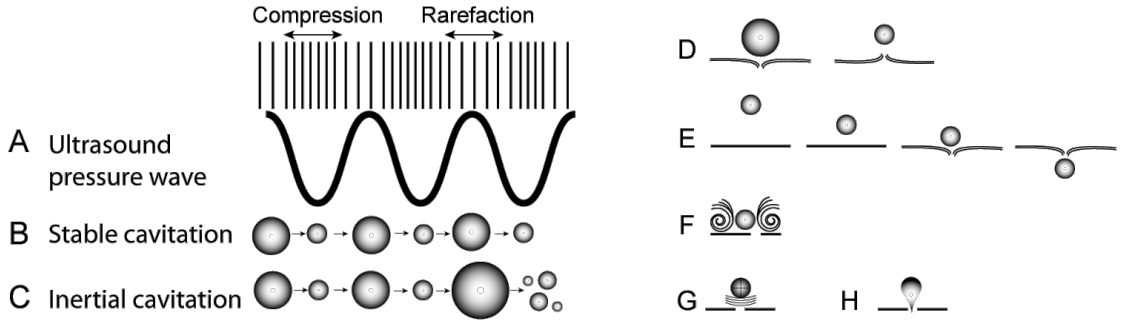

Figure 3: Biophysical effects of stable and inertial cavitating microbubbles. Figure adapted from (24). (A) Schematic representation of an acoustic pressure wave. (B) Stable cavitation of microbubbles caused by low intensity ultrasound. (C) Inertial cavitation of microbubbles caused by high intensity US. The effects of stable cavitation on the cell membrane are illustrated in (D), (F), while the effects of inertial cavitation are demonstrated in (G) and (H). The push and pull from a stably oscillating microbubbles disturb the cell membrane integrity (D). Acoustic radiation force displaces the microbubble against the cell membrane causing membrane disruption (E). Microstreaming created by the stably oscillating microbubbles create mechanical stress on the cell membrane, causing pore formation (F). Collapse of inertial cavitating microbubbles creates shock waves generating high stresses on the cell membrane, resulting in membrane disruption (G). A liquid jet is formed when a microbubble collapses near the cell surface puncturing the cell membrane (H).

How close the MB has to be to the cell to cause pore formation has been studied in single–cell experiments. One study concluded that membrane perforation occurred with 75% probability when bubble–cell distance was equal to 75% of the maximum bubble radius (28). The size of the pores and how long it takes for the pore to close depends on the intensity of the US wave (mW/cm^2) and the time exposed to US (28). That being said, pore sizes have been measured to be from 10 nm to 1 μm in size and occur within several to tens of microseconds. It is reported that the pores last from minutes up to a few hours (28). Pores can also be created by the force of the US wave pushing the MBs against the plasma membrane (acoustic radiation force) disrupting it, and the MB may even be pushed inside the cell (**Figure 3E**). A stable cavitating MB also create microstreaming in the fluid surrounding the cell causing mechanical stress on the plasma membrane, which can result in pore formation (**Figure 3F**). The implosion of MBs (following inertial cavitation) also creates pores due to the high stress on the plasma membrane (**Figure 3G**). Moreover, an imploding MB creates a liquid jet towards the cell surface, which punctures the membrane creating a pore (27) (**Figure 3H**).

1.2.5 Intracellular effects of sonoporation

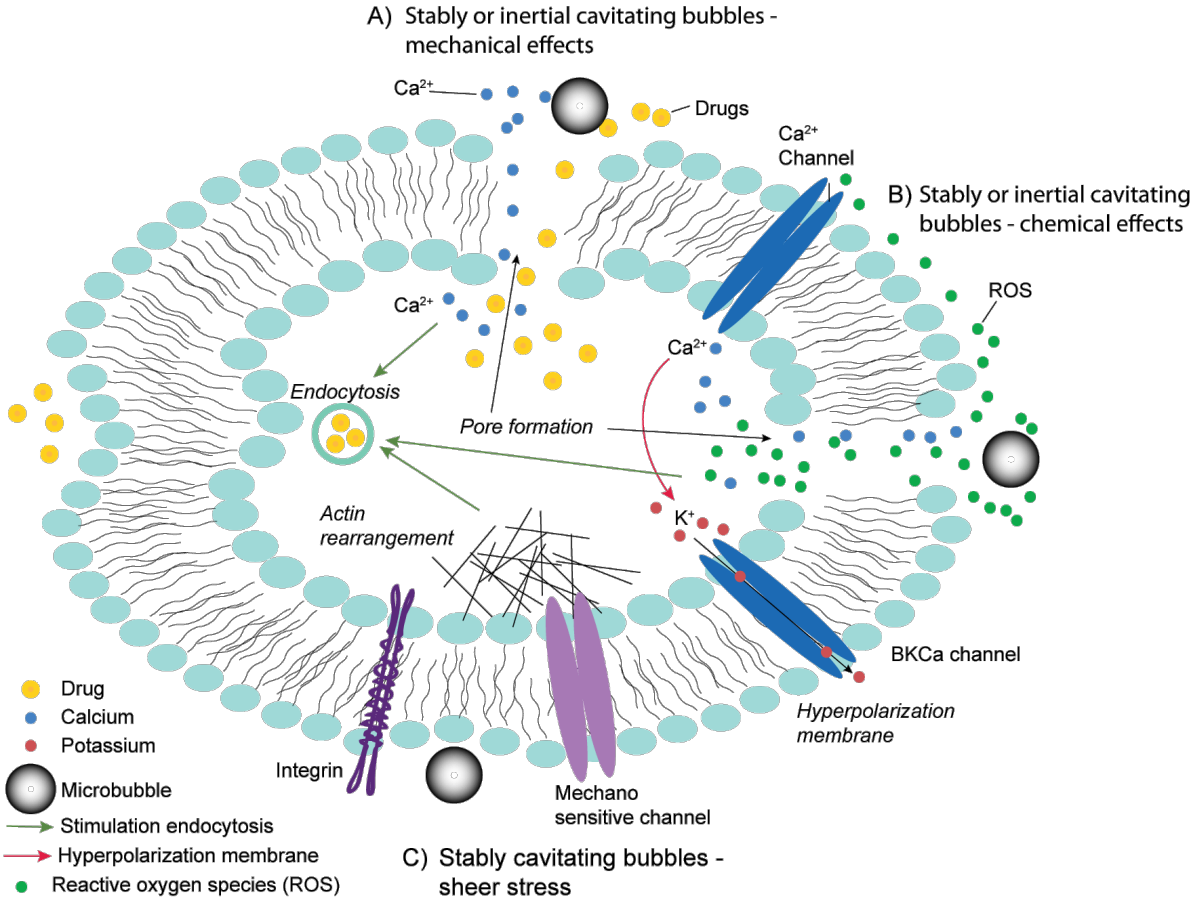

Figure 4: Intracellular effects of stably and inertial cavitating microbubbles. Adapted from (27). Pore formation allows molecules, such as calcium (Ca^{2+}) and drugs, to passively diffuse into the cell (A). Microbubble cavitation causes production of reactive oxygen species (ROS), which can modulate ion channels or cause membrane disruption via lipid peroxidation. Hyperpolarization of the cell membrane can be caused by potassium efflux via Ca^{2+}–dependent potassium (BK_{Ca}) channels due to Ca^{2+} influx mediated by ROS. Also, Ca^{2+} influx can stimulate endocytosis (B). The cell membrane can be deformed by the microstreaming generated by stably cavitating microbubbles, leading to cytoskeletal rearrangements and differences in membrane tension. The changes in membrane tension are detected by mechanosensors, which can initiate a signalling cascade that influences endocytosis/exocytosis processes (C).

The creation of pores in the plasma membrane creates a range of biological effects. Pores enables membrane impermeable molecules such as Calcium (Ca^{2+}) and drugs to diffuse passively into the cell (27, 28) (**Figure 4A–B**). The stress on the cell created by a cavitating MBs creates reactive oxygen species (ROS), which are involved in modulation of ion–channels. The production of ROS can also lead to lipid peroxidation which causes membrane disruption. As a result of Ca^{2+} influx mediated by ROS potassium (K^+) diffuse out of the cell via Ca^{2+}–dependent potassium (BK_{Ca}) channels, which results in hyperpolarization of the plasma membrane (**Figure 4B**). Moreover, Ca^{2+} influx stimulates endocytosis (**Figure 4**). Further biological effects from stably cavitating MBs include cytoskeletal rearrangements and

differences in membrane tension as a result of deformation of the membrane caused by sheer stress. The deformation of the membrane is sensed by mechanosensors, such as integrins and stretch-activated ion channels, which transduce these signals into downstream processes such as endocytosis and exocytosis processes (27) (**Figure 4C**). In addition to pores created by membrane perforation the oscillating MB can create gaps between cells, so–called interendothelial gaps, in the blood vessels (28) (**Figure 5**).

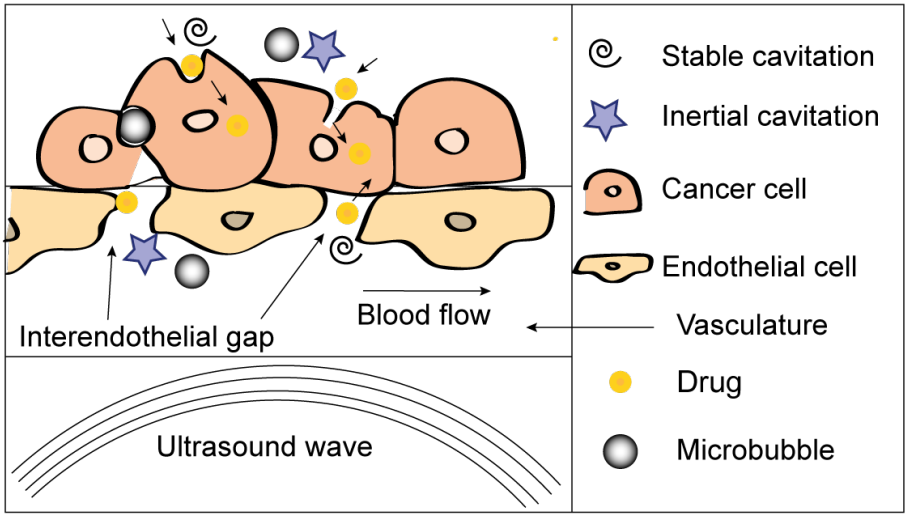

Figure 5: Passive and active delivery routes enhanced by sonoporation. Figure adapted from (2). Sonoporation perforates the membrane by acoustic cavitation allowing passive diffusion of macromolecules into the cell. The interendothelial junction may be opened by acoustic cavitation, providing an active route for macromolecules and drugs. Stable cavitation stimulates endocytosis, actively delivering macromolecules into the cells via vesicles.

Pore formation and interendothelial gaps creates a "drug delivery route" bypassing the abnormal tumour vasculature that normally hinders drug distribution to large areas of the tumour (8) (**Figure 5**). However, the creation of pores allow for deeper drug penetration, hopefully increasing the efficacy of the drug (4). Due to the many challenges of treating PDAC, including late detection due to its asymptomatic nature (5), extreme hypoxic (9) and desmoplastic nature (4), elevated TIFP and increased tumour blood viscosity (10), surgery is not possible for most patients (85%) (4), thus, there is a dire need for improved drug delivery for treatment of PDAC.

1.2.6 Previous research

The biomechanical mechanisms of sonoporation are thoroughly studied (27-29), however, the intracellular effects are not well documented. One study found that apoptosis–related proteins in sonoporated leukemia cells (HL–60) and found a reduction in poly adenosine diphosphate

ribose polymerase (PARP) signalling and a simultaneous increase in cleaved–PARP, and B–cell lymphoma 2 (Bcl–2) had a decreased signal following sonoporation, while Bcl–2–associated X (Bax) had a slight increased signal. These results indicate that these proteins have an active role in sonoporation–induced apoptosis (30). The effect of clinical US in leukaemia cells (MOLM–13) and monocytes have been found to react differently to US. MOLM–13 had increased signalling of p38 when exposed to US (161 mW/cm^2) plus MBs, while the monocytes had an increased signal at all US intensities (0.35, 1.17 and 161 mW/cm^2) plus MBs, but also at high US without MBs. Extracellular signal–regulated kinases 1 & 2 (ERK 1/2) had an overall increase in signal in MOLM–13 cells, but the signalling monocytes were downregulated (20). The endoplasmic reticulum (ER)–stress response has been found to be induced in HL–60 leukemia cells by sonoporation. The ER–stress sensors PKR–like ER kinase (PERK) and inositol–requiring enzyme 1 (IRE1) was activated upon exposure to sonoporation with increasing signal in a time–dependent manner (31).

1.2.7 Choice of signalling pathways

1.2.7.1 Unfolded protein response

Cell signalling induced by sonoporation is largely untouched territory and there are nearly limitless signalling pathways and signalling proteins to investigate. ER–stress has been shown to be induced in leukaemia cells by sonoporation (31), however, assessment of phosphorylation status of ER–stress proteins was not included. ER–stress can be induced by various biochemical, physiological, pathologic and mechanical stresses leading to oxidative stress, altered glycosylation, DNA damage and energy disturbance/ fluctuation, nutrient deprivation and Ca^{2+} depletion (32). ER–stress is sensed by three ER–transmembrane receptors; IRE1, PERK, and activating transcription factor 6 (ATF6), which triggers the unfolded protein response (UPR) (33) (**Figure 6**). One of the downstream signalling proteins of PERK is the eukaryotic initiation factor 2α (eIF2α). Upon phosphorylation eIF2α initiates a signalling cascade resulting in decreased global protein translation via amplification of the selective translation of the mRNA encoding for ATF4 (**Figure 6**). ATF4 is a transcription factor that induces the expression of genes involved in amino acid metabolism, autophagy, apoptosis, antioxidant responses and GADD34. Under prolonged ER–stress PP1C, encoded by GADD34, dephosphorylates eIF2α counteracting PERK activity (33) (**Figure 6**). Attenuation of global protein translation have a significant adverse effect on cellular survival (34), and is therefore an interesting target in cancer therapy.

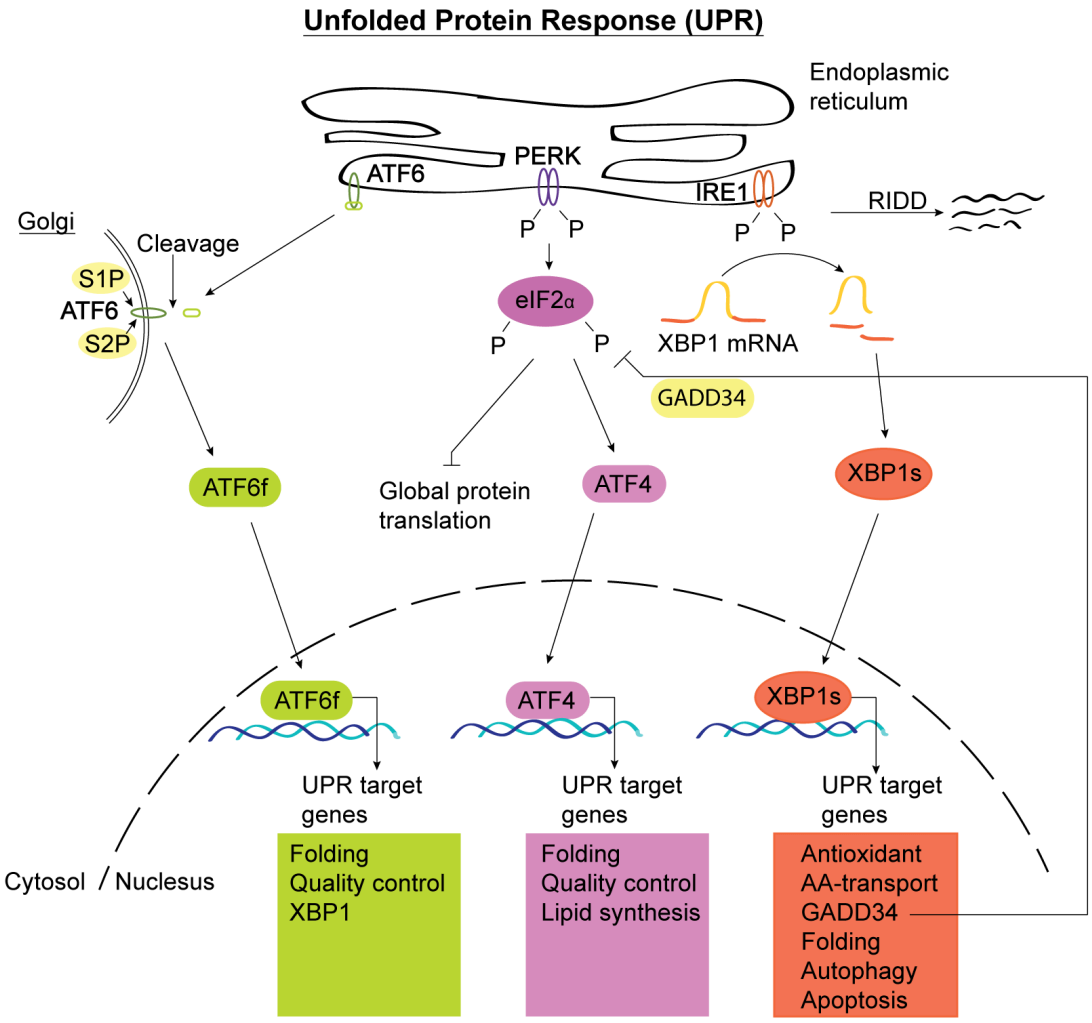

Figure 6: The unfolded protein response (UPR) signalling. Figure adapted from (33). The stress sensors IRE1, PERK, and ATF6 regulates the UPR. Activation of PERK phosphorylates eIF2α leading to attenuation of global protein synthesis via activation of the transcription factor ATF4, which induces the expression of genes involved in antioxidant responses, apoptosis, amino acid (AA) metabolism, autophagy, and GADD34. Under sustained ER–stress GADD34 feeds back to dephosphorylate eIF2α. ER–stress leads to dimerization and autophosphorylating of IRE1, which activates its endoribonuclease activity in the cytosolic domain. Active IRE1 modulates the processing of the mRNA encoding XBP1 (transcription factor), leading to upregulation of UPR target genes related to folding, quality control, and ER–associated degradation (ERAD). Furthermore, IRE1 degrades certain mRNAs through regulated IRE1–dependent decay (RIDD). During ER–stress, ATF6 is processed at the Golgi apparatus, where the cytosolic domain is released and then translocate to the nucleus increasing the expression of some ER chaperones, ERAD–related genes, and XBP1. See text for definitions of abbreviations.

1.2.7.2 MAPK pathway

The UPR may also interact with the mitogen activated protein kinase (MAPK) pathway, a highly conserved family of serine/threonine protein kinases involved in a variety of fundamental cellular processes. MAPKs include ERK1/2, Stress–Activated Protein Kinase/Jun–amino–terminal Kinases (JNKs) and the p38 family (**Figure 7**). ERK 1/2 regulates cell proliferation, differentiation and survival. The JNKs can mediate apoptosis and

autophagy, but also cell survival. Depending on the type of activation (mechanical, biochemical, physiological) activation of p38 can induce both cell proliferation and cell cycle arrest (35). In cancer, on the one hand, the initiation of the UPR can restore tumour homeostasis and enhance tumour growth. On the other hand, it can also lead to apoptosis (32). Since ER–stress can be induced by sonoporation (31), and ERK 1/2 and p38 have been found to be activated by sonoporation with MBs in leukemia cells (20). The involvement of eIF2α and the MAPKs in survival and apoptotic pathways makes them interesting targets in the investigation of the effect of sonoporation-induced signalling.

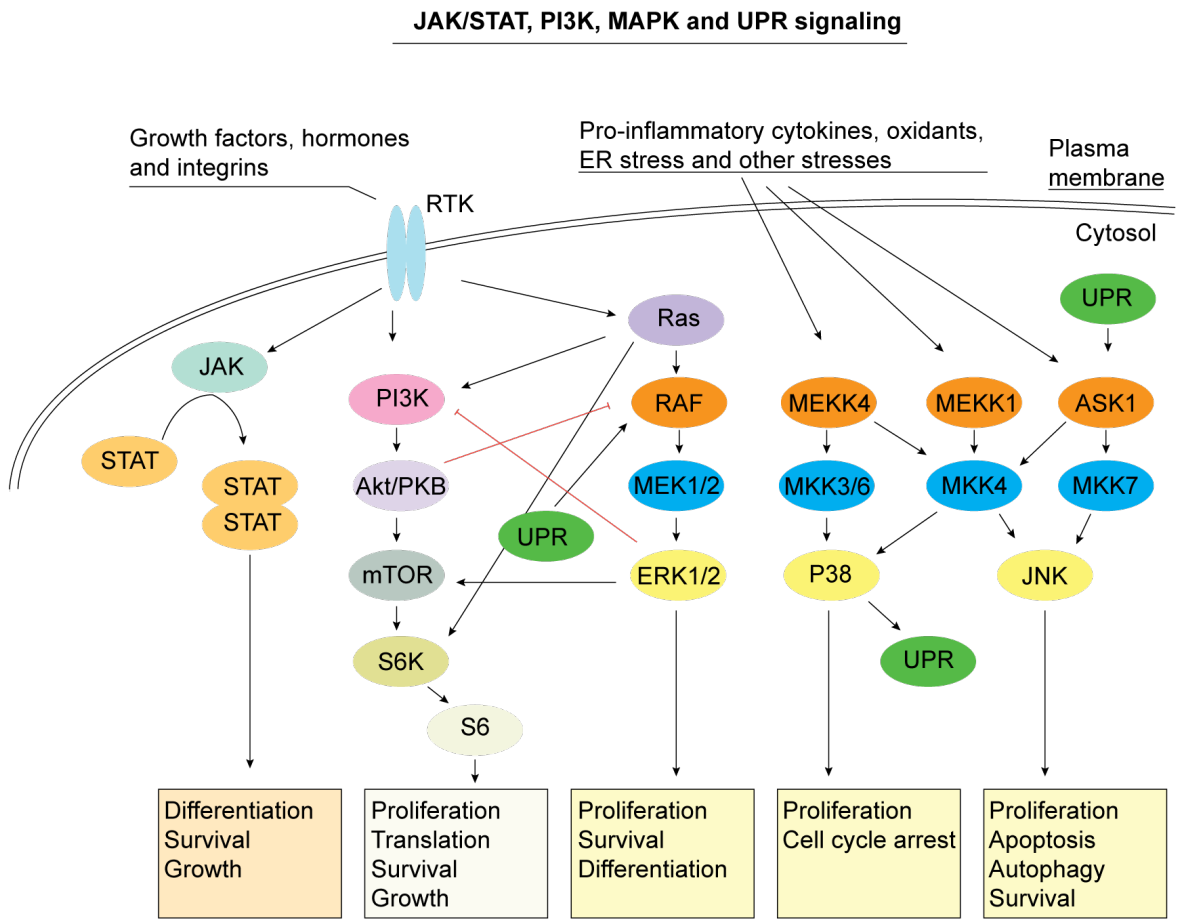

Figure 7: Mitogen Activated Protein Kinase (MAPK) signalling – Cross–talk with the Unfolded Protein Response (UPR). Figure adapted from (35-39). Schematic of JAK/STAT, PI3K, MAPK and UPR signalling with points of cross–talk. Growth factors, hormones and integrins stimulate receptor tyrosine kinases (RTKs), which again activates the JAK/STAT pathway and the PI3K pathway upstream of ribosomal protein S6 (S6). There is cross–talk between the PI3K and MAPK pathway. PI3K can be activated by Ras and inhibited by ERK 1/2. Oncogenic Ras can also directly activate S6K. Akt can inhibit RAF, and ERK 1/2 can activate mTOR. The MAPK signalling pathways are activated by extracellular signals, such as ER–stress (and other cellular stresses), cytokines and growth factors, which activates MKKKs, MKKs and then MAPKs. Under ER–stress conditions the UPR activates ASK1–MKK4/7–JNK signalling and correspondingly promotes ERK1/2 activation. Furthermore, MEKK4–MKK3/4/6–p38 signalling also modulates the UPR via p38–dependent phosphorylation of CHOP and ATF6 (not shown).

1.2.7.3 JAK/STAT pathway

Signal Transducers and Activators of Transcription 3 (STAT3) is a constitutively active transcription factor in many cancers, including haematological malignancies and pancreatic cancer, which promote angiogenesis, survival, immune evasion, cell proliferation and migration/invasion (**Figure 7**). STAT3 is an interesting therapeutic target because by blocking downstream STAT3 signalling tumour progression has been successfully inhibited (40). Several factors contribute to STAT3 activation in cancer, including overexpression of protein tyrosine kinases, epigenetic modulation of negative regulators of STAT3 and increased secretion of growth and cytokines factors in the tumour microenvironment (41). In relation to sonoporation, it would be interesting to see whether the constitutively active STAT3 is influenced by the US and MB treatment.

1.2.7.4 PI3K-mTOR pathway

Ribosomal protein S6 (S6) is a downstream substrate in the phosphatidylinositol 3–kinase (PI3K)–mammalian target of rapamycin (mTOR) pathway (39) (**Figure 7**). PI3K is activated directly by growth factor receptors, or indirectly by insulin receptor substrate (IRS) or (GRB2–associated binder (GAB) docking proteins (not shown) (39). The mTOR complex 1 (mTORC1) is activated via PI3K and Akt/PKB (**Figure 7**), and by energy status, amino acid levels and cellular stress through a number of phosphates and kinases. mTORC1 complex phosphorylates eukaryotic initiation factor 4E (eIF4E)–binding protein (4E–BP) and S6K (p70 ribosomal S6 Kinase), leading to activation of several downstream substrates, including S6 (**Figure 7**). Phosphorylation of S6 mediates proliferation, translation, survival and growth (39). **Figure 7** shows cross-talk between the PI3K-mTOR and MAPK pathway (42). Ras can directly activate both PI3K and S6K (**Figure 7**). Considering the interconnecting links between the UPR, MAPK and PI3K-mTOR pathway, and as sonoporation has been shown to influence ER-stress (activating the UPR) (31) and MAPKs (20) it would be interesting to investigate S6.

1.2.7.5 Rho/ROCK pathway

Myosin Light Chain 2 (MLC2) and myosin–binding subunit of myosin phosphatase 1 (MYPT are part of the Rho/Rho–associated coiled–coil–forming kinase (ROCK) signalling pathway that regulates the cytoskeleton. Actin–myosin contractions enables the cells to change shape and move during development, but also in inflammation and wound healing (43) (**Figure 8**). More specifically, what enables cells' motility is the assembly of integrins in the plasma membrane forming focal adhesions, not only enables locomotion,

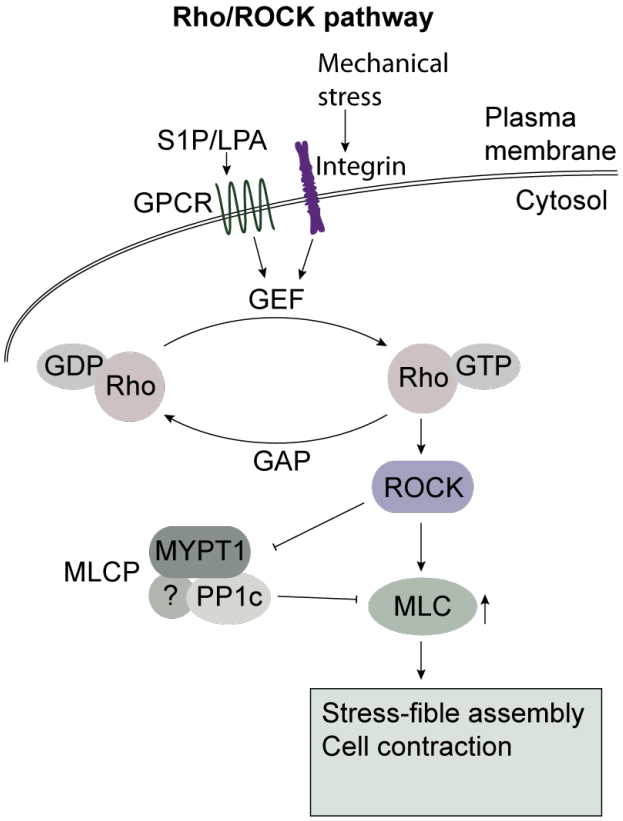

Figure 8: Rho/ROCK pathway simplified. Figure adapted from (44). lysophosphatidic acid (LPA) or sphingosine–1–phosphate (S1P) binds to G–protein–coupled receptors (GPCRs), which activates Guanine nucleotide exchange factors (GEFs). GEFs phosphorylate Rho Kinase (Rho), while GTPase activating proteins (GAPs) dephosphorylate Rho. GTP–bound Rho subsequently activates Rho–associated coiled–coil–forming kinases (ROCKs) to phosphorylate myosin light chain (MLC). MLC phosphatase (MLCP) consists of the myosin–binding subunit myosin phosphatase target subunit (MYPT1), the catalytic subunit protein phosphatase type 1 (PP1c) and a small non–catalytic subunit of unknown function. De–phosphorylation of MYPT by ROCKs inhibits the dephosphorylation of MLC, thereby increasing myosin II activity and stress–fibre formation and contractility. MLCP dephosphorylates MLC. Abbreviation: Guanosine–5'–triphosphate (GTP).

but strengthens the cells ability to resist mechanical injury. The Rho/ROCK pathway regulates this focal adhesion assembly by activation of Rho and ROCK. In fact, sonoporation (mechanical stress), has been shown to affect the cytoskeleton (45, 46) (**Figure 8**). ROCK inhibits MLC phosphatase (MLCP), thereby promoting phosphorylation of MLC (47).

Furthermore, Rho/ROCK, which also mediates cytoskeletal reprogramming during invasion and metastasis, is activated by hypoxia–inducible factors 1 (HIF–1) and 2 (HIF–2) in cancer (48). Since pancreatic cancer is known to be severely hypoxic (49), it would be interesting to investigate the role of MLC2 and MYPT1 in pancreatic cell lines. De–regulation of for example small GTPases (RhoA) and kinases, such as ROCK1/2 in cancer further contribute to the invasive behavior of cancers (43). MYPT1 is one of three sub–regulatory units of MLCP, the second is the catalytic subunit protein phosphatase type 1, (PP1c), and the third is a small a small non–catalytic subunit of unknown function (44) (**Figure 8**). The GTP–bound Rho activates ROCKs, which phosphorylate MLC. Phosphorylation of MYPT by ROCKs, however, inhibits the dephosphorylation of MLC, thus increasing myosin II activity and stress–fibre formation and contractility (44) (**Figure 8**). Both the amino terminus and the carboxyl terminus of MYPT have a binding site for myosin. Also, the amino–terminal of MYPT binds PP1c, and the carboxy–terminal half contains binding sites for the small non–catalytic subunit and RhoA. Phosphorylation of residues in the carboxy–terminal results in the inhibition of MLCP activity and a concomitant increase in phosphorylated MLC and cell contractility. ROCK II phosphorylates MYPT at Thr697, Ser854 and Thr855. The ROCK II–mediated phosphorylation of Thr855 induces its dissociation from myosin, which might inhibit myosin phosphatase activity. Thr697 phosphorylation is also implicated in the inhibition of MLCP activity, but how this regulates the catalytic activity of PP1c is unknown (44). In relation to sonoporation, it would be very interesting to see whether sonoporation affects for example cancer cells invasive behaviour via the Rho/ROCK pathway.

1.3 Preclinical results

Sonoporation used to increase drug uptake is a growing area of research (50), and has been tested in multiple animal models. One group demonstrated that local sonoporation to the kidney transiently affected the glomerular filtration barrier resulting in increased the transfer of oligonucleotides in mice (51). Another group, studying oral squamous cell carcinoma in hamster models, found that the chemotherapeutic carboplatin combined with low intensity US had a synergetic effect enhancing the effect of the drug, prolonging survival and had no additional side–effects (52). Furthermore, in a study performed with a rat pancreas carcinoma model, treated with drug loaded MBs and US, resulted in a 12–fold higher drug tissue concentration and a significantly lower tumour growth, compared to the control (53). Studies performed at the University of Bergen (UIB) have investigated the effect of treating PDAC with US and MBs, in addition to a chemotherapeutic agent, in an orthotopic xenograft mouse

model of luciferase expressing the pancreatic cell line MIA PaCa–2. The mice were divided into a control group (saline treatment only), one group was treated with gemcitabine alone, and one group was treated with Gemcitabine combined with US and SonoVue® MBs. Sonoporation was induced in a localized region of the primary tumour with a custom–made focused US transducer using clinically safe acoustic conditions. In the combination group the tumour growth was significantly inhibited, compared to the control and the group treated with gemcitabine only, indicating improved uptake in the combination group (24).

1.4 Clinical trials

These promising results led to the world first phase I clinical trial testing Gemcitabine combined with LIUS and SonoVue® MBs (21). Other groups have investigated the effect of HIUS on drug uptake (54), however, LIUS in combination with a chemotherapeutic agent had not yet been tested in humans before (4). In this trial, ten terminally ill PDAC patients were treated with Gemcitabine plus LIUS and MBs (SonoVue®), compared to historical controls having received gemcitabine monotherapy. One of the aims of the study was to evaluate the safety and potential toxicity of gemcitabine combined with sonoporation in inoperable pancreatic cancer patients. No additional toxicity or increased frequency of side effects were found, and the patients tolerated an increased number of gemcitabine cycles compared to the historical control (Control: n = 63 patients; average of 8.3 ± 6.0 cycles, versus sonoporation + gemcitabine–treated patients: 13.8 ± 5.6 cycles, p = 0.008, unpaired t–test). The median survival of the patients increased from 8.9 months to 17.6 months (p =0.011). The study concluded that "*it is possible to combine ultrasound, microbubbles, and chemotherapy in a clinical setting using commercially available equipment with no additional toxicities. This combined treatment may improve the clinical efficacy of gemcitabine, prolong the quality of life, and extend survival in patients with pancreatic ductal adenocarcinoma*" (4).

Another phase 1 trial has successfully disrupted the blood brain barrier with pulsed US and microbubble treatment. An US device system (SonoCloud) was implanted in in patients with recurrent glioblastoma, which was treated monthly using pulsed US in combination with systemically injected microbubbles followed by systemic infusion of the chemotherapeutic carboplatin. They reported that the treatment was found to be safe and well tolerated by patients, in addition to increased drug concentrations and slowed tumour growth (55).

The evidence that sonoporation has potential to improve drug delivery is growing, however, the intracellular mechanisms behind slowed tumor growth and increased tolerance of chemotherapy in PDAC is largely unknown.

1.5 Choice of cell lines

Several *in vitro* sonoporation studies have been performed with leukemia cells (20, 30, 31, 56), which are suspension cells, making them easier to work with, compared to adherent cells. However, the main objective of this project was to investigate the effect of sonoporation on post translational modifications of proteins (*i.e.*, phosphorylation) in adherent pancreatic cell lines. Therefore, the initial testing was done with the leukemic cell line MOLM–13. To get a good representation of patient heterogeneity three pancreatic cell lines MIA PaCa–2, PANC–1 and BxPC3 were included. MIA PaCa–2 and PANC–1 differs in morphology and immunohistochemistry, expresses polymorphism and pleomorphism, respectively. One similarity between two of the cell lines is that both have epithelial–mesenchymal transition (EMT) differentiation. However, PANC–1 does not express E–cadherin, making it more aggressive in terms of metastasis (57). The three cell lines differ in origin adhesiveness, invasiveness, genotype and angiogenic potential (58)

1.6 Ultrasound treatment of cell culture

1.6.1 Challenges

To treat cells with US can be a challenge since there are many parameters that needs to be optimised. In addition, cell signalling cascades are very sensitive and can be induced by reagents, such as heated trypsin–EDTA (37ºC) used to detach adherent cells (59, 60), and by mechanotransduction triggered by handling the cells (61). Trypsin–EDTA is discussed in **chapter 1.6.4.**

1.5.3 Adherent cells

The PDAC tumour is known to be severely hypoxic, therefore, in order to study the PDAC cell line MIA PaCa–2 cells in a similar hypoxic environment, the low oxygen transfer bioreactors called “Petaka G3” was used to culture PDAC cell lines as PDAC tumours.

There is no research done on the treatment of pancreatic cells with US in a Petaka. Therefore, an optimisation of the parameters of treating pancreatic cell lines with US in a Petaka was essential.

1.6.4 Cell detachment in Petaka

In order to study cell signalling in adherent cells, they need to be detached. The commonly used cell detachment method of cell scraping is possible using a magnet (62), however, due to the lack of necessary equipment to implement this, enzymatic cell detachment was used in this project. Trypsin is a proteolytic enzyme, used to detach cells from the substrate, that detaches the cells by cleaving peptides at the C–terminal side of arginine and lysine amino acid residues and works optimally when heated to 37^{o}C (physiologic temperature) (60). However, trypsin heated to 37^{o}C may affect the integrity of cell surface proteins (60) . Trypsin is available in different concentrations. To detach strongly adherent cell lines trypsin from 2.5% to 0.25% (10× to 1× power, respectively) are used (60). To increase the enzymatic activity disodium ethylenediaminetetraacetic acid (EDTA) is added to the trypsin solution. EDTA works as a chelating agent neutralizing calcium and magnesium ions that obscure the peptide bonds on which trypsin acts (63). The 10× trypsin used in this project did not have EDTA added. In this thesis "trypsin" refers to the "trypsin–EDTA" solution, unless otherwise stated. Trypsin has been identified to activate cell signalling via the G protein–coupled receptor protease–activator receptor 2 (PAR2) by cleaving the amino–terminal exodomain. In epithelial and smooth muscle cells PAR2 activation stimulates the MAPK pathway, and trypsin activated PAR2 may also activate MAP phosphatase activity and reduce phosphorylated–ERK 1/2 (p–ERK 1/12) level induction by other receptors (59). Furthermore, one study determined that trypsin induced RhoA signalling (64). At a temperature of 4^{o}C trypsin is still 50% active, but the tyrosin kinases remain inactive (59). Thus, test cell detachment with ice–cold trypsin was tested to see if the phosphorylation status of the proteins of interest differ between regular warm (37^{o}C) and cold trypsinization.

1.7 Western Blot

WB, also called immunoblotting, is the gold standard of identifying presence or absence of a protein in a biological sample, and for detecting change in posttranslational modifications (*i.e*, phosphorylation/de–phosphorylation, acetylation, methylation, and ubiquitination) by antibody (Ab) binding to a specific protein of interest (1). A simplified overview of WB is explained in **Figure 9**. Protein is extracted from tissue or cells and protein concentration is quantified before preparing the samples by adding loading dye and denaturing the proteins by heating them. The loading dye contains sodium dodecyl sulfate (SDS), which is a strong anionic detergent added to coat hydrophobic regions of proteins with negative charge, thus overpowering positive charges in proteins, which endures a uniformly distributed negative

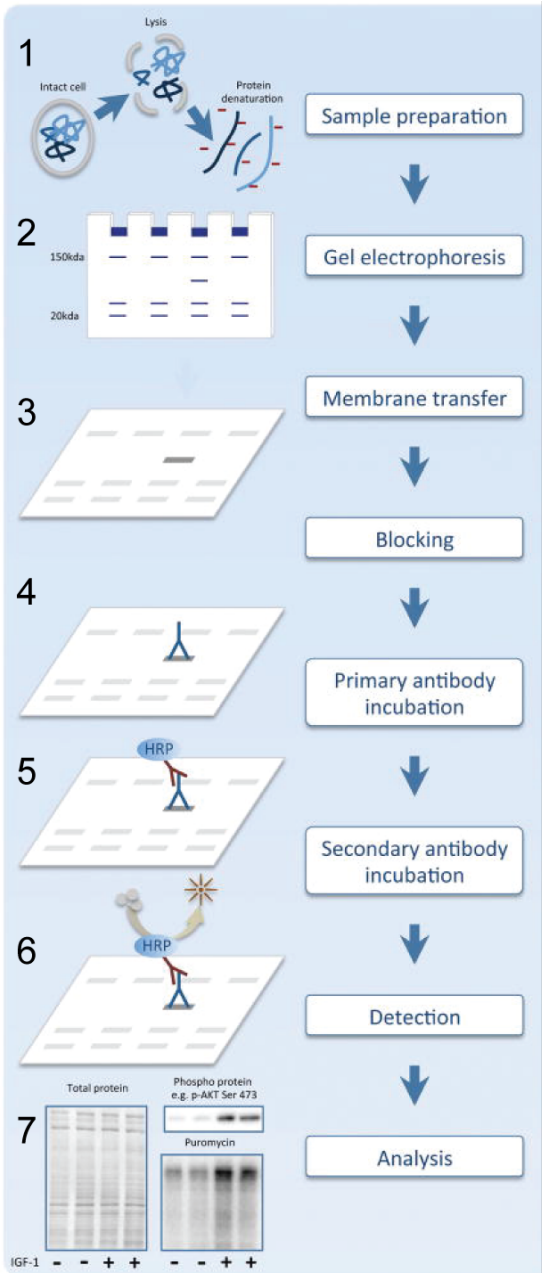

Figure 9: Sequential stages of the Western blot process. Figure adapted from (1). Extraction of cellular proteins from cells (1); quantification of protein concentration and electrophoretic separation of proteins within a gel matrix (2); transfer to a membrane with a high affinity for proteins (3); "blocking" the membrane to reduce non-specific binding (4); antigen detection by antibodies specific for the protein(s) of interest (5); incubation with a secondary antibody linked to a label (e.g., chemiluminescent or fluorescent) (6); development and detection of the signal, which is theoretically proportional to the degree of antigen/antibody binding and quantification of the resulting bands using densitometry software.

charge of the protein lysate (64). The loading dye also contains glycerol, which makes the sample heavier than the running buffer surrounding the gel, thereby ensuring that the sample collects at the bottom of the well. The protein samples are separated during gel electrophoresis based on size and electric charge, then transferred to a membrane with high affinity for proteins. The membrane is then incubated in a blocking buffer, which contains a 5% membrane-blocking agent in Tris-buffered saline and 0.05% Tween 20, which aids in the removal of residual SDS from earlier steps. The blocking buffer also improve the sensitivity of the assay by reducing background interference and improving the signal-to-noise ratio. After blocking, the membrane is incubated with antigen-specific primary antibody, typically over-night, after which the membrane is washed with purified water and blocking buffer to remove residual primary Ab. The next step is incubation with secondary antibody, which is conjugated to a chemiluminescent or fluorescent protein. After further washing steps the signal (phosphorylation), which is theoretically proportional to the degree of antigen/antibody binding, can be detected and quantified based on protein bands using densitometry software. A dark band means you have higher expression of protein or a stronger phosphorylation, while relatively weaker bands means lower expression of the protein of interest, or lacking signal.

2.0 Aims

The primary aim of this project is to elucidate the pathways activated by sonoporation. The goal is to identify biomarkers for PDAC that ca be used to optimise sonoporation therapy.

The specific objectives were to

- develop methodology for *in vitro* optimisation of sonoporation
- do initial investigations of protein signalling pathways activated by sonoporation in the AML cell line MOLM–13
- investigate protein signalling pathways activated by sonoporation in the pancreatic cell lines MIA PaCa–2, PANC-1 and BxPC-3 cultured in the bioreactor Petaka G3 LOT

3.0 Materials and Methods

All reagents were purchased from Sigma–Aldrich (Inc. St Louis, MO, USA) unless otherwise stated.

3.1.1 Cell culturing

The acute myeloid leukemia (AML) cell line MOLM–13 was purchased from DSMZ, (Deutche Sammlung von Mikroorganismen und Zellkulturen GmbH, Braunschweig, Germany) and maintained in Roswell Park Memorial Institute (RPMI) –1640 medium supplemented with 1% (v/v) L–glutamine solution (L–G) and 10% (v/v) heat–inactivated fetal bovine serum (FBS).

The pancreatic cell lines were kindly provided by Anders Molven laboratory at the University of Bergen and were originally purchased from ATCC® Europe (Wesel, Germany). MIA PaCa–2 cells originates from a 65–year–old male Caucasian and were cultured in Dulbecco's Modified Eagle's Medium – High glucose (DMEM) supplemented with 2.5 % (v/v) horse serum (HS; Gibco™ by Thermo Fisher Scientific, Waltham, MA, USA), 2% (v/v) L–G, 10% (v/v) FBS and 1% (v/v) Sodium Pyruvate (Gibco™ by Thermo Fisher Scientific, Waltham, MA, USA). The BxPC–3 epithelial cells originate from an adenocarcinoma tumour from a 62–year–old female and were cultured and maintained in RPMI–1640 medium supplemented with 2% (v/v) L–G, 10% (v/v) FBS and 1% (v/v) Sodium Pyruvate (Gibco™ by Thermo Fisher Scientific, Waltham, MA, USA). The epithelial PANC–1 cells originate from epithelioid carcinoma in the pancreatic duct in a 56–year –old Caucasian male and cultured and maintained in DMEM– High glucose supplemented with 10% (v/v) FBS (Sigma–Aldrich, Inc., St. Louis, MO, USA), 1% (v/v) L–G (Sigma–Aldrich, Inc., St. Louis, MO, USA); 1% (v/v) Na–P (Gibco™ by Thermo Fisher Scientific, Waltham, MA, USA).

The cells were cultured in 75cm^2 cell culturing flasks (T75 flasks, VWR International Ltd., Leicestershire, UK) with ventilated lids and placed in a humidified incubator with 5% CO_2 at 37˚C (Thermo Fisher Scientific, Waltham, MA, USA) unless otherwise stated. A sterile laminar flow bench with a high efficiency particulate air filter was used for all cell culturing.

3.1.2 Cell passaging

All cell lines were passaged 2–4 times a week in accordance with manufacturers recommendations. Cells were counted using a Bürker or a Fuchs–Rosenthal counting

chamber. For passaging all reagents were pre–heated to room temperature (RT). MOLM–13 cells were passaged by centrifuging the cells at 400 G for 5 min, resuspending in fresh medium and supplementing with fresh medium to the desired cell concentration. The adherent pancreatic cell lines were passaged by enzymatic dissociation from the flask at approximately 80% confluency incubating with trypsin solution after washing the cells with Phosphate Buffered Saline (PBS) until the cells were detached from the flask. The trypsin was neutralized with 6.5 times the trypsin volume of fresh medium, and the solution was centrifuged at 400 G for 5 min at RT before resuspending in fresh medium obtaining the desired cell density in a new cell culture flask.

3.1.2 Cryopreservation and thawing of cells

For cryopreservation the cells were counted and resuspended at the desired cell concentration (1.0×10^6 – 5.0×10^6 cells/mL) in 95% complete growth medium and 5% Dimethyl sulfoxide (DMSO). To prevent cell damage from freezing too fast the aliquots were placed in a freezing container (Nalgene® Mr. Frosty) over–night at -80°C, which allows the cells to decrease in temperature by 1°C/hour protecting the cells. After 24h the cells were placed in -80°C freezer for long term storage. For thawing, the cells were thawed under running water at RT and pre–heated medium was added within 10 min of retrieval from -80°C storage. The cells were centrifuged 400 G for 5 min at RT to remove the freezing medium containing cytotoxic DMSO. Then, the cells were resuspended in fresh medium and incubated as previously described. For the adherent cells each cell line was kept until a passage number of maximum 20 passages, and a new batch of cells was started thereafter. The stock was obtained during the first few passages.

3.2 Antibodies

3.2.1 Positive controls and antibodies

The antibodies (**Table 7 – Appendix**) corresponding to the proteins of interest for the pancreatic cell lines were tested prior to treating the cells with sonoporation to determine the presence and/or level of protein expression in the cell line. To induce phosphorylation or dephosphorylation different chemicals, referred to as positive controls (**Table 9 – Appendix**), known to induce phosphorylation or dephosphorylation, were used to stimulate the cells. These tests were used to test the antibodies and optimise the amount of protein extract necessary to perform WB analysis.

3.3 Viability assays

3.3.1. Trypan Blue apoptotic cell stain

The nucleic acid trypan blue stain (0.4%, 1 μg/mL, 1:1 dilution; duplicates) was used for cell count following cell treatment, and to distinguish between dying/dead cells and viable cells. Only cells with a compromised plasma membrane take up the dye (63). The cells were counted using a Fuchs–Rosenthal counting chamber immediately after treatment (65).

3.3.1.2 Hoechst 33342 apoptotic stain

Hoechst 33342 is a fluorescent nucleic acid stain that will only stain dying and apoptotic cells with a compromised plasma membrane (64). Upon binding to A–T rich regions of dsDNA the Hoechst stain will undergo an approximately 30–fold increase in fluorescence. When exited by ultraviolet (UV) light (360 nm) the Hoechst stained cells will emit a blue fluorescence (460 nm) (65). The Hoechst solution was prepared (11.8 mL sterile PBS, 3.2 mL 37% formaldehyde and 0.03 mL (20 mM) Hoechst 33342 stock solution (10 mg/mL)) prior to treatment of cells. 100μL Hoechst solution was added to 100μl cell suspension (suspension cells) or cell culture media (adherent cells). (cell suspension: Hoechst is 1:1) (63). The plate was covered with Parafilm M, the lid and aluminium foil to preserve it, and stored at 4^{o}C until imaging (64). Images were captured using a 5×/0.6NA 20× objective coupled to an inverted Axiovert microscope (Carl Zeiss Microscopy GmbH, Göttingen, Germany) using Zen Pro software (Carl Zeiss Microscopy GmbH, Göttingen, Germany). Image exposure time was set to 33 ms, and the light source (DAPI) was set to max. The images were analysed in Fijii software (ImageJ) number of Hoechst 33342 stained apoptotic cells and total number of cells were counted, and the percentage of apoptotic cells calculated. and figures made in Graph Pad Prism (GraphPad Software, La Jolla, CA, USA).

3.3.1.3 WST–1 metabolic assay

The WST–1 assay (Roche, Ltd., Basel, Switzerland) provides an estimation of the amount of metabolically active cells in the sample. WST–1 is a tetrazolium salt that is cleaved to a soluble formazan. This reaction is dependent on nicotinamide adenine dinucleotide phosphate (NAD(P)H) in viable cells, and the amount of formazan dye formed directly correlates to the number of metabolically active cells. The method is sensitive detecting low cell numbers with longer incubation times (66). When light passes through the sample the density of the solute/colour determines how much light passes through. A sample of low density, such as a sample with few cells, or many apoptotic cells (not metabolically active), will have a low

absorbance, meaning little light has been absorbed by the sample. In a sample of high density with many metabolically active (live) cells less light will pass through the sample and more will be absorbed, meaning the sample will have a high absorbance. It is recommended to incubate the cells with the WST–1 reagent 0.5 – 4.0 hours, and optimisation for each cell line is recommended by manufacturer (67). The absorbance was measured using a plate reader (Spectra Max Plus 384) at 450 nm and 620 nm. The results were analysed in Microsoft Excel (Microsoft Office 2018) and figures made in Graph Pad Prism (GraphPad Software, La Jolla, CA, USA). The metabolic activity can be calculated by applying the following equation:

$$\%\ Metabolic\ activity = (Sample\ Abs.at\ 450\ nm - Sample\ Abs.at\ 620\ nm) - (Blank\ Abs.at\ 450\ nm - Blank\ Abs\ at\ 620\ nm)$$

3.3.2 Viability optimisation MOLM-13

3.3.2.1 Hoechst 33342

To reduce work and ensure more high-throughput analysis of dead cells following Hoechst staining, a new semi-manual method of counting dead cells was tested. This whole process was performed by two individuals to identify irregularities in the process. Following sonoporation (**chapter 3.5.3**) the Hoechst assay was performed according to protocol (**chapter 3.3.1.2**). Three images per replicate were then uploaded to Fijii software (ImageJ) and analysed separately.

Count of total number of cells:

- Image uploaded
- Image converted to 16-bit
- Brightness/contrast and threshold adjusted
- Cells were counted by the software.

Count of dead cells:

- Image uploaded again
- Manual identification of dead cells aided by a cell counter function in Fijii.

3.3.2.2 WST-1

To optimise incubation–time following sonoporation and the optimal cell concentration to seed a test was performed. 100 µl of untreated MOLM–13 cell suspension of different concentrations (0.05×10^6, 0.1×10^6, 0.2×10^6, 0.4×10^6, 0.8×10^6, 1×10^6) were seeded (triplicates) in a 96–well plate. 100 µl RPMI was used as a control. The cells were incubated for 24h Then, 10 µl WST–1 reagent was added to each well and the plate was incubated for 0.5 h, 1h, 2h and 4h. The absorbance was read on a plate reader (Spectra Max Plus 384) at 450 nm and 620 nm. The results were analysed as described in **chapter 3.3.1.3.**

3.3.3 Viability optimisation MIA PaCa-2

3.3.3.1 WST-1 - Cell number and incubation time for MIA PaCa-2

In order to determine the optimal number of cells to seed, and the optimal incubation time for WST–1 assay following US treatment of MIA PaCa–2 cells a test was performed. 1×10^6 MIA PaCa–2 cells (maintained in DMEM) were seeded in Petakas and incubated for 24h Then, the cells were sonoporated at 358 mW/cm^2 for 5 min and incubated for 60 min. The cells were detached with pre-heated 1× trypsin as describer previously. Then, 0.1×10^4, 0.2×10^4, 0.4×10^4, 0.8×10^4, 1.6×10^4, 3.2×10^4 and 6.4×10^4 cells were seeded (duplicates) in a 96–well plate. The cells were incubated further 24h before adding 10 µl WST–1 reagent. Absorption was read with an ELISA plate reader (Spectra Max Plus 384) at 450 nm and 620 nm after 1h, 2h and 4h incubation. The results were analysed as described in **chapter 3.3.1.3.**

3.3.3.2 Viability test of MIA PaCa-2 in Petakas

To assess the optimal seeding density for viability assays for MIA PaCa–2, cells cultured in Petakas, were either serum-starved or (cultured in DMEM without any additives) or treated with high US (**Table 3**) and Sonazoid MBs (5.6 µL/mL). Cell not treated were the control. After 60 min. of incubation following sonoporation, cells from each sample (High US, Serum–Starved, Control) were seeded for Trypan blue counting, Hoechst 33342 and WST-1 assays.

- Trypan Blue

  MIA PaCa-2 cells were stained with a 0.4% solution of trypan blue (1:1 dilution; duplicates). Stained and unstained cells were counted immediately following treatment using a Fuchs-Rosenthal counting chamber.

- Hoechst 33342

32×10^4 cells were seeded (triplicates) from each sample (High US, Serum-Starved, Control) and incubated for 24h before adding 100 µl Hoechst 33342 solution. The plate was preserved and imaged as described previously (**chapter 3.3.1.2**). The Hoechst seeding test was repeated seeding 0.8×10^4 and 1.6×10^4 (triplicates) with untreated MIA PaCa–2 cells, which was assessed visually.

- WST-1

32×10^4 cells were seeded (triplicates) from each sample (High US, Serum-Starved, Control) and incubated for 24h. before adding 10µl Cell Proliferation Reagent WST-1 /well. The plate was incubated for 2h before reading the absorbance on a plate reader (Spectra Max Plus 384) at 450 nm and 620 nm. The results were analysed as described in **chapter 3.3.1.3.**

3.5 Ultrasound treatment of cells *in vitro*

3.5.1 MOLM–13

The custom–made suspension cell plate sonicator used in this project is made for regular 24–well plates (68) (**Figure 10A–B**). The device has six US transducers focused in the middle of each well. The six wells allow for testing different treatments simultaneously, for example MBs or drugs. The plate sonicator is controlled by a custom program written in LabVIEW (National Instruments Corporation, Austin, TX, USA) with a user–friendly interphase (**Figure 10B**). Prior to the experiment a file is written indicating the name, frequency, pressure, intensity, and duration required for each experiment. This file is read by the software and all parameters are automatically calculated (68) .

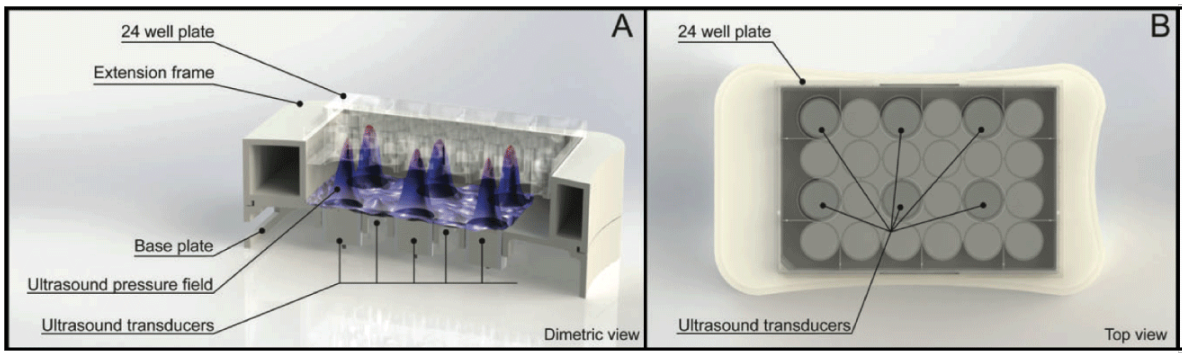

Figure 10: Computer generated renderings of the custom–made suspension cell plate sonicator for 24–well plates. Cutway diagram showing assembly (A) Figure from (68). Top view showing position of the ultrasound transducers (B).

3.5.2 Cell culture before experiments

MOLM–13 cells were cultured and seeded at 0.5×10^6 cells/mL until they experienced log–phase growth. Then, 2.5 mL 0.4×10^6 cells/mL MOLM–13 cell suspension (maintained in RPMI–1640) was seeded per well (1×10^6 cells/well) in 6 wells, corresponding to the US transducers of the plate sonicator, and kept stored in the incubator for 1–2h until sonoporation (69).

3.5.3 Ultrasound and microbubble treatment

MOLM–13 cells were treated with three different US conditions (**Table 1**). The US intensities used in the studies of MOLM–13 were 74 mW/cm^2, 501 mW/cm^2 and 2079 mW/cm^2, later referred to as Low, Medium and High (**Table 1**). Before US treatment the plate covered with a self–adhering thin membrane (TopSeal ™ –A; Perkin Elmer, Waltham, MA, USA), measured to have < 1% pressure attenuation at 1 MHz, and was placed inverted in the water bath. The TopSeal™ has been measured to have < 1% pressure attenuation at 1 MHz (70).

Table 1: Ultrasound settings for MOLM–13 studies

Sample definition	Intensity (mW/cm^2)	MI	Duty cycle (%)	MHz	Duration (min)
Control	0	0	0	0	0
Low	74	0.2	4	1.108	10
Medium	501	0.3	16	1.108	10
High	2079	0.4	37	1.108	10

MOLM–13 cells were treated with and without MBs at Low, Medium and High US intensity (**Table 1**) for 10 min. Following US treatment cells were harvested for viability assays. The trypan blue assay was performed within 5 min of sonoporation, while cells for Hoechst 33342 were incubated for 24h before fixing the cells. Protein extraction was performed within 5 min and after 2h incubation following sonoporation. The procedure for cells treated with MBs extracting proteins within 5 min of sonoporation is described below. Before MB addition Sonazoid MBs were prepared according to manufacturer's recommendations; the MBs were resuspended in 2 mL sterile NaCl (0.9%) and diluted 1:10 before addition to the cells (cells : MBs are 1:1). MBs were added immediately before sonoporation. Cells not treated with US were used as control. After sonoporation cells from 6 wells were collected. Then, cells were seeded for viability assays and cells were prepared for protein extraction within 5 min

following sonoporation. Protein was extracted as per protein extraction protocol and prepared for WB (**chapter 3.7**).

3.5.4 MIA PaCa–2

The custom–made adherent cell plate sonicator has a water bath that sits on the electronics case containing a 128–element array (90 cm^2 treatment area) of US transducers. The carriage has a removable acoustic absorber, the Aptflex F28, which is placed above the Petaka absorbing the US, thereby, minimises standing waves. The Petaka is placed in the carriage with the upper surface facing down (68) (**Figure 11**).

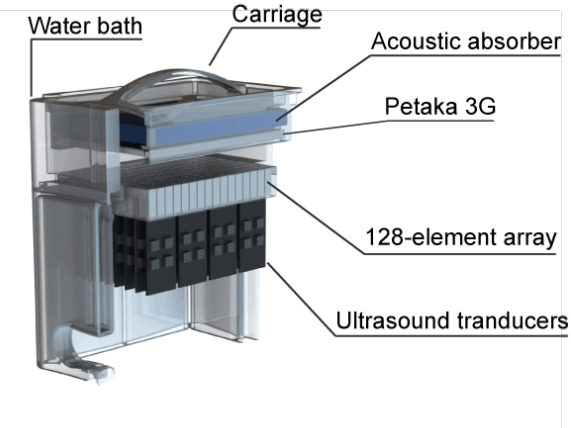

Figure 11: Computer generated rendering of the custom–made adherent cell plate sonicator. Cutway diagram showing assembly. The Petaka is placed in the carriage containing the acoustic absorber before it is positioned in the water bath. The sonicator contains a 128–element array of ultrasound transducers covering the whole cell culture surface of the Petaka.

The plate sonicator is controlled by a custom program, based on the program for the 24–well plate sonicator, written in LabVIEW, with a user–friendly interphase. Prior to the experiment a file is written indicating the name, frequency, pressure, intensity, and duration required for each experiment. This file is read by the software and all parameters are automatically calculated (68).

3.5.5 Cell culture before experiments

MIA PaCa-2 cells were cultured at a density between 2×10^6 and 7×10^6 cells in T75 flasks until reaching full confluency.

3.5.6 Protocol for seeding adherent cells in Petaka

The cells were detached by pre-heated 1× trypsin. Trypsin was neutralized with medium and the cell suspension was centrifuged at centrifuged at 400 G for 5 min. Cells were then counted and resuspended. Then, 3×10^6 cells in 26 mL medium (1.15×10^5 cells/mL) were injected into the Petaka. Air pockets were removed before sealing the ventilation port with adhesive tape to avoid new air leaking into the Petaka during incubation and handling. The Petaka was incubated for 24h in a horizontal position to allow the cells to adhere. After 24h the Petaka was placed in a vertical position. The Petaka was then incubated further 24–36 h to achieve log–phase growth and to ensure there is enough cells for WB analysis.

3.5.7 Protocol for detachment of adherent cells in Petaka

To detach the cells from the Petaka the ventilation port seal was removed, and the supernatant aspirated. Then, to wash residual medium and debris 10 mL ice–cold PBS was injected with a 30mL syringe and the Petaka swirled to cover all cells. The PBS was aspirated before injecting 3 mL ice–cold trypsin, swirling the Petaka to cover all cells, and incubating on ice for ~30 min to detach the cells. Next, the trypsin was neutralized by injecting 10 mL ice–cold DMEM with a 30mL syringe, swirling the Petaka. The supernatant was then transferred to a 50mL tube and centrifuged at 400 G for 5 min at 4°C. Protein was extracted as per protein extraction protocol and prepared for WB (**chapter 3.7)**

3.6 *In vitro* optimisation

3.6.1 Optimisation of cell lysis

To be able to plan how many WBs could be performed from one experiment using Petakas the protein concentration from 1×10^6 MIA PaCa–2 cells were quantified. The cells were harvested when passaging cells, counted and quantified using DC™ Protein Assay Kit as per protein quantification protocol (**chapter 3.7.2**).

3.6.2 Optimisation of growth rate for MIA PaCa–2 in Petaka

In order to ensure optimal conditions for cell growth in the Petaka MIA PaCa–2 cells, cultured in Petakas, compared to MIA PaCa–2 cells grown in T75 flasks, was investigated. The objective was to ascertain the cells growth rate to identify at which time–point the cells were in log phase, and to identify when the cell growth plateaus. The growth rate was determined by the mean of mean cell count per surface area.

MIA PaCa–2 cells (1×10^6/26 mL), were seeded in two Petakas, and one T75 culturing flask, and incubated for 48 h. The Petakas and the T75 flasks were cultured for further 5 days and monitored daily using a Leika microscope. The cells were imaged approximately every 24h for 5 days, the first images taken 24h after seeding. Images were captured using a 5×/0.6NA 20× objective coupled to an inverted Axiovert microscope (Carl Zeiss Microscopy GmbH, Göttingen, Germany). Image exposure time was set to 6.5 ms, and the light source was set to max. The images were saved in 16bit czi format. A total of 50 images per Petaka were captured. MIPAR batch processor (MIPAR, Worthington, OH, USA) was used measure the surface area occupied by the MIA–PaCa–2 cells. The exact recipe settings can be seen in the appendix (**Table 10**). **Figure 12** shows a general overview of the process with the major steps.

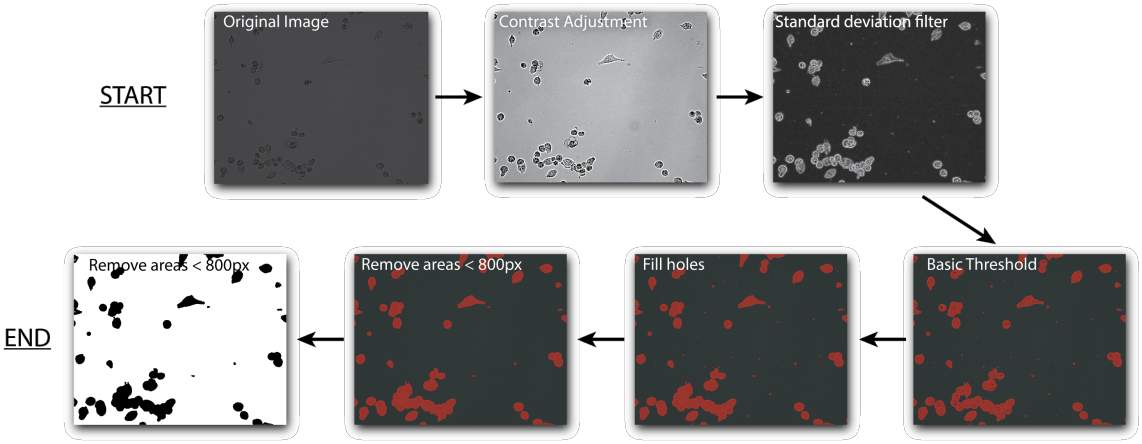

Figure 12: Overview protocol of Hoechst Imaging analysis. Images captured using a 5×/0.6NA 20× objective coupled to an inverted Axiovert microscope (Carl Zeiss Microscopy GmbH, Göttingen, Germany; image exposure time; 6.5 ms. Light source; max.16bit image czi format). 50 images captured per Petaka. MIPAR batch processor (MIPAR, Worthington, OH, USA) was used measure the surface area occupied by the MIA PaCa–2 cells. The contrast was adjusted, and the background was flattened to correct for illumination inhomogeneity. A dark texture filter was used to highlight dark components of the image via a grayscale closing method. A standard deviation filter was used to accentuate the cell edges by brightening pixels which have dissimilar neighbours. A range threshold was applied, holes were filled, and areas of 800 pixels or less were rejected to remove false positives. The percentage of selected pixels as a ratio of the original image size was considered the percentage surface area covered by cells.

3.6.3 Optimisation of cell detachment

3.6.3.1 Optimisation of timing of cell detachment with cold 1× trypsin and 10× trypsin

The objective was to determine how long it would take to detach untreated MIA PaCa–2, PANC–1 and BxPC–3 cells with ice–cold 1× trypsin and 10× trypsin 3×10^6 cells of each cell line were seeded in two T75 flasks per cell line and incubated for 48 h. The cells were washed once with ice–cold sterile PBS, then, ice–cold 1× trypsin or 10× trypsin was added, and the

flask put on ice. The flasks were monitored by microscope until the cells were detached and the time it took for the cells to detach was noted.

3.6.3.2 Optimisation of cell detachment–western blot

Since trypsin may affect cell signalling results (59, 60), the possible influence of cell detachment with 1× trypsin was investigated. Three methods of cell detachment were tested, trypsin– 4ºC (1), trypsin RT (2) and scraping (3). Cell detachment by scraping in a Petaka is possible using a magnet (62), however, due to the lack of necessary equipment to accomplish this, enzymatic cell detachment was used in this project. For this test 3×10^6 MIA PaCa–2 cells, (maintained in DMEM,) were seeded in six T75 flasks and incubated for 48 h. For each detachment method one flask of cells was stimulated with A23187 (1µM) + PMA (0.1µM) for 30 min to investigate influence on phosphorylation. Untreated cells were used as controls.

Detachment following stimulation:

1. Trypsin 4ºC:
    - Cells were washed twice with ice–cold PBS.
    - 1× trypsin was added, and the cells were kept on ice until the cell detached from the flask.
    - After the cells were detached the trypsin was neutralized with ice–cold DMEM.

2. Trypsin 37ºC:
    - Cells were washed twice with PBS (37ºC).
    - 1× trypsin (37ºC) was added and the cells were kept in the incubator until the cell detached from the flask.
    - After the cells were detached the trypsin was neutralized with medium (37ºC).

3. Cell detachment by scraping refers to scraping to loosen the cells from the flask with RIPA lysis buffer (supplemented with (1:100) Halt™ Protease & Phosphatase Inhibitor Cocktail and 0.5 M EDTA Solution) after washing with PBS:
    - cells were washed twice with ice–cold PBS.
    - 1 mL RIPA lysis buffer was added and the flask swirled to cover the cells, then incubated on ice for ~ 20 min

Protein was extracted from all samples as per protein extraction protocol and prepared for WB (**chapter 3.7).** 30 μg protein was loaded in the gel from each sample.

3.6.3.3 Optimisation of cell detachment with 10× trypsin –Viability and western blot

In order to determine whether 10× trypsin affects cell signalling a test was performed with the MIA PaCa–2, PANC–1 and BxPC–3 cell lines. 3×10^6 cell of each cell line was seeded in two T75 flasks per cell line and incubated for 48 h. For each cell line one flask of cells was stimulated with A23187 (1μM) + PMA (0.1μM) for 30 min Untreated cells were used as controls. The viability assay Trypan blue, WST–1 and Hoechst 33342 was used to assess how 10× trypsin affected the cells viability. Following stimulation cells were detached with cold trypsin as described in **chapter 3.6.3.2** and viability assays performed is previously described (**chapter 3.3.1.1–3.3.1.3**). WST-1 32×10^4 cells, Hoechst 33342 1.6×10^4 cells. After viability assays were seeded protein was extracted as per protein extraction protocol and prepared for WB (**chapter 3.7).**

3.6.4 Optimisation of incubation time following sonoporation

MIA PaCa–2 cells were sonoporated with Sonazoid MBs and cells were harvested after 5 min, 1h, 2h, and 4h incubation in Petakas to investigate phosphorylation kinetics. Five Petakas were seeded with 3×10^6 MIA PaCa–2 cells (maintained in DMEM) and incubated for 48 h as previously described (**chapter3.5.6**). Then, the cells were sonoporated at 358 mW/cm^2 (referred to as High US) for 5 min One Petaka was not sonoporated (control), the second was lysed 5 min after sonoporation, the third Petaka after 1h, the fourth after 2., and the fifth after 4h incubation. Protein was extracted as per protein extraction protocol and prepared for WB (**chapter 3.7).**

3.6.5. Optimisation of western blot

To be able to determine the approximate protein level expressed of each protein investigated, optimisation of each Ab corresponding to the protein of interest was performed. These tests were also used to check that antibodies and recommended antibody concentrations worked as expected/intended. MIA PaCa–2 cells were stimulated with drugs of relevant targets (**Table 2**), known to induce phosphorylation of the proteins in question. For each test 3×10^6 MIA PaCa–2 cells (maintained in DMEM) were seeded in T75 culturing flasks and treated/stimulated after 48 h incubation with their respective stimuli for different time–periods

(**Table 2**). Protein was extracted as per protein extraction protocol and prepared for WB (**chapter 3.7)**, and 30 µg, 40 µg and 50 µg protein were loaded per well.

Table 2: Positive controls – Induction of phosphorylation

Antibody/Epitope	**Stimuli**
ERK 1/2 (Thr202/Tyr204)	*TNFα 15 min
SAPK/JNK (Thr183/Tyr18)	A23187 + **PMA 30 min
p38 (Thr180/Tyr182)	A23187 4h
MLC (Ser19)	A23187 4h
p–eIF2α (Ser51)	A23187 4h
MYPT1 (Ser 853)	
MYPT1 (Ser 696)	

*TNFα = Tumour necrosis factor
**PMA = Phorbol 12–myristate 13–acetate

3.6.6 Ultrasound and microbubble treatment of MIA PaCa–2

MIA PaCa–2 cells were treated with three different US conditions (**Table 3**) in the custom-made adherent cell plate sonicator (**Figure 10**). The US intensities used in the studies of MIA PaCa–2 are referred to as Low, Medium and High and refers to 3 mW/cm^2, 50 mW/cm^2 and 358 mW/cm^2 respectively (**Table 3**).

Table 3: Ultrasound settings for MIA PaCa-2 studies

Sample definition	**Intensity (mW/cm^2)**	**MI**	**Duty cycle (%)**	**MHz**	**Duration (min)**
Control	0	0	0	0	0
Low	3	0.1	20	2.0	5
Medium	50	0.2	80	2.0	5
High	358	0.378	160	2.0	5

The MIA PaCa–2 cells were treated with 5.6 µL/mL Sonazoid MBs. The concentration of microbubbles was based on a–priori knowledge. Four Petakas were seeded with 3×10^6 MIA PaCa–2 cells (maintained in DMEM), cultured and detached as described in **chapters 3.5.5 – 3.5.7**. Sonazoid MBs were prepared according to manufacturer's recommendations; the MBs were resuspended in 2 mL sterile NaCl (0.9%) and diluted 1:10 before immediately before injecting 1 mL MB–suspension (4.8×10^6 ppmL) into the Petaka (cells:MBs are 1:1). The experiment was repeated in full for the samples not treated with MBs. Here, NaCl only was

injected instead of a NaCl-MB suspension to mimic the treatment with MBs. Cells treated with MBs that were not treated with US was used as control, however, the cells were left for 5 min in the sonicator in order to treat the samples as equal as possible. The Petakas were injected with MBs immediately before sonoporation. Cells were sonoporated for 5 min at Low, Medium or High US intensity (**Table 3**) and then incubated for 2h. The cells were imaged immediately after sonoporation and then incubated for 2h. In experiments where microbubbles were added the cells were imaged immediately after sonoporation. After incubation for 2hours, the cells were detached by cold–trypsinization (1× trypsin) as described earlier. The trypsin was neutralized with ice–cold DMEM, the cell suspension resuspended, and cells were extracted for trypan blue counting. Then, the samples were centrifuged at 400 G for 5 min (4°C), resuspended in cold DMEM and diluted to 32×10^4 cells/µl and 1.6×10^4 cells/µl for WST–1 and Hoechst assays, respectively. 100 µl of each sample (Ctr., Low US, Medium US, High US) was seeded (triplicates) in a 96–well plate and incubated for 24h. After seeding for viability assays the samples were prepared for protein extraction for WB analysis as described earlier. After 24h viability assays were performed as described earlier (**chapter 3.3.1.1–3.3.1.3**).

3.7 Western blot

3.7.1 Protein extraction

Following treatment all cell lines were subject to the same extraction procedure. Samples were kept on ice between centrifugation steps. The cell suspension of each sample was centrifuged at 400 G for 5 min, supernatant aspirated and the cells washed with 10 mL cold PBS and again centrifuged at 400 G for 5 min Then, the supernatant was removed, and the pellet resuspended in 1 mL cold PBS in an Eppendorf tube and centrifuged at 400 G for 5 min Next, the supernatant was carefully removed by micropipette and the pellet was dissolved in RIPA lysis buffer supplemented with 1:100 Halt™ Protease & Phosphatase Inhibitor Cocktail and 1:100 0.5 M EDTA solution. To ensure that the pellet would dissolve and get a homogenous cell lysate, the pellet was dissolved by mechanical homogenization (repeated pipetting in RIPA buffer). For protein extraction 100 µl RIPA /1×10^6 cells, and 50 µl RIPA/ 1×10^6 cells were used for MOLM–13 and MIA PaCa–2 cells, respectively. The lysates were immediately incubated on ice and left for 15 min before centrifuging at 14000 G for 15 min Finally, the lysates were aliquoted, labelled according to sample and immediately stored at –80°C.

3.7.2 Protein quantification and sample preparation

The protein concentration was quantified using the colorimetric DC™ Protein Assay Kit (Bio–Rad Laboratories, Hercules, CA, USA(71)) with a serial dilution working range of 0.0 µg/mL – 2000 µg/mL. First, 5 µl of protein extract was added to a 96–well plate (triplicate). Then, 25 µl of working reagent A' (2% (v/v) of reagent S mixed with reagent A) and 200µl reagent B was added. All extracts were measure in triplicates to ensure precision. The plate was incubated in RT for 15 min before determining the protein concentration by reading the absorbance on an ELISA plate reader (Spectra Max Plus 384) at 720 nm. The protein extracts were denatured at 100°C for 5 min in 1× Loading buffer (200mM Tris–HCl (pH 6.8), 400 mM DTT, 8% SDS, 0.4% bromophenol blue, 40% glycerol), then cooled on ice for 10 min before loading the samples in the gel.

3.7.3 Sample reparation MOLM–13

For WBs with MOLM–13 26 µg protein extract was loaded in the gel.

3.7.4 Sample preparation pancreatic cell lines

For WBs with pancreatic cell lines (MIA PaCa–2, PANC–1, BxPC–3) 30–50 µg protein extract was loaded in the gel depending on the cell line and protein concentration of the cell lysate.

3.7.5 Gel electrophoresis

The protein extracts were separated by size using 10% sodium dodecyl sulfate–polyacrylamide gel electrophoresis system (SDS–PAGE; Mini–PROTEAN Tetra Electrophoresis System; Bio–Rad Laboratories, Hercules, CA, USA), according to manufacturer's protocol. SDS is a strong anionic detergent added to coat hydrophobic regions of proteins with negative charge, thus overpowering positive charges in proteins (1). By adding SDS in the loading buffer, gel and buffers denaturing of the proteins is ensured and gives the protein lysate a uniformly distributed negative charge.

When exposed to an electrical current the proteins will migrate towards the positive electrode (anode) and be separated in the gel by size. The gel was hand–cast using the Mini–PROTEAN® tetra hand–caste system with 1.0 and 1.5 mm Spacer Plate and Short Plate (Bio–Rad Laboratories, Hercules, CA, USA). ~ 7.5 mL resolving gel (25% (v/v) 1.5 M Tris–HCl (pH 8.8), 1% (w/v) SDS, 1% (w/v) ammonium persulfate (APS; Bio–Rad Laboratories,

Hercules, CA, USA), 0.06% (v/v) TEMED (Bio–Rad Laboratories, Hercules, CA, USA) and 27% (v/v) 30% Acrylamide/Bis solution.) was added to the cast. 500µL ultrapure water (MQ–H_2O; processed by Milli–Q® Type1 Ultrapure Water System; Merck Millipore, Billerica, MA, USA) was carefully added on top of the gel to ensure a flat surface. The gel was left to solidify for ~ 1h. Then, the MQ–H_2O was removed, and ~ 2.5 mL stacking gel (12.5% (v/v) 1 M Tris–HCl (pH 6.8), 1% (w/v) SDS, 1% (w/v) APS, 0.1% (v/v) TEMED and 6.5% (v/v) 30% Polyacrylamide/Bis solution) was added on top of the resolving gel. A 1.0 mm/10welled or 1.5mm/15 welled comb (Bio–Rad Laboratories, Hercules, CA, USA) was immediately inserted in the cast and left to solidify for ~15 min Next, the gel was placed in the Mini–PROTEAN® electrophoresis system (Bio–Rad Laboratories, Hercules, CA, USA). Running buffer 0.3% (w/v) Tris Salt, 1.5 (w/v) Glycine and 0.1% (w/v) SDS was added to the marked level and the combs were removed submerged in buffer. 3–5 µL Precision Plus Protein™ All Blue Standards (Bio–Rad laboratories, Hercules, CA, USA) was added to the first and last well to help identify the separated proteins.

3.7.8 Electrophoretic transfer of proteins

The separated proteins were transferred from the gel to a nitrocellulose membrane (Bio–Rad Laboratories, Hercules, CA, USA) using a wet transfer (Mini Trans–Blot® Cell; Bio–Rad Laboratories, Hercules, CA, USA). The transfer buffer (0.3 (w/v) Tris Salt and 1.5% (w/v) Glycine) was prepared in advance and cooled to 4ºC. For one gel two pieces of extra thick blot paper (Bio–Rad Laboratories, Hercules, CA, USA), two black sponges and the membrane was soaked in transfer buffer for ~ 10 min Then the gel holder cassette was assembled carefully as follows: a sponge, a blot paper, the gel, nitrocellulose membrane, a blot paper and finally a sponge. All the parts were kept wet and assembled to avoid air pockets between the gel and the nitrocellulose membrane. Next, the gel holder cassette was placed in the electrode module with the gel facing the negative electrode (cathode), which was inserted in the buffer tank with a frozen cooling unit to avoid the transfer to overheat and deregulate the proteins. The buffer tank was placed in a bucket of ice to aid with the cooling of the transfer. Transfer buffer was filled to the designated mark. The proteins were transferred at 240 Ampere for 150 min After transfer the membrane was washed in MQ–H_2O, then soaked in Ponceau red solution for ~ 1 min to confirm the loading consistency of protein samples. An image was captured for later reference of loading consistency.

3.7.9 Immunostaining

After staining with Ponceau red the membrane was incubated in 10 mL blocking buffer (5% (w/v) non–fat milk solution (Skim Milk Powder; Sigma–Aldrich, Inc., St. Louis, MO, USA) in 1× Tris Buffered Saline (TBS) supplemented with and 0.1% (v/v) Tween® 20 (Sigma–Aldrich, Inc., St. Louis MO, USA) for 1hour in RT. Subsequently, the membrane was incubated with the respective primary antibodies corresponding to the assayed proteins (**Table 7 – Appendix**) over–night at 4°C. The antibodies were diluted according to the manufacturer's recommendations (**Table 7 – Appendix**) in blocking buffer. COX IV mAb was used as a loading control (**Table 7 – Appendix**). After over–night incubation with primary Ab the membrane was washed with MQ–H_2O thrice and incubated in blocking buffer for 10 min in RT. This washing step was repeated twice before incubating the membrane with rabbit or mouse secondary peroxidase Ab corresponding to the species of the primary Ab target (**Table 8 – Appendix**) for 1h. Then, the membrane was again washed thrice in MQ–H_2O and blocking buffer and placed in 1× TBS and imaged as soon as possible. The protein bands were visualized by incubating the membrane in 3 – 4 mL SuperSignal™ ELISA Pico Chemiluminescent Substrate (Thermo Fisher Scientific, Waltham, MA, USA), or 2 – 3 mL SuperSignal™ West Femto Maximum Sensitivity Substrate (Thermo Fisher Scientific, Waltham, MA, USA) for the Ab with weaker signal. Imaging (and analysis) was performed with Luminescent image Analyzer (ImageQuant LAS4000 Inc., both GE Healthcare, Chicago, IL, USA).

3.8 Statistics

The results are expressed as mean values ± SD, unless otherwise indicated.

4.0 Results

4.1 Results MOLM–13

4.1.1 Optimisation of WST–1 for MOLM–13

A pilot study was performed to determine which cell concentration to seed, and how long incubation–time following sonoporation was optimal for WST–1 metabolic assay for MOLM–13 cells (**Figure 13**). Untreated cells were seeded at concentrations between 0.5×10^6 and 1.0×10^6 and incubated between 0.5 and 4h. The fluorescence absorbance increases with increasing number of viable cells, as expected. At 0.8×10^6 cells the reaction is saturated because the WST–1 reagent has been used up or metabolized.

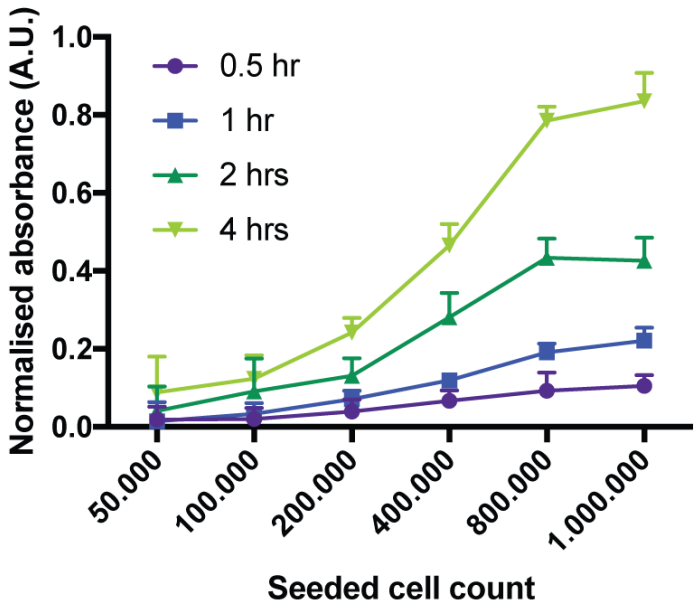

Figure 13: WST–1 based metabolic assay for MOLM–13. Metabolic activity evaluated in untreated MOLM–13 cells, seeded at concentrations between 0.5×10^6 and 1.0×10^6 and incubated between 0.5 and 4h). The absorbance was read on an ELISA plate reader (Spectra Max Plus 384) at 450 nm and 620 nm.

4.1.2 Viability – trypan blue and Hoechst staining of sonoporated MOLM–13

MOLM–13 cells (0.4×10^6/mL) were sonoporated with or without Sonazoid MBs (cells:MBs were 1:1) at Low US (74 mW/cm^2), Medium US (501 mW/cm^2) or High US (2079 mW/cm^2) for 10 min (control was not sonoporated) as described in **chapter 3.5.3**. Viability assays were performed as per **chapter 3.3.1** (trypan blue) and **3.3.2.1** (Hoechst 33342). 5 min after sonoporation there was no change in cell concentration in both the samples with and without MBs, compared to the control, and no significant cell death was observed. Some cell uptake of trypan blue was observed in samples treated with MBs at 0h with increasing US intensity (**Figure 14A+B**). After 24h cells in all samples not treated with MBs had proliferated (measured as increase in cell concentration) with little cell death observed (**Figure 14C**). However, in the samples treated with MBs the samples with Medium and High US intensity showed a trend of decreasing proliferation ability and increasing cell death, compared to the control, after 24h (**Figure 14D**). Of the Hoechst stained cells there was no difference in percent apoptotic cells between the samples, compared to the control without MBs. However, with MBs added there is a clear trend of increasing percent apoptotic cells with increasing US intensity (**Figure 14F**).

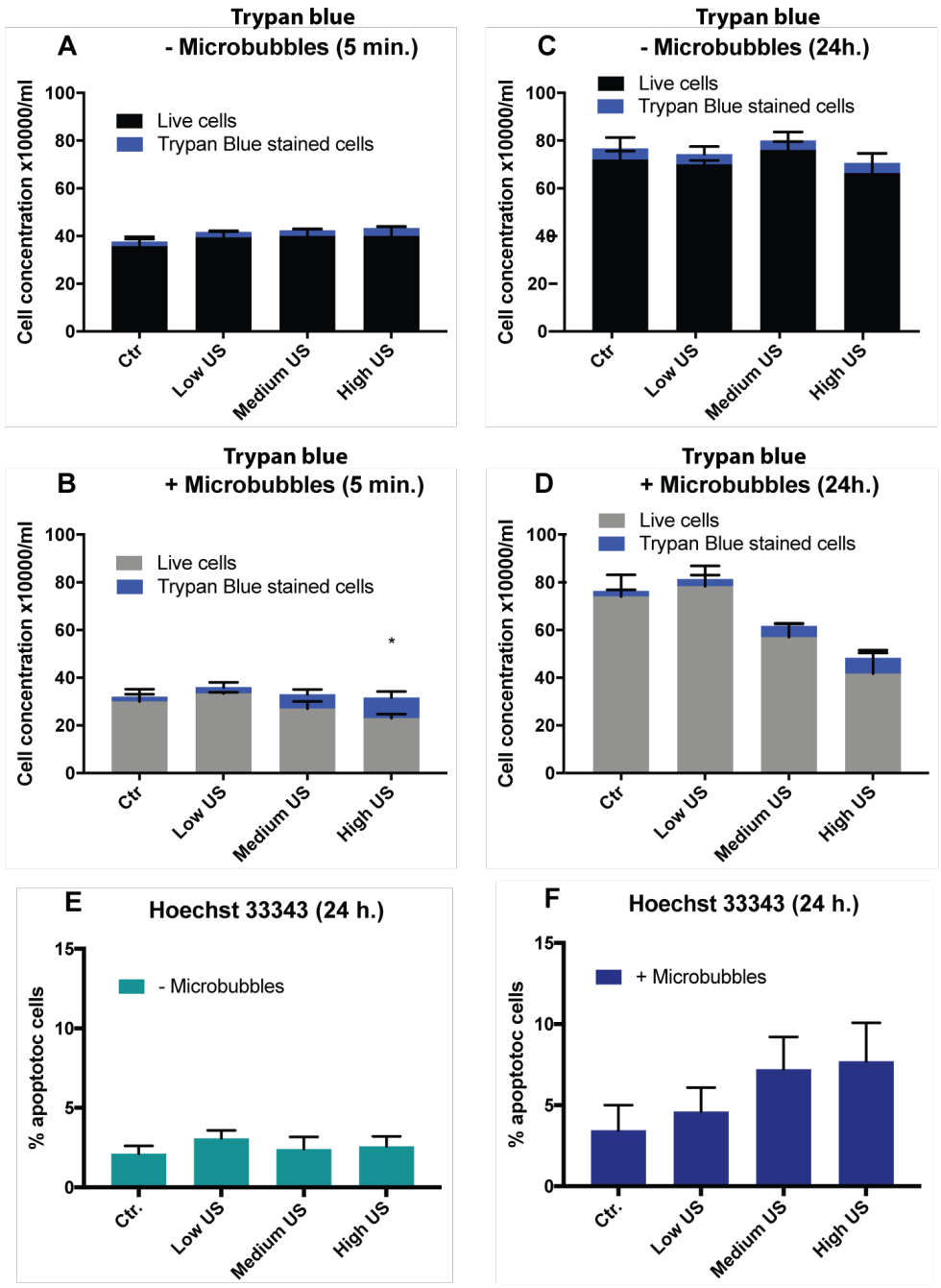

Figure 14: Trypan blue (proliferation) and Hoechst 33342 (apoptosis) assessment of sonoporated MOLM–13 cells. Cells were sonoporated with (+) or without (–) Sonazoid microbubbles (MBs, cells:MBs were 1:1) at Low (74 mW/cm^2), Medium (501 mW/cm^2) or High (2079 mW/cm^2) ultrasound (US). Control was not sonoporated. Trypan blue stained cells (1:1 dilution) were counted after 5 min and after 24h incubation (5% CO_2, 37˚C). After 5 min there was no change in cell count +/– MBs, compared to the control (A+B). After 24h all samples –MBs had proliferated (C). However, after 24h Medium and High US intensity +MBs had a decrease in proliferation, and increase in cell death, compared to the control (D). Hoechst stained cells –MBs revealed no difference in percent apoptotic cells between the samples, compared to the control (E). However, +MBs had increasing percent apoptotic cells with increasing US intensity (F).

4.1.3 Western Blot analysis MOLM–13

MOLM–13 cells (0.4×10^6/mL) were sonoporated with or without Sonazoid MBs (cells:MBs were 1:1) at Low US (74 mW/cm^2), Medium US (501 mW/cm^2) or High US (2079 mW/cm^2) for 10 min. Control cells were not sonoporated but treated with MBs (**Figure 14**). Cell lysates were analysed by WB to evaluate the relative protein expression using 26.7 µg protein/well. p38 was increasingly phosphorylated with increasing US intensity in samples with MBs harvested 5 min post sonoporation and in the control (Ctr.) and high US intensity (2079 mW/cm2). 2h post sonoporation p38 had an increase in phosphorylation in samples with MBs only. Phosphorylation of ERK 1/2 was increased both with and without MBs 5 min post US, but a lower phosphorylation after 2h incubation (**Figure 15**). No phosphorylation of eIF2α was seen 5 min post sonoporation but increasing phosphorylation with increasing US intensity after 2h with MBs was observed. S6 was phosphorylated in all samples. STAT3 (Tyr705) was not phosphorylated 5 min post sonoporation, however, some phosphorylation in the Ctr. and Low US intensity (74 mW/cm^2) 2h post sonoporation. STAT3 (Ser727), however, was phosphorylated in all samples. SAPK/JNK was not phosphorylated after 5 min but JNK was phosphorylated after 2h (**Figure 15**).

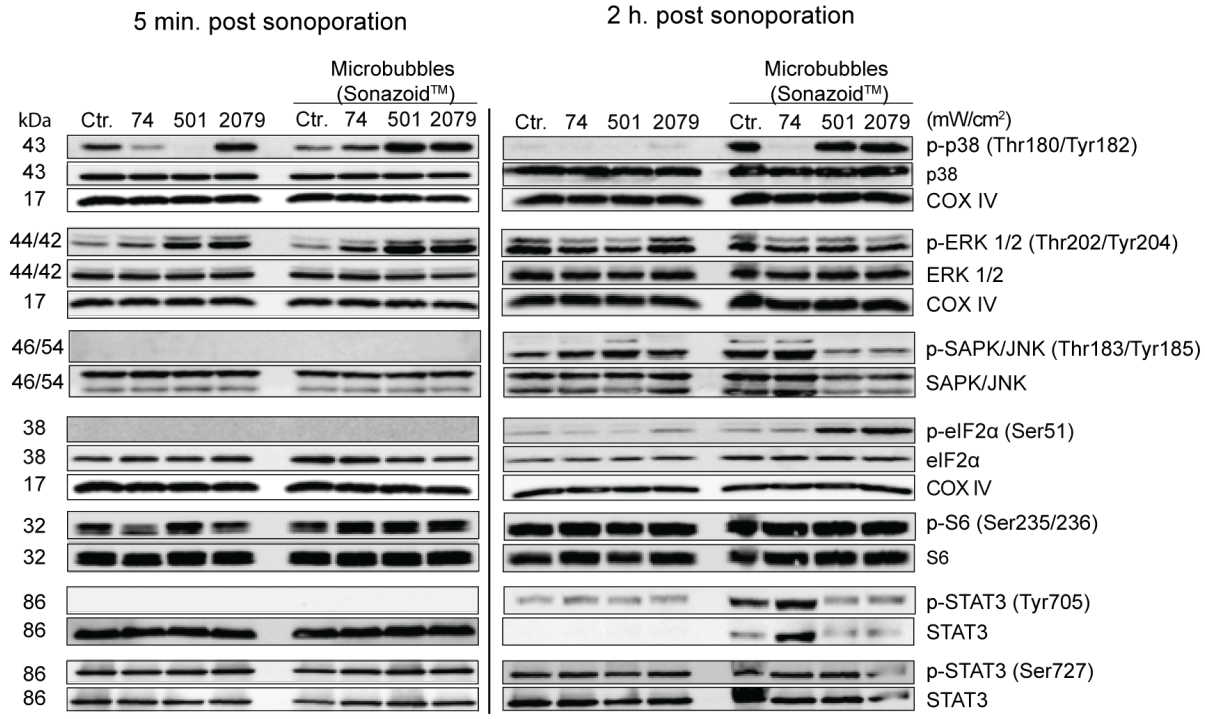

Figure 15: Western blot of sonoporated MOLM–13 cells. MOLM–13 cells (0.4×10^6/mL) were sonoporated with or without Sonazoid microbubbles (cells:MBs were 1:1) at Low ultrasound (US; 74mW/cm^2), Medium US (501mW/cm^2) or High US (2079mW/cm^2) for 10 min Control was not sonoporated. Cell lysates were analysed by western blot to evaluate the relative protein expression using 30.0 µg protein/well. p38 was increasingly phosphorylated with increasing US intensity in samples with MBs harvested 5 min post sonoporation and in the control (Ctr.) and high US intensity (2079 mW/cm^2). 2h post sonoporation p38 had an increase in phosphorylation in samples with MBs only. ERK 1/2had increasing phosphorylation with and without MBs 5 min post sonoporation but had a weaker signal after 2h incubation. SAPK/JNK was only phosphorylated after 2h. eIF2α was not phosphorylated 5 min post sonoporation but were increasingly phosphorylated with increasing US intensity after 2h with MBs. S6 was phosphorylated in all samples. STAT3 (Tyr705) was not phosphorylated 5 min post sonoporation, however, weakly phosphorylated Ctr. and Low US intensity (74 mW/cm^2) 2h post sonoporation. STAT3 (Ser727), however, was phosphorylated in all samples.

4.2 Results Pancreatic cell lines

4.2.1 Optimisation of cell lysis

To be able to plan how many WBs could be performed from one experiment using Petakas the protein lysates from 1×10^6 MIA PaCa–2, PANC–1 and BxPC–3 cells using 50 µl RIPA buffer according to WB protocol (**chapter 3.7**) and quantified using DC™ Protein Assay Kit as per protein quantification protocol (chapter 3.8.0). MIA PaCa–2 (*n=3*) and PANC–1 (*n=3*) had a mean protein concentration of 2.774 µg/µl and 3.495 µg/µl, respectively. BxPC–3 had a protein concentration of 2.208 µg/µl (*n=1*) (**Table 4**). This resulted in 4, 5 and 3 WBs for MIA PaCa–2, PANC–1 and BxPC–3, respectively, using 30 µg/well. When using 40 µg/well the result was 3, 4 and 2 for MIA PaCa–2, PANC–1 and BxPC–3, respectively (**Table 4**).

Table 4: Quantification of 1×10^6 cells lysed in 50 µl RIPA buffer

Cell line	Protein concentration. (µg/µl)	# of western blots with 30 µg/well	# of western blots with 40 µg/well
MIA PaCa–2 (*n=3*)	2.774	4	3
PANC–1 (*n=3*)	3.495	5	4
BxPC–3 (*n=1*)	2.208	3	2

4.2.2 Viability optimisation MIA PaCa-2

4.2.2.1 WST-1 - Cell number and incubation time for MIA PaCa-2

In order to determine the optimal number of cells to seed, and the optimal incubation time for WST–1 assay following US treatment of MIA PaCa–2 cells a test was performed (**Figure 16**). The absorption increased with increasing cell number seeded, as expected. The cells incubated for 1h peaked at 1.6×10^4 cells seeded and then the curve plateaued. Cells incubated for 2hours had a steady increase in absorbance with increasing cell number seeded and at 6.4×10^4 cells the absorbance increased markedly. The cells incubated for 4h increased steadily with increasing cell number seeded (**Figure 16**).

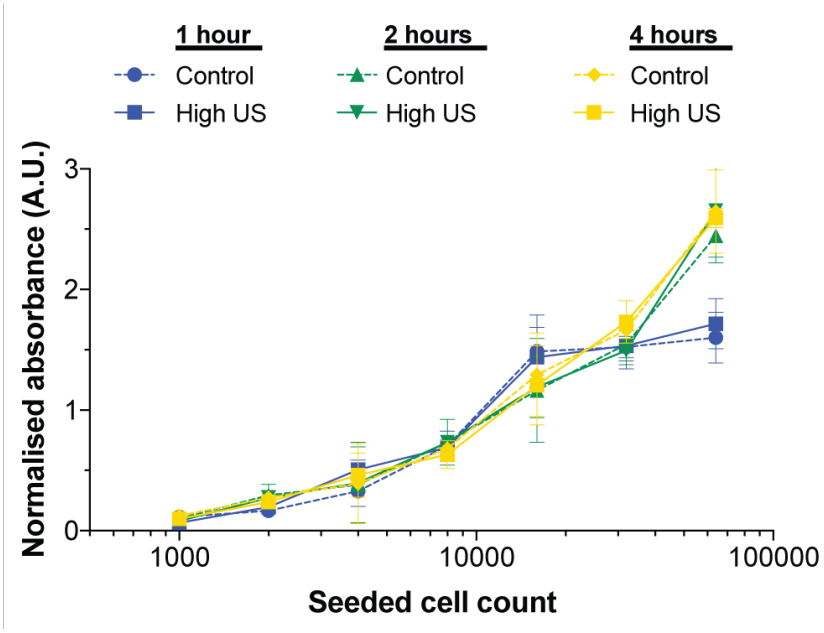

Figure 16: Optimisation of cell number seeded and incubation time for WST–1 for MIA PaCa–2 in Petaka. Metabolic activity evaluated in sonoporated (358 mW/cm^2 for 5 min) MIA PaCa–2, cultivated in Petakas, by WST–1–bases assay. Untreated cells were used as control. Different cell numbers (between 1×10^4 and 6.4×10^4; duplicates). Absorbance read 1h, 2h and 4h following sonoporation. Results analysed in Graph Pad Prism (GraphPad Software, La Jolla, CA, USA).

4.2.2.2 Viability test of MIA PaCa-2 in Petakas

To determine the optimal conditions for viability assays for MIA PaCa-2 cells treated with US in Petakas a test was performed. Treatment and procedure for viability assays (Trypan blue, Hoechst 33342 and WST-1) are described in **chapter 3.3.3.2.** The trypan blue resulted in no trypan blue stained cells (data not shown).

A significant difference was found between the serum–starved cells and the control, and between the serum–starved cells and cells treated with High US (**Figure 17B**). The control and the cells treated with High US had a similar absorbance (**Figure 17B**).) The decreased metabolic activity seen in serum–starved cells, compared to the control, was expected. The cell density used for WST-1 (3.2×10^3 cells) was therefore used in further assays. For the Hoechst assay, the cells were too densely seeded for semi-automated counting. The software (Fijii) used to count the cells were unable to distinguish between single cells for the Control and cells treated with High US. The serum–starved cells, however, could be been quantified by this method (**Figure 17B)**.

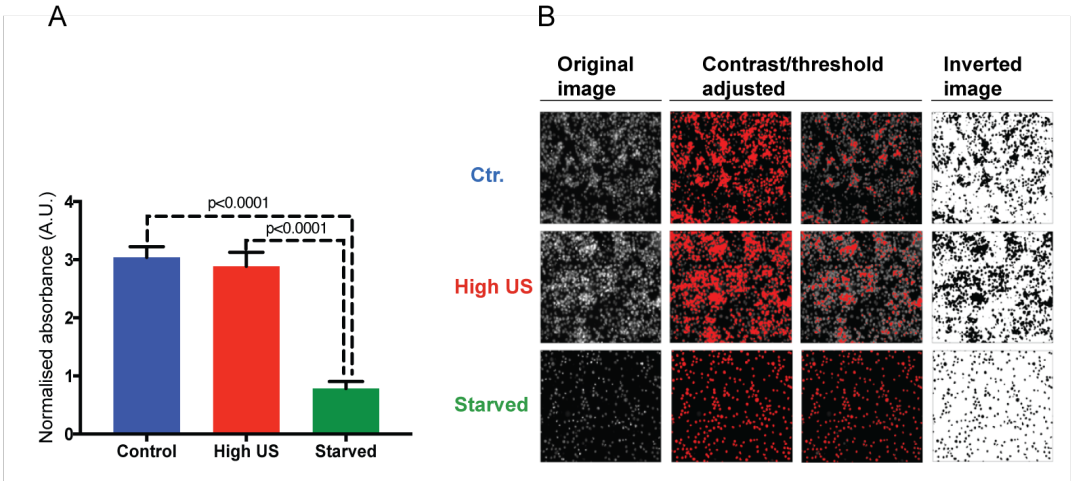

Figure 17: Viability test for MIA PaCa–2. WST–1 analysis (A). Hoechst analysis (B). MIA PaCa–2 were incubated (5% CO_2, 37˚C) in Petakas for 24h Serum supplemented medium was replaced in one Petaka (Starved) with serum–free medium and all Petakas were incubated further 24h One Petaka was treated with ultrasound (US) at 358 mW/cm^2 (High US). Untreated cells were kept as control (Control). 3.2×104 cells/100 µl/well were seeded (triplicates) in a 96–well plate for WST–1 and Hoechst and incubated for 24h 10 µl WST–1 reagent/well (1:10 dilution) was added and absorbance read after 2h on an ELISA plate reader (Spectra Max Plus 384) at 450 nm and 620 nm. (A). Cells were fixed with 100 µl Hoechst reagent/well. Images captured with an inverted Axiovert fluorescent microscope (Carl Zeiss Microscopy GmbH, Göttingen, Germany) (B).

The Hoechst test was repeated seeding 0.8×10^4 and 1.6×10^4 (triplicates) with untreated MIA PaCa–2 cells. The seeding density was evaluated by light microscopy and not by the software due to poor image quality. It was determined that 1.6×10^4 cells/well was satisfactory for further sonoporation studies (**Figure 18**).

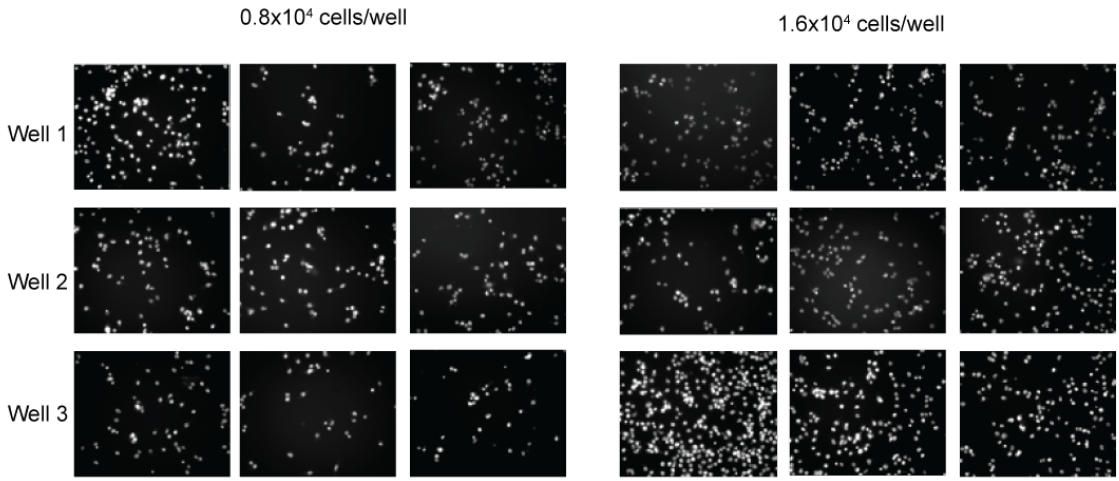

Figure 18: Hoechst seeding test. 100 µl untreated MIA PaCa–2 cells (0.8×10^4 cells/well and 1.6×10^4 cells/well) were seeded (triplicates) in a 96–well plate and fixed with 100 µl Hoechst reagent (1:1 dilution). Images captured with an inverted Axiovert fluorescent microscope (Carl Zeiss Microscopy GmbH, Göttingen, Germany). The seeding density at 1.6×10^4 cells/well, evaluated visually, was determined to be satisfactory for further studies with MIA PaCa–2.

4.2.4 Optimisation of growth rate for MIA PaCa–2 in Petaka

To determine the optimal seeding cell density and incubation time before cell treatment the growth rate of 1×10^6 MIA PaCa–2 cells seeded in Petakas, compared to 1×10^6 cells growth in regular cell culture flasks, was investigated (*n=3*). The Petakas and flasks were monitored by microscope and imaged daily for five days from 24h after seeding. The growth rate was determined by mean cell count per surface area. The cells cultured in Petakas experienced log–phase growth between 48 h and 72h reaching a maximum confluency at approximately 60% and the cell growth plateaued after 72h (**Figure 19A**). In T75 flasks the cells experienced log–phase growth between 48 h and 96 h and reached a maximum confluency at approximately 85% confluency and cell growth plateaued after 120 h (**Figure 19B**).

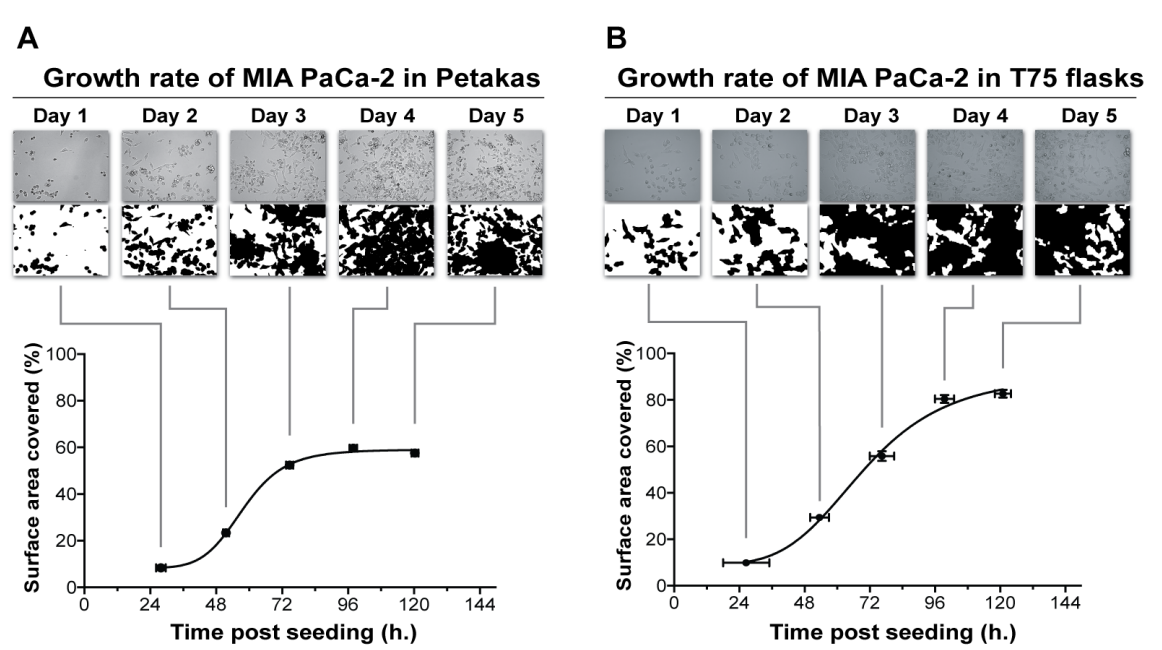

Figure 19: Estimation of MIA PaCa–2 growth rate by mean cell count per surface area – visual representation. MIA PaCa–2 cells, seeded in Petkas and T75 cell culture flasks (75cm^2) were imaged for five consecutive days starting 24h after seeding. The growth rate was estimated by mean cell count per surface area (50 images/petaka/flask; *n=3*).

Figure 20 displays the same growth rate in single Petakas (**Figure 20A**) and flasks (**Figure 20B**). Only minor discrepancies occurred between Petakas and between the flasks.

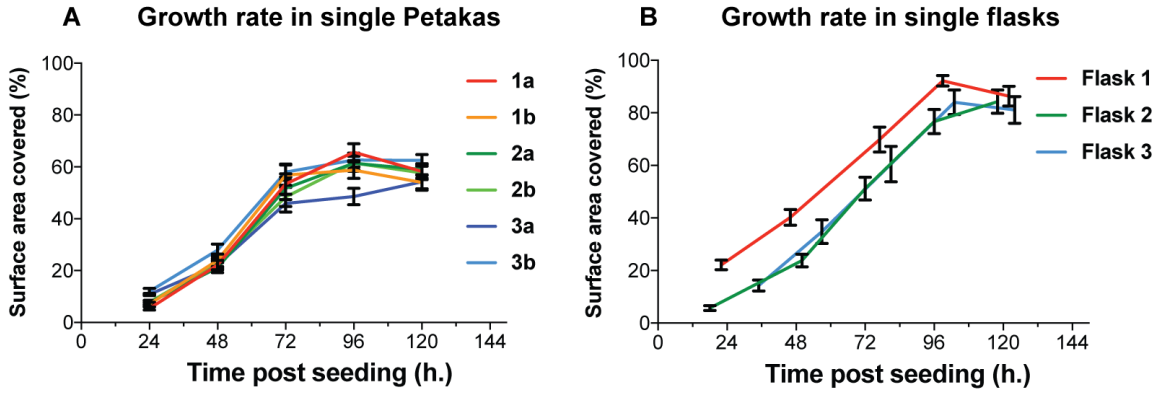

Figure 20: Estimation of MIA PaCa–2 growth rate by mean cell count per surface area. MIA PaCa–2 cells, seeded in Petkas (1a – 3b) and T75 cell culture flasks (Flask 1 – 3) were imaged for five consecutive days starting 24h after seeding. The growth rate was estimated by mean cell count per surface area (50 images/petaka/flask; *n=3*). Mean growth in single cells was uniform, with a slight deviation in Petaka 3a (A). Mean growth in flask was uniform, however flask 1 was seeded with more cells than expected (B).

4.2.5 Optimisation of timing of cell detachment with cold 1× trypsin and 10× trypsin

To optimise planning of sonoporation studies a test was performed to determine the time it takes for the cells (untreated) to detach from the flask using ice–cold 1× trypsin and 10× trypsin. A description of the process can be found in **chapter 3.6.3.1.** With 1× trypsin MIA PaCa–2, PANC–1 and BxPC–3 took 30 min, 70 min and 2h 45 min, respectively (**Table 5**).

Table 5: Timing of cell detachment with ice–cold 1× trypsin.

Cell line	± time to detach cells
MIA PaCa–2	30 min
PANC–1	70 min
BxPC–3	2h 45 min

With 10× trypsin MIA PaCa–2, PANC–1 and BxPC–3 took 7 min, 21 min and 22 min, respectively (**Table 6**).

Table 6: Timing of cell detachment with ice–cold 10× trypsin.

Cell line	± time to detach cells
MIA PaCa–2	7 min
PANC–1	21 min
BxPC–3	22 min

4.2.6 Optimisation of cell detachment–western blot

MIA PaCa–2 cells were stimulated with A23187 (1μM) + PMA (0.1μM) for 30 min to induce phosphorylation. Lysates for WB were prepared according to **chapter 3.7** and 30 μg, 40 μ g and 50 μg protein extract was used to evaluate the protein level and phosphorylation status of the MAPK p38 (**Figure 21**). With 30 μg the signal was very weak prompting the need to use long exposure time with SuperSignal™ West Femto Maximum Sensitivity Substrate to develop the membrane as SuperSignal™ West Pico did not produce a signal (**Figure 21**). With 40 μg and 50 μg protein there was a clear difference in phosphorylation status of p38 in the stimulated sample between the different detachment methods (**Figure 21**). No phosphorylation was detected in the stimulated samples detached with pre–heated trypsin or by scraping. In further WBs 40 μg protein was used per well for MIA PaCa–2 cells.

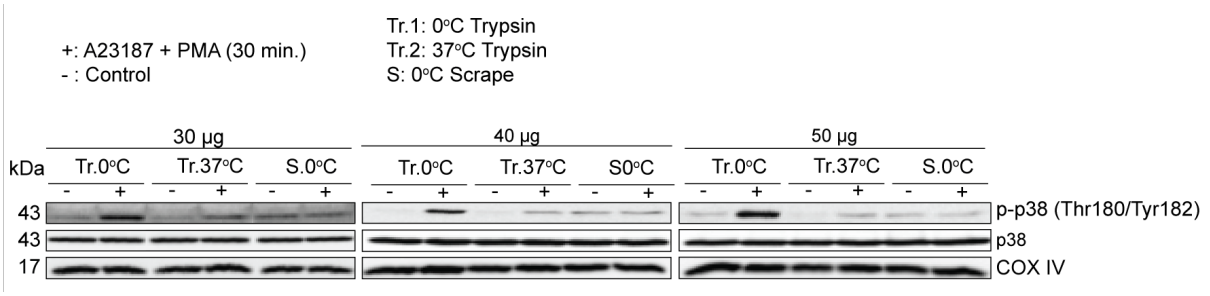

Figure 21: Western blot of cell detachment by cold (4°C) and warm (37°C) 1× trypsinization vs. scraping. MIA PaCa–2 cells were treated with A23187 (1µM) + PMA (0.1µM for 30 min (+). Untreated cells were kept as control (–). Cells were detached by cold 1× trypsin (4°C), warm trypsin (37°C) or by scraping. COX IV was used as a loading control. Western blot analysis of p38 shows a weak phosphorylation using 30 µg, while samples loaded with 40 µg and 50 µg shows a clear activation in the samples detached with ice–cold 1× trypsin.

4.2.7 Optimisation of cell detachment with 10× trypsin –Viability

In order to determine whether detaching cells with 10× trypsin affected cell viability trypan blue count (cell count), Hoechst 33342 (apoptosis) and WST–1 (metabolic) assay were performed as per **chapter 3.6.3.3**. Trypan blue stained cells counted within 5 min of detachment with 10× trypsin did not result in cell death (**Figure 22A**). Of the Hoechst stained cells, there was no difference in percent apoptosis occurring between the cell lines (**Figure 22B**). The assessment of metabolic activity in live cells by WST–1 showed a relative very low absorbance of MIA PaCa–2 cells, but the absorbance of PANC–1 and BxPC–3 was similar (**Figure 22C**).

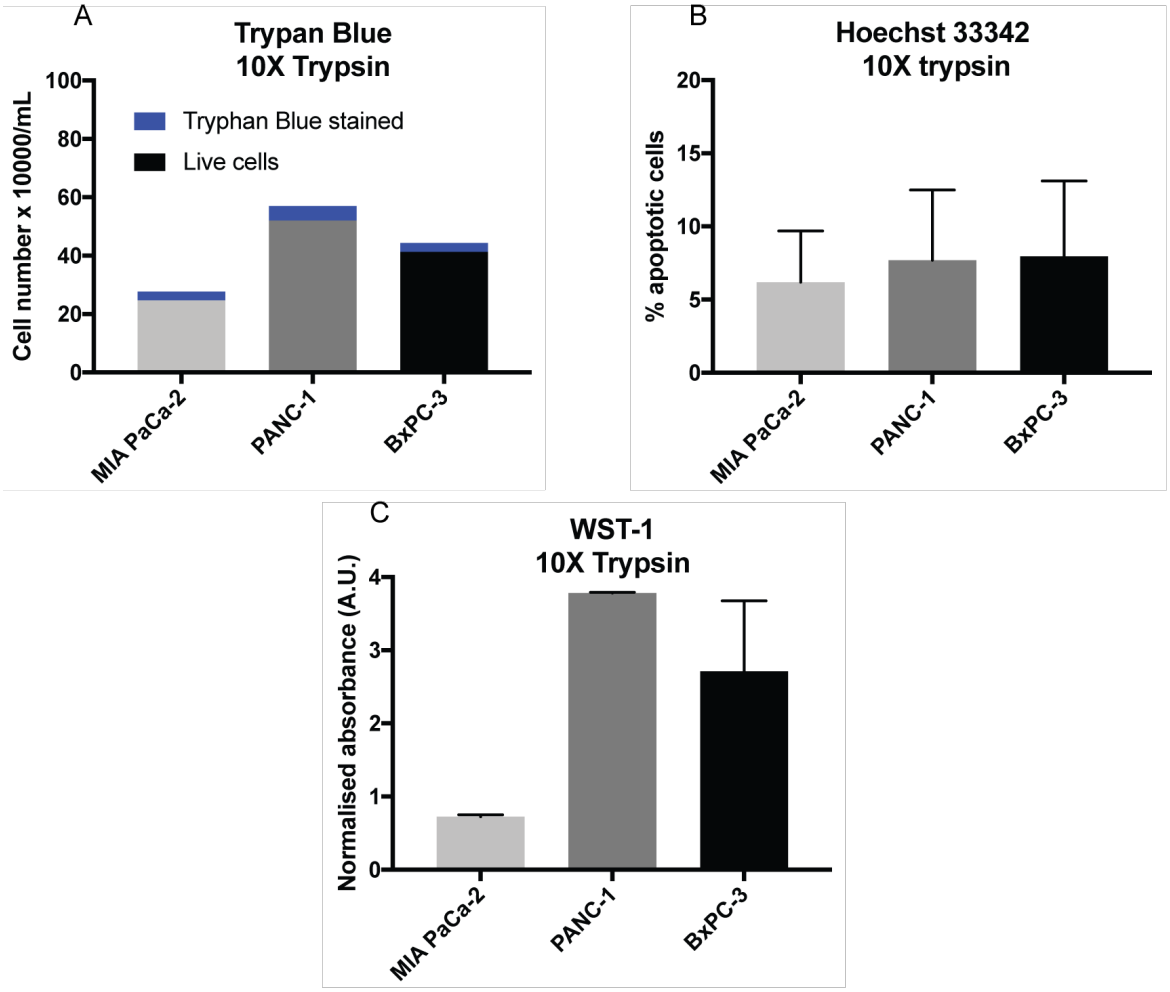

Figure 22: 10× trypsin test – trypan blue, Hoechst 33342 and WST–1 assessment. MIA PaCa–2, PANC–1 and BxPC–3 were stimulated with A23187 (1µM) + Phorbol 12–myristate 13–acetate (PMA) (0.1µM) for 30 min and detached by cold 10× trypsinization. Cells stained with trypan blue (cells: trypan blue was 1:1) were counted within 5 min of detachment, while cells for Hoechst and WST–1 were incubated for 24h (37°C, 5% CO_2) before adding Hoechst (1:1) and WST–1 (1:10). Hoechst images were captured using a 5×/0.6NA 20× objective coupled to an inverted Axiovert microscope (Carl Zeiss Microscopy GmbH, Göttingen, Germany) using Zen Pro software (Carl Zeiss Microscopy GmbH, Göttingen, Germany). Image exposure time was set to 32.991 ms, and the light source (DAPI) was set to max. The images were analysed in Fiji software (ImageJ) and figures made in Graph Pad Prism (GraphPad Software, La Jolla, CA, USA). Absorbance of WST–1 stained cells were read after 2h on a plate reader (Spectra Max Plus 384) at 450 nm and 620 nm. The results were analysed in Microsoft Excel (Microsoft Office 2018) and figures made in Graph Pad Prism (GraphPad Software, La Jolla, CA, USA).

4.2.8 Optimisation of cell detachment with 10× trypsin – Western blot

Since cell signalling is essential in this project, the relative phosphorylation status of selected proteins was analysed in MIA PaCa–2, PANC–1 and BxPC-3 by WB as described in chapter 3.6.3.3. ERK 1/2 was strongly phosphorylated in stimulated MIA PaCa–2 and PANC–1 samples, while BxPC–3 had a relative weaker phosphorylation in the stimulated samples (**Figure 23**). p38 was only phosphorylated in stimulated BxPC–3 cells and SAPK/JNK was

only phosphorylated in PANC–1. MLC was not phosphorylated in any cell lines and MLC lacked total MLC protein (**Figure 22**).

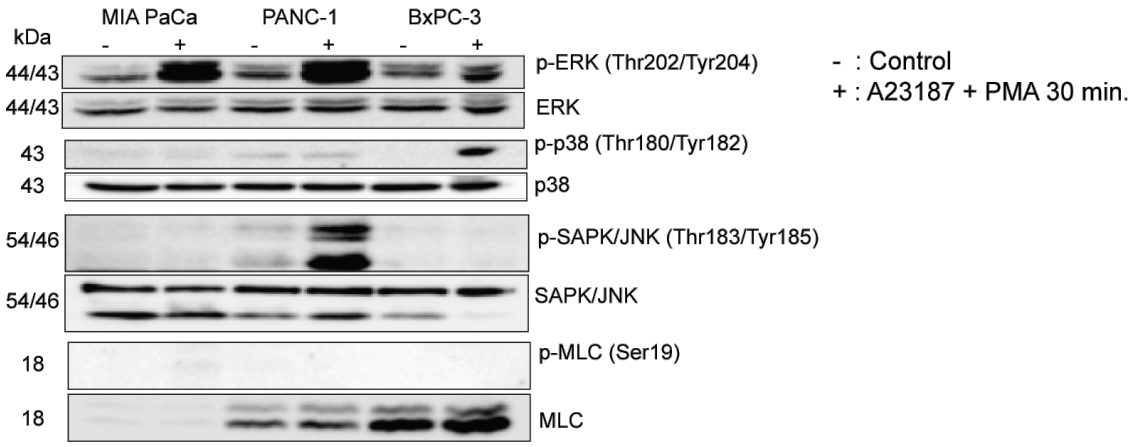

Figure 23: Western blot of cell detachment by 10× trypsin with three pancreatic cell lines. MIA PaCa–2, PANC–1 and BxPC–3 cells were treated with A23187 (1μM) + Phorbol 12–myristate 13–acetate (PMA) (0.1μM) for 30 min (+). Untreated cells were kept as control (–). ERK 1/2 was strongly phosphorylated in the treated MIA PaCa–2 and PANC–1 samples and a weak activation in BxPC–3. MLC was not phosphorylated in any cell line and total MLC appears absent in MIA PaCa–2. p38 was weakly phosphorylated in stimulated BxPC–3 cells, and SAPK/JNK was phosphorylated in stimulated PANC–1 cells.

4.2.9 Optimisation of western blotting

To determine the presence and phosphorylation status of chosen signalling proteins in MIA PaCa–2 the cells were stimulated with various chemicals, known as positive controls (**Figure 24**). The test was also to ascertain whether the antibodies corresponding to chosen proteins worked in MIA PaCa–2 cells. WB was performed with 40 μg protein extract. ERK 1/2 was stimulated (phosphorylated) by all stimuli but was markedly stimulated by A23187+PMA (**Figure 24**). SAPK/JNK resulted with phosphorylation in the control only, while p38 was phosphorylated by TNFα. eIF2α was phosphorylated in both the control and stimulated sample (A23187). Both MUPT1 epitopes (Ser853/Ser696) were phosphorylated in both the control and stimulated sample (A23187) (**Figure 24**). All tested antibodies worked, although some antibodies require SuperSignal^{TM} West Femto Maximum Sensitivity Substrate for development of the membranes due to weak signal.

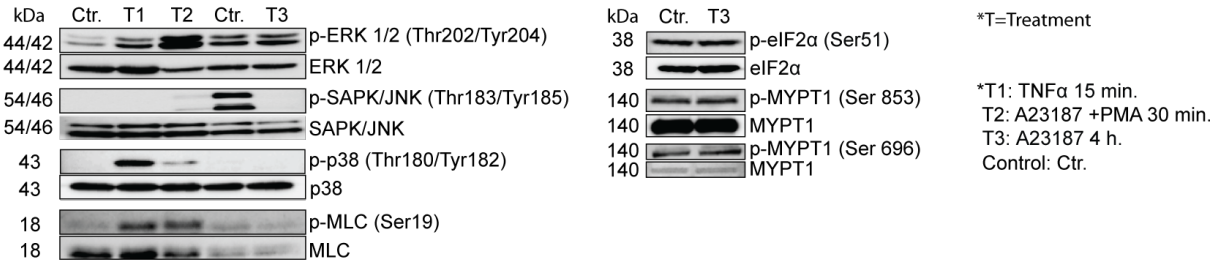

Figure 24: Validation of antibodies for sonoporation studies with MIA PaCa–2 – Western blot. MIA PaCa–2 cells were treated with Tumour necrosis factor (TNFα; 15 min; T1), A23187 + Phorbol 12–myristate 13–acetate (PMA; 30 min; T2), or A23187; 4h; T3). 40 µg protein was used for western blot. ERK 1/2 was stimulated (phosphorylated) by all stimuli but was markedly stimulated by A23187+PMA. SAPK/JNK was phosphorylated in the control only, while p38 was phosphorylated by TNFα. eIF2α was phosphorylated in the control and stimulated sample (A23187). MYPT1 (Ser853/ Ser696) was phosphorylated both in the control and stimulated sample (A23187).

4.2.10 Optimisation of incubation time following sonoporation

To determine the optimal incubation time to detect cell signalling in MIA PaCa–2 cells, following sonoporation in Petaka, a test was performed. The process is described in **chapter 3.6.4**. ERK 1/2had a time-dependent increase in phosphorylation, peaking at 1h, while MLC showed no phosphorylation before 2h, where the signal was strong (**Figure 25**). eIF2α had a time–dependent steady increase in phosphorylation (**Figure 25**). Based on these results it was determined to proceed with 2h incubation time for further sonoporation studies of MIA PaCa–2.

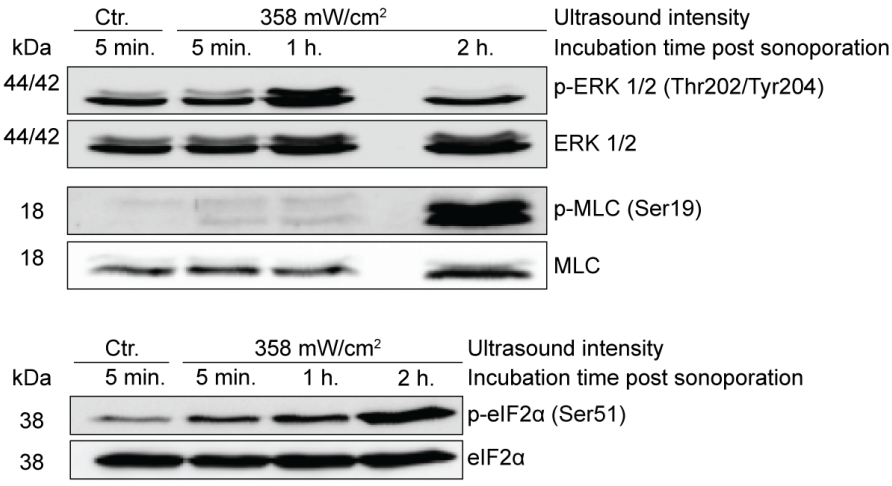

Figure 25: Western blot of test of incubation time post sonoporation of MIA PaCa–2. Cells were sonoporated at 358 mW/cm^2 with Sonazoid MBs (5.6 µL/mL). for 5 min and incubated (5% CO_2 at 37˚C) for 5 min, 1h or 2h. Control was not sonoporated. ERK 1/2had a time-dependent increase in phosphorylation, peaking at 1h, while MLC showed no phosphorylation before 2h, where the signal was strong. eIF2α had a time–dependent steady increase in phosphorylation.

4.3 Sonoporation of MIA PaCa–2 cells

4.3.1 Viability sonoporated MIA PaCa–2

MIA PaCa–2 cells were treated with three different US conditions with and without Sonazoid MBs as described in **chapter 3.6.6.** The cells treated with US only differed in total cell count, of which the Low US sample had a higher cell count, and none of the samples had a significant number of trypan blue stained cells (**Figure 26A**). Of the samples treated with US and MBs the total cell count was again higher for Low US compared the other samples, and here more cells were stained by trypan blue (**Figure 26B**). The Hoechst assay showed that in cells treated with US only (– MBs) the Low and Medium US samples had a higher percentage apoptotic cells, compared to the control, while High US had less than half the percentage of apoptotic cells (**Figure 26C**). Of the Hoechst stained cells treated with US and MBs the control had the most apoptotic cells and the treated samples varied in the percentage of apoptotic cells (**Figure 26D**). The WST–1 metabolic assay showed that in cells only treated with US (– MBs) the control had a very low absorbance compared to the treated samples, which had a decreasing absorbance with increasing US intensity (**Figure 26E**). The absorbance of the samples treated with US and MBs was very similar, with a slight increase in Medium and High US (**Figure 26F**).

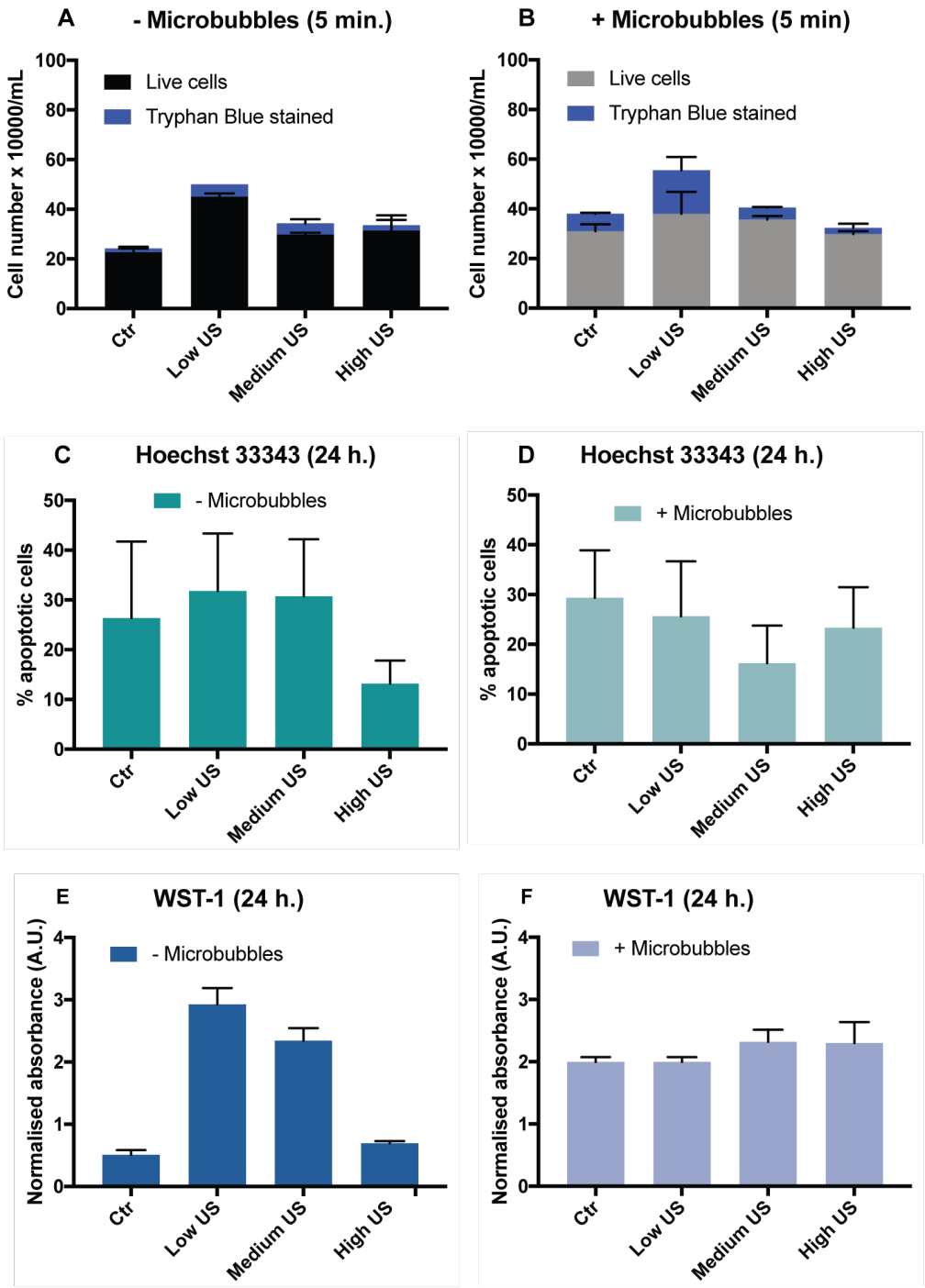

Figure 26: Viability assays of sonoporated MIA PaCa–2 cells. MIA PaCa–2 cells, cultured in Petaka 3G bioreactors, were sonoporated at Low (3mW/cm^2), Medium (50mW/cm^2) and High (358mW/cm^2) ultrasound (US) with/without Sonazoid MBs (5.6 µL/mL) and incubated at 37°C 5% CO2 for 2h after sonoporation. Cells were detached by ice–cold 1× trypsin. Trypan blue count performed immediately after detachment, while cells for Hoechst and WST–1 were incubated for 24h (37°C, 5% CO_2) before adding Hoechst (1:1) and WST–1 (1:10). Images were captured using a 5×/0.6NA 20× objective coupled to an inverted Axiovert microscope (Carl Zeiss Microscopy GmbH, Göttingen, Germany) using Zen Pro software (Carl Zeiss Microscopy GmbH, Göttingen, Germany). Image exposure time was set to 32.991 ms, and the light source (DAPI) was set to max. The images were analysed in Fijii software (ImageJ) and figures made in Graph Pad Prism (GraphPad Software, La Jolla, CA, USA). Cells for WST–1 were incubated for 2h before reading the absorption on a plate reader (Spectra Max Plus 384) at 450 nm and 620 nm.

4.3.2 Western blot sonoporated MIA PaCa–2

MIA PaCa–2 cells were treated with three different US conditions with and without Sonazoid MBs as described in **chapter 3.6.6.** ERK 1/2 was weakly phosphorylated without MBs and showed a stronger phosphorylation with increasing US intensity with MBs (**Figure 27**). p38 was only weakly phosphorylated at High US with MBs and SAPK/JNK was not phosphorylated in any samples. eIF2a and STAT3 were phosphorylated in all samples, which show that these are constitutively active in these cells. For eIF2α this was also seen during optimisation of western blot (previous section). S6 showed an increase in phosphorylation at higher US intensities. MLC was weakly phosphorylated without MBs and a clear increase at High US with MBs. No phosphorylation was observed for both MYPT1 (Ser853) and MYPT1 (Ser696) (**Figure 27**).

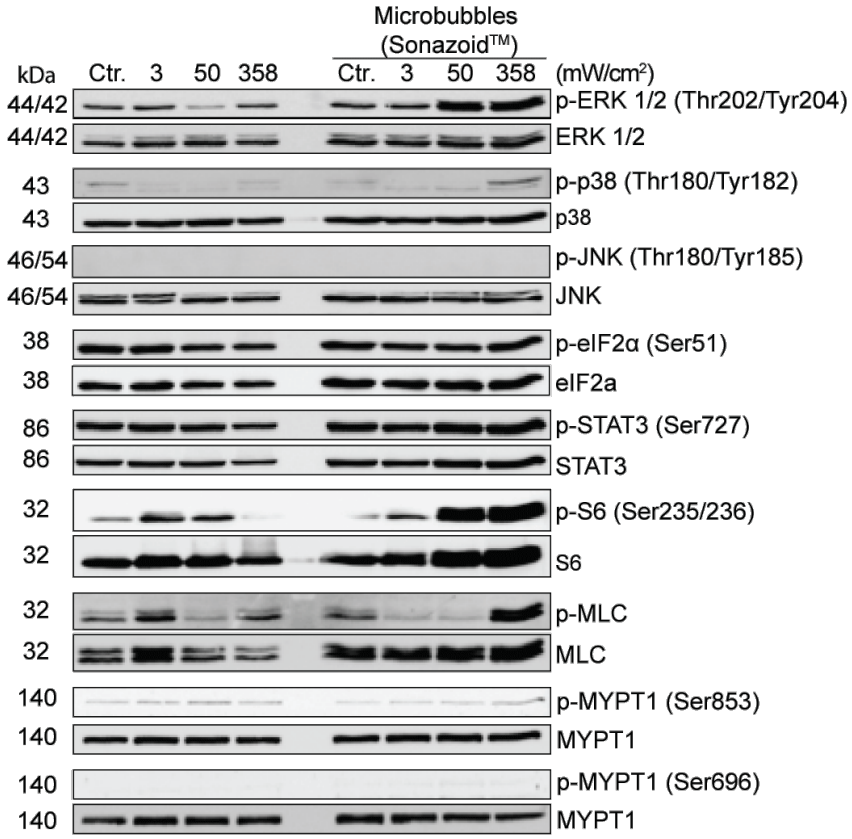

Figure 26: Western blot analysis of sonoporated MIA PaCa–2 cells. MIA PaCa–2 cells, cultured in Petaka 3G bioreactors, were sonoporated at Low (3 mW/cm^2), Medium (50 mW/cm^2) and High (358 mW/cm^2) ultrasound (US) with and without Sonazoid MBs (5.6 μL/mL), incubated at 37^{o}C 5% CO_2 for 2h following sonoporation. Cells were detached by ice–cold 1× trypsin. ERK 1/2 was weakly phosphorylated without MBs and had a stronger phosphorylation with increasing US intensity with MBs. p38 had only a weak signal at High US with MBs and SAPK/JNK was not activated in any samples. eIF2a and STAT3 were phosphorylated in all samples, while S6 showed an increase in phosphorylation at higher US intensities. MLC had a weak phosphorylation without MBs and a clear increase in phosphorylation at High US with MBs. MYPT1(Ser853) had a weak activation, while MYPT1(Ser696) was not phosphorylated.

5.0 Discussion

The mechanisms and biological effects of sonoporation are well studied (27-29), however there is insufficient data on the intracellular effects of sonoporation. Cell signalling induced by sonoporation has been investigated previously in suspension cells, such as in leukemia cell lines (20, 30, 31), but in pancreatic cell lines there is little research into the intracellular effects of sonoporation.

This project addresses this gap in current research, namely investigating signalling proteins and pathways affected by sonoporation in pancreatic cell lines, aiming to identify biomarkers for PDAC that ca be used to optimise sonoporation therapy. An important part of this investigation is *in vitro* optimisation of sonoporation. Numerous of parameters had to be optimised before continuing to sonoporation of pancreatic cell lines. Studying sonoporation in adherent cell lines, such as pancreatic cell lines, entails different conditions that can affect the outcome, for example detaching the cells from the flask to be able to analyze them. Therefore, the initial investigation of intracellular effects induced by sonoporation was performed with the leukemic cell line MOLM–13. With previous results to refer to (20), it was possible to optimise treatment parameters, as well as getting an indication of which signalling pathways were induced by sonoporation. Clearly, there was no guarantee that the same pathways would be induced in pancreatic cell lines, nevertheless, it was a good starting point. Also, since the custom–built US technology we used to treat adherent cell lined was not yet available at the beginning of the project, it was natural to start with the suspension cell line MOLM–13 as a model system. For suspension cells there was an US machine (also custom–made) available.

5.1 Choice of signalling pathways

There are almost endless signalling proteins and pathways to choose from when studying cell signalling. The choice is slightly narrowed by one of the objectives of this current project, which was to identify biomarkers to identify a successfully sonoporated cell that ca be used to optimise sonoporation therapy. Thus, signalling proteins involved in cellular stress response, the induction of apoptosis and survival are interesting. As a starting–point, signalling proteins known to have been induced by sonoporation in previous studies were investigated. These include the MAPK proteins ERK 1/2, p38 (24), and SAPK/JNK and the molecular switch for global protein translation eIF2α (31). In studies of adherent pancreatic cell lines proteins involved in adherence and migration is interesting, such as STAT3 (migration/invasion) (40) and MLC2 and MYPT, which are part of the Rho/ROCK pathway that mediates

cytoskeletal reprogramming during invasion and metastasis (48). Ribosomal protein S6 is downstream of the PI3K–mTOR pathway which has cross-talk with the UPR (**Figure 7**). ER–stress, which activates the UPR, has been shown to be induced by sonoporation (31), and was therefore included in this current investigation.

5.2 MOLM–13

MOLM–13 cells were treated with three US intensities and MBs (sonoporated). Cells were also treated with US alone to evaluate its effect on the cells. Protein were extracted for WB analysis of chosen signalling proteins. Three different viability assays, trypan blue, Hoechst 33342 and WST–1, were considered as an assessment of cell viability following sonoporation. COX IV was used as a loading control. The protocol is described in detail in chapter **3.5.1. – 3.5.3.**

5.2.1 Trypan blue

The first viability assay, trypan blue, is a DNA–binding dye that only stains dying and apoptotic cells (72). For MOLM-13 trypan blue was used for total cell count following treatment, as well as an assessment of the number of dead cells. Trypan blue was employed both immediately following treatment and after 24h to assess whether the treatment had affected the cells ability to proliferate (measured by change in cell concentration). Cell death can also be assessed by a range of other methods. However, the trypan blue assay provides immediate information on cell concentration and can be used to measure change in cell proliferation. Furthermore, it is a quick way to evaluate cell death. Therefore, it was decided to employ trypan blue for sonoporation studies in both MOLM–13 and pancreatic cell lines.

5.2.2hoechst 33342

The second viability assay used in this project, Hoechst 33342, is also a fluorescent DNA–binding dye. Hoechst not only stains apoptotic cells in different stages, early, late apoptotic and necrosis, but also mitotic cells (73). This assay allows for a direct, visual evaluation of cell morphology, compared to trypan blue stain, which only provides a percentage of dead cells in the sample. Hoechst 33342 was included to assess whether cells died by apoptosis. Traditionally, the apoptotic cells are counted manually in the microscope, however, there are many disadvantages using this method. The fluorescent dye fades when exposed to light over time, therefore, if the user takes too long the apoptotic cells may no longer be distinguishable

from the viable cells, and which cells are in fact apoptotic is a subjective evaluation. However, if images are captured this can be documented and the analysis double-checked. Using images, it was possible to get a more accurate result, compared to manual counting. The method is not perfect, however, also here, the program may not be able to identify all cells, or to distinguish two adjacent cells from each other if they are too close. Adjustments are made manually to correct for contrast to enable the software to identify each cell as a dot, then, the dots are counted by the software. Consequently, resuspension of the cells immediately before seeding, and seeding density, is very important using this semi–automated method. With too many clustered and overlapping cells the software will be unable to identify single cells for total cell count. Furthermore, the identification of apoptotic cells is also here a subjective evaluation by the user, however, the advantage of having images stored for analysis at a later time–point enables the user to take his/her time to do the analysis properly. Furthermore, it is important to be able to identify the different stages of apoptosis and to be able to distinguish apoptotic cells from mitotic cells, which also are stained by Hoechst.

5.2.3 WST–1 assay

A third viability assay was considered for MOLM–13 studies, namely the WST–1 based metabolic assay, which provides an estimation of number of cells and of metabolically active cells in a treated sample. Here, the cells that survive the treatment are evaluated, as opposed to assessing cell death. The WST–1 salt changes colour when metabolised by the cells and the absorbance of light passing through the sample is measured. Resuspension of the cells and seeding density are important in this assay as well. If the cells are seeded too densely the results may be false because the reaction is saturated (WST–1 reagent is metabolised) before the absorbance is read. Additionally, it is important that all samples have the same seeding density. Therefore, a test was performed where different cell concentrations (between 0.5×10^6 and 1.0×10^6) of MOLM–13 cells (untreated) were seeded and subject to the WST–1 assay. At 0.8×10^6cells (**Figure 13**) the reaction is saturated, and the curve flattens. This cell concentration is interesting due to the experimental setup of sonoporation of MOLM–13 cells. In order to have enough cells to make sufficient lysate for WB analysis, 0.41×10^6 cells/mL were used in the sonoporation experiment with MOLM–13. For experiments the cells are seeded when they are in log–phase, and during the 24h incubation period following treatment cell number may double, and then, according to these results, the WST–1 reagent is saturated by too many cells (**Figure 13**). In addition, the absorbance was low. Therefore, it was

determined to not use this assay for MOLM–13 studies. Nevertheless, cell viability of MOLM–13 cells were evaluated by trypan blue count and Hoechst 33342.

5.2.4 Sonoporated MOLM-13 – Western blot and viability

The treated MOLM–13 cells were also analysed by western bot where the relative phosphorylation status of selected signalling proteins was evaluated.

5.2.4.1 MAPK pathway

p38, belonging to the MAPKs, was downregulated in Low and Medium US, but upregulated in High US samples without MBs (**Figure 15**). The MAPK are part of a signalling cascade that can be activated by many extracellular signals, stress signals, such as pro–inflammatory cytokines and for example the epidermal growth factor (EGF), which binds to the EGF receptor (EGFR) initiating a signalling cascade that activates the MAPK. However, intracellular signals may also activate the MAPK. There is substantial cross–talk between signalling pathways, and MAPKs are also activated by ER–stress via the UPR (35). The UPR activates p38 via ASK1 and MKK4 (**Figure 7**). One study found that ER–stress proteins were activated by sonoporation (20), and also here, it is possible that p38 is activated by ER–stress via the UPR. After 5 min of sonoporation cells were phosphorylated by High US without MBs, indicating that High US alone has an effect on the cells, and with MBs added the phosphorylation increased with increasing US intensity (**Figure 15**). Analysis of p38 2h after sonoporation showed that with MBs added, however, there was no phosphorylation of p38 without MBs, while the control, Medium and High US samples with MBs were phosphorylated (**Figure 15**). The results suggest that the phosphorylation is induced at higher US intensities with MBs. Importantly, the WB was performed once, which is not sufficient to draw any definite conclusions. Both cell proliferation or cell cycle arrest can be stimulated by the activation of p38, depending on the kinetics of activation and downstream signalling pathways activated (35). In sonoporated cells with MBs at Medium and High US the cell proliferation ability was reduced, and some cell death occurred (**Figure 14**). Cell death, assessed by the percentage apoptotic cells, showed that there was no difference between the treated samples and the control without MBs, indicating that US alone does not have an effect. However, with MBs added there was an increase in percentage apoptotic cells (**Figure 14E**), also reflected in the reduced proliferation ability (**Figure 14D**). With this in mind, these results indicate that p38 may be involved in the reduction of proliferation. p38 also mediates

cell cycle arrest (**Figure 7**), although, this was not investigated in this thesis cell cycle arrest has been shown to be induced by sonoporation (30). The phosphorylation at higher US intensities with MBs indicate activation, which may influence cell cycle arrest. However, the WB analysis of p38 is inconsistent and needs to be confirmed.

ERK 1/2, one of the MAPKs, was increasingly phosphorylated 5 min after sonoporation both without and with MBs, but after 2h the signal decreased (**Figure 15**). ERK 1/2 is activated extracellularly by hormones, integrins and practically all growth factors and intracellularly by the UPR via ER–stress activation (35). ERK 1/2 activation promotes cell proliferation, differentiation and cell survival. However, the fact that proliferation ability was reduced with MBs added (**Figure 14**), may be influenced by any number of other signalling proteins. Though, the increasing ERK 1/2 phosphorylation (**Figure 15)** implies that ERK 1/2 may be induced by sonoporation initiating proliferation and cell survival pathways. The estimation of percentage apoptotic cells showed no difference between treated samples and the control without MBs (**Figure 14E**), consistent with proliferation and survival signals initiated, while the percentage apoptotic cells increased with increasing US intensity with MBs (**Figure 14F**), which is reflected in the reduced ERK 1/2 phosphorylation after 2h (**Figure 15**).

The third MAPK, JNK showed no phosphorylation 5 min after sonoporation, but was phosphorylated after 2h with and without MBs (**Figure 15**). There was no difference between the control and samples, indicating that sonoporation had no effect (**Figure 15)**. JNK, as p38, is activated by pro–inflammatory cytokines, oxidants, ER–stress and other cellular extracellular stresses (35) (**Figure 7**) in addition to the UPR (intracellularly). JNK is phosphorylated by MKK4, which also activates p38, and MKK7 via ASK1. ASK1 is activated by the UPR, or by MEKK1, which is activated by extracellular signals. JNK promotes apoptosis, autophagy, but also cell survival. The fact that JNK was not phosphorylated after 5 min of sonoporation can indicate that it has a delayed response. Cell proliferation, measured by trypan blue, showed that only cells with MBs were affected by the treatment (**Figure 14**). Additionally, the percentage apoptosis, measured by Hoechst 33342, showed the same trend, namely that only cells with added MBs were influenced by the sonoporation. In relation to JNK signalling, no phosphorylation at 5 min and the phosphorylation at 2h may indicate that cell survival signals were activated initially, but after 2h the apoptotic signals had been activated (**Figure 15**). Though, the results need to be confirmed.

5.2.4.2 UPR pathway

The UPR, activated by ER–stress, also activates an important signalling protein called eIF2α, which upon phosphorylation attenuates global protein translation (33). This signalling cascade, depicted in **Figure 6**, starts with the activation of PERK, an ER–stress transmembrane sensor that phosphorylates eIF2α, which leads to an increase in the selective translation of the mRNA encoding for ATF4, a transcription factor that induces the expression of several genes, including apoptosis and autophagy and GADD34. GADD34 works as a negative feedback on eIF2α dephosphorylating it during prolonged ER–stress. In sonoporated MOLM–13 cells no phosphorylation was detected in after 5 min, but after 2h there was a clear increase in phosphorylation with increasing US intensity (**Figure 15**). After 24h the Medium and High US samples with MBs had a reduced proliferation ability, compared to the control, correlating with the increasing phosphorylation of eIF2α after 2h (**Figure 14D)**. This indicates that eIF2α had a delayed activation and global protein translation was downregulated, but also that the UPR was initiated. Activation of PERK, upstream of eIF2α, has been shown to have a delayed response to stress (31), which correlates with the WB analysis of eIF2α above. As for the assessment of percentage apoptosis in relation to eIF2α, the author refers to the above explanation that the activation of the UPR, which has a myriad of downstream signals that affects apoptotic signals. The results, however, needs to be confirmed.

5.2.4.3 PI3K–mTOR pathway

The WB analysis showed that of Ribosomal protein S6 was phosphorylated in all samples, with/without MBs at 5 min and 2h, including the control (**Figure 15**). This suggests that S6 is constitutively active in MOLM-13. As the viability assays (proliferation by trypan blue and apoptosis by Hoechst 33342) indicate, that there was only an evident effect in cells with MBs after 24h of sonoporation (**Figure 14A–F**), suggesting a delayed response not detectable after 2h. Sonoporation has been shown to influence ER-stress (31), therefore, further investigation of the effect sonoporation may have on S6 should include sampling at different time–points after sonoporation to elucidate possible effects. Additionally, the viability assays should be confirmed.

5.2.4.4 JAK/STAT pathway

STAT3 (Tyr705) was not phosphorylated 5 min post sonoporation, however, after 2h the control and Low US intensity (74 mW/cm^2) were weakly phosphorylated (**Figure 15**). The results from 5 min post sonoporation appear credible since STAT3 (total protein) had even loading in all samples. The samples from 2h post sonoporation, however, were unexpected.
Total STAT3 without MBs is absent and with MBs the loading is uneven, thus confirmation of the results is essential. STAT3 is activated by phosphorylation at Tyr705 (74), one of the epitopes tested here, indicating that STAT3 had an immediate downregulation by sonoporation, which returns after 2h (**Figure 15**). This suggests that sonoporation may have an immediate, but brief effect on STAT3 downregulating it, which is interesting since blocking STAT3 has been shown to slow tumour growth (40). Phosphorylated STAT3 (Ser727), which is associated with transcription and cell survival (75), though, was weakly phosphorylated in all samples 5 min post sonoporation (**Figure 15**). After 2h all samples were phosphorylated, indicates that sonoporation had little effect on STAT3. Considering that STAT3 is a constitutively active transcription factor in many cancers (40), including acute myeloid leukaemia (AML), from which the MOLM–13 cell line originates (76), stimulation might just aggravate the constant STAT3 signalling in MOLM–13. STATs regulate cellular growth, differentiation, survival and development, and with a constitutively active ligand/receptor engagement, abnormal STAT signalling may contribute to tumour development by stimulating cell cycle progression and/or cell survival (76). STAT3 alone probably cannot cause tumour progression, however, it plays an important role being constitutively turned on in many cancers (40).

5.2.5 Concluding remarks MOLM–13

The initial experiments with MOLM–13 enabled us to establish protocols and test the methods used to analyse sonoporated cells. It was demonstrated that it is possible to induce cell signalling with sonoporation and that we were able to detect a signal. shown

5.3 Pancreatic cell lines

5.3.1 Ultrasound treatment of cells – challenges

When studying cell signalling there are several aspects to be aware of that can affect the signalling resulting in false or skewed results. This applies particularly to adherent cells, which has to be detached from its substrate to be analysed. Trypsin is an enzyme that detaches

the cells by cleaving peptides on the cell surface, however, trypsin is not selective and can affect cell surface epitopes (60), which can have a downstream effect on intracellular signalling by either activating or de–activating cell surface receptors (59). For example, trypsin was fond to activate PAR2, which stimulates the MAPK pathway, including MAP phosphatase, which reduce p–ERK level induction by other receptors (59). Furthermore, one study determined that trypsin induced RhoA signalling (64), and Blc2, p53 and p33 were all found to be up or downregulated by trypsin (77). We used heated trypsin (37ºC) for cell passaging and initially also for cell detachment following treatment, since it is at this temperature it works optimally (60). However, cold trypsin, which is still 50% active at around 4ºC, would be a better option for cell signalling studies as it affects the surface epitopes to a lesser degree since the tyrosin kinases remain inactive at this temperature (59). Therefore, we have investigated the effect of trypsin on the cells, comparing cold and warm trypsinization. Cell detachment by scraping was also included in the test to check its effect on signalling. Although it is possible to detach cells in a Petaka using a magnet (62), we did not have the available technology to do this, so we had to utilise enzymatic cell detachment. See discussion of testing 1× and 10× trypsin below (**chapter 5.3.6 – 5.3.8.2**). Furthermore, the lack of commercially available technology to treat cells cultured in a Petaka with US was a time–limiting factor. It is possible to treat adherent cells in regular cell culture plates; however, we chose to use the hypoxic bioreactor Petaka 3G in order to mimic the severely hypoxic PDAC tumour. Using the Petaka the need for a hypoxic chamber is eliminated.

5.3.2 Optimisation of cell lysis

In order to determine how many WBs could be performed with 1×10^6 MIA PaCa–2, PANC–1 and BxPC–3 cells were quantified using 50 µl RIPA buffer (**Table 4**). This was important to assess the number of experiments to prepare sufficient lysate to investigate the chosen proteins of interest from one experiment. The protein concentration of the different cell lines varied: MIA PaCa–2 (2.774 µg/µl), PANC–1 (3.495 µg/ µl) and BxPC–3 (2.208 µg/µl), which provided 4, 5 and 3 WBs, respectively (**Table 4**). Since the protein concentration varied, the WBs were planned accordingly.

5.3.3 WST–1 – Optimisation of cell number seeded and incubation time – MIA PaCa–2

As explained previously (**chapter 3.3.1.3**) the WST–1 assay provides an estimation of metabolically activity in the cells. The WST–1 salt is metabolized by the cells and thereby

changes colour. The disadvantage of this assay is that if the cell concentration is too high the WST–1 reagent will be saturated before the reaction is finished and the results will be unreliable. Thus, to optimise this assay for MIA PaCa–2 cells were sonoporated (358 mW/cm^2, 5 min) and different cell concentrations (1×10^3 – 6.4×10^4) were seeded and incubated for 24h. The cells were then incubated for 1, 2 or 4h after adding the WST–1 reagent. The cells incubated for 1h had a rapid increase in absorption between 0.8×10^4 and 1.61×10^4 cells seeded, and then the curve plateaus, indicating the reaction is saturated (**Figure 16**). Cells incubated for 2h had a steadier increase in absorption with increasing cell number seeded, but with a rapid increase in absorption between 3.2×10^4 and 6.4×10^4 cells seeded. When incubated for 4h the absorption increased more rapid after 0.8×10^4 cells seeded. Considering that this test was only performed once it is difficult to draw a conclusion, however, based on these results it was decided to continue with 3.21×10^4 cells incubated for 2h in further studies with MIA PaCa–2, as under these conditions the increase in absorption was steady.

5.3.4 Optimisation of viability assays

To get an indication on how the cells' viability was affected by sonoporation, and to determine the optimal seeding density, a test was performed using High US, Serum–starvation (positive control) and untreated MIA PaCa–2 cells. Trypan blue, Hoechst 33342 and WST–1 (both assays: 3.2×10^4 cells/well) assays were included in the test. There were barely any trypan blue stained cells in any of the samples (data not shown). The WST–1 assay revealed no significant difference between the control and High US, while the starved sample showed a significant reduction in metabolic activity, compared both to the control and High US (**Figure 17A**). Keeping in mind that the cells were incubated for 24h before performing the assay itself, may have allowed the cells in High US sample to recover from sonoporation. In contrast, the sample with starved cells showed a significant reduction in absorption, suggesting that starvation affected the cells. It is well known that serum–starvation can affect the viability of cells. Partial starvation may strengthen some sub–populations (in MCF7 breast cancer cell line), but complete serum–starvation will affect their ability to proliferate (78). The starvation affects the rate of DNA synthesis after 20 h of starvation, and mitotic activity is inhibited (79). Serum–starvation can also activate apoptotic pathways, resulting in cell death (80). In the current test the cells were starved completely for 24h, therefore, the reduction in metabolic activity in the starved cells can likely be attributed to the lack of

proliferation due to inhibition of mitotic activity, as well as induction of apoptosis. High US did barely affect the cells' metabolic activity, compared to the control (**Figure17A**), however, considering that the cells are incubated for 24h following sonoporation the cells may have recovered from the treatment overnight. It was decided that 3.2×10^4 cell/well was acceptable for WST–1 assay to evaluate MIA PaCa–2 cells in further studies. The images of the Hoechst stained cells, processed as explained earlier (**chapter 3.3.2.1**), correlates with the WST–1 analysis (**Figure 17B**). The control and High US samples appear similar in cell density, while that starved sample had fewer cells, indicating cell death and/or lack of proliferation occurring during the 24h incubation period following treatment. The test also revealed that the seeding density was too high in the control and High US samples for the software to be able to distinguish between single cells, even with manual adjustments of contrast and threshold. In fact, it was possible to count the serum–starved cells (Fig 17B, but it was not performed since it was not possible to quantify the control and High US and, therefore, there would be no ground for comparison. As 3.2×10^4 cells was too dense to distinguish single cells, a new Hoechst test was performed seeding 0.8×10^4 and 1.6×10^4 cells/well (**Figure 18**). The images were evaluated visually due to poor image quality, as opposed to counting the cells with the software. For the purpose of determining seeding density this was sufficient. Based on a sample of images (three/well) representing the average cell density, it was decided to proceed with 1.6×10^4 cells/well in future Hoechst 33342 assays with MIA PaCa–2 (**Figure 18**).

5.3.5 Optimisation of growth rate

Culturing cells is normally done in cell culture flasks, which have ventilated caps allowing exchange of gasses. The Petaka, however, has minimal gas exchange, it is essentially a hypoxic bioreactor (81), hence it was assumed that the cells would behave differently in terms of growth rate. It was important to find optimal conditions for cell growth in relation to treating the MIA PaCa–2 cells with sonoporation to avoid the cells turning too hypoxic and entering senescence. The main objective was to ascertain when the cells experience log–phase growth. In order to determine in which time–period the cells in Petakas experience log–phase growth the cells were cultivated until they reached their maximum confluency, which is when they run out of space, nutrients and/or oxygen, resulting in slowing of DNA synthesis rate and inhibition of mitotic activity (79). MIA PaCa–2 cells were cultivated in Petakas and T75 flasks over the course of 6 days to compare the growth rate between the two cell culture methods. The growth rate was calculated by estimating the percentage surface area covered

by the cells in Petakas and flasks by imaging the cells. The cells in Petakas experienced log–phase growth between 48 and 72h (**Figure 19A**), while in the flasks log–phase growth was reached between 24 and 96 h (**Figure 19B**). Cells in Petakas reached full confluency around 60% surface area covered and the growth plateaued (**Figure 19A**). Cells in the flasks continued to grow further 24h, compared to the cells in Petakas, and reached full confluency around 80% of surface area covered by the cells (**Figure 19B**).

Cell growth in single Petakas was relatively even, but cells in one Petaka (**Figure 20A– "3a")** that appeared to experience less growth, compared to the rest. This might be due to an air pocket observed in this Petaka. When seeding cells in Petakas they are first placed in a horizontal position in the incubator for 24h for the cells to adhere, and then placed vertically for continued incubation. Between 24 and 48 h an air pocket appeared in the top of the Petaka, resulting in no medium covering the cells in this area, possibly drying and killing these cells. The air was removed at 48 h and fresh medium was refilled (2 mL) to ensure cell growth. Nevertheless, the mean growth between the Petakas was quite similar (**Figure 20A**).

Cell growth in single flasks was also relatively even in rate (**Figure 20B**). The deviation here was that flask # 1 appears to have been seeded with a higher cell number, compared to flask # 2 and 3 (**Figure 20B**). From these observations, it was decided to treat cells in Petakas between 48 and 72h of seeding as the cells experienced log–phase growth between those time–points.

5.3.6 Optimisation of timing of cell detachment with cold 1× trypsin

The time is takes untreated cells to detach from the flask with cold 1× trypsin and 10× trypsin was tested in three pancreatic cell lines; MIA PaCa–2, PANC–1 and BxPC–3. With 1× trypsin MIA PaCa–2 cells were detached by 30 min on ice, while PANC–1 and BxPC–3 took 70 min and 2h 45 min, respectively (**Table 5**). With 10× trypsin MIA PaCa–2, PANC–1 and BxPC–3 took 7 min 21 min and 22 min, respectively (**Table 6**). Due to the complex and time–consuming experimental setup of the main experiment, sonoporation at different US intensities with/without MBs, it would be impractical to include PANC–1 and BxPC–3 in further studies. Furthermore, it is not known whether incubation with trypsin on ice over such long periods of time affects the results. However, due to the potential time saved with using 10× trypsin for cell detachment, this was tested before excluding PANC–1 and BxPC–3. Between 7 and 22 min is feasible in a large experiment, in terms of the timing of all the steps after cell detachment, including seeding of cells for viability assays and protein extraction. Especially for PANC-1 and BxPc-3 detachment with more concentrated trypsin is necessary

to do signalling studies in these cell lines. However, before determining whether it was feasible to continue with all three cell lines, WB analysis was performed for 1×trypsin and 10× trypsin, in addition to viability testing of the cells detached with 10× trypsin.

5.3.7 Optimisation of cell detachment with cold 1× trypsin – western blot

As mentioned above, it is known that trypsin may affect cell signalling by cleaving cell surface receptors (59, 82), including integrins, which are implicated in activation of several pathways (**Figure 7**) (47). Since investigating cell signalling was the main objective of this project, consequently, examining the effect on signalling of different cell detachment methods was essential. Three detachment methods cold 1× trypsin, pre–heated 1× trypsin and scraping were then tested in MIA PaCa–2 (**Figure 21**). The cells were stimulated with A23187 (1μM) +PMA (0.1μM) for 30 min, a combination of stimuli known to induce phosphorylation. The cells were detached as described in **chapter 3.6.3.2**. Included in this test was also testing different amounts of protein extract for WB, as different cell lines may express different levels of the various proteins. For example, p38, JNK2 and c–Jun have been found to be upregulated in the cervical cancer and HeLa cells, compared with levels in non–cancerous tissues (83). Therefore, 30 μg, 40 μ g and 50 μg protein extract were used to evaluate the protein level and phosphorylation status of the MAPK p38. There was a relatively weak phosphorylation detected using 30 μg/well prompting the need to use long exposure time with the more sensitive SuperSignal™ West Femto Maximum Sensitivity Substrate to develop the membrane as no signal was detected using SuperSignal™ West Pico (**Figure 21**). There was a clear difference in phosphorylation status of p38 between the different detachment methods. Using 40 μg and 50 μg protein for cell detachment with ice–cold 1× trypsin resulted in phosphorylation of p38 in the stimulated sample (**Figure 21**). However, no phosphorylation was detected in the stimulated samples detached with pre–heated trypsin or by scraping (**Figure 21**), which was unexpected. Therefore, in further WBs 40 μg protein was used per well for MIA PaCa–2 cells, and all cell detachment of treated cells was performed with ice–cold trypsin (except cell passaging) from this point forward. This test confirms that optimisation is particularly important in signalling studies.

5.3.8 Optimisation of cell detachment with cold 10× trypsin

The three cell lines MIA PaCa–2, PANC–1 and BxPC–3 were stimulated with A23187 (1μM) + PMA (0.1μM) for 30 min to induce phosphorylation. The cells were detached by cold 10× trypsinization as described in **chapter 3.6.3.2.** Cells were harvested for trypan blue count,

Hoechst and WST–1 assays and cells were prepared for WB as previously described (**chapter 3.3.1 –3.3.3**) (1.6×10^4 cells/well for Hoechst 33342).

5.3.8.1 Optimisation of cell detachment with cold 10× trypsin – viability

Few cells were stained by trypan blue, indicating no immediate toxic effects resulting from this harsher treatment (**Figure 22A**). The uneven cell number between cell lines may be due to poor resuspension of cells before harvesting cells for the assay. The low number of trypan blue stained cells indicate that 10× trypsin detachment did not affect the cells to a large degree. The Hoechst 33342 analysis showed no difference in percentage apoptosis between the cell lines (**Figure 22B**). The assessment of metabolic activity in live cells by WST–1 showed a relative very low absorbance of MIA PaCa–2 cells, but the absorbance of PANC–1 and BxPC–3 was similar (**Figure 22C**). The inconclusive were unexpected and needs to be confirmed. To get a better impression of how 10× trypsin might influence signalling WB was performed with selected proteins.

5.3.8.2 Optimisation of cell detachment with cold 10× trypsin – western blot

ERK 1/2 was strongly phosphorylated in stimulated MIA PaCa–2 and PANC–1 samples, while BxPC–3 was relatively weaker phosphorylated in the stimulated samples (**Figure 23**). The results for stimulated BxPC–3 sample are blurred. This might be due to a deformed well used to load the protein, but this can also have happened when applying the membrane to the gel during transfer causing smudging of this sample. Regardless, there is a weak phosphorylation of ERK 1/2 in BxPC-3 (**Figure 23**). ERK 1/2 mediates cell proliferation, survival differentiation. When cells are stressed survival mechanisms are initiated, which might explain the induction of phosphorylation across all cell lines. p38 was only weakly phosphorylated in stimulated BxPC–3 cells. Recalling that p38 was phosphorylated in MIA PaCa–2 cells tested with cold 1× trypsin (**Figure 22**), it is possible that cold 10× trypsin indeed affected p38 signalling. Trypsin has been found to affect MAPK signalling, including p38 (84). SAPK/JNK was only phosphorylated in stimulated PANC–1 cells (**Figure 23**). JNK mediates apoptosis and autophagy and cell survival (35). The lack of detected phosphorylation in MIA PaCa–2 and BxPC–3 might indicate that they are more sensitive to trypsin than PANC–1, or that it is more difficult to activate this pathway in these cell lines. No phosphorylation was detected in MLC in any cell lines and protein lading was not successful for MIA PaCa-2 (**Figure 23**). The lack of total MLC in MIA PaCa–2 could be an

error, or MLC in MIA PaCa–2 is possibly extremely sensitive to trypsin. The Ponceau red staining of the membrane showed even loading of protein (**Figure 28 – Appendix**), therefore, the lack of total MLC protein is unknown. Due to the inconsistent results from the 10× trypsin test, including viability and WB analysis, it was decided to continue with cold 1× trypsin for cell detachment for the purpose of this current project.

5.3.9 Optimisation of western blotting

To determine the presence and phosphorylation status of chosen signalling proteins in MIA PaCa–2 the cells were stimulated with various chemicals, also called positive controls (**Table 2+9**). The test was also to ascertain whether the antibodies corresponding to chosen proteins worked in MIA PaCa–2 cells. Cells were stimulated with Tumour necrosis factor (TNFα) for 15 min (T1), A23187 + PMA for 30m min (T2), or A23187 for 4h (T3). WB was performed with 40 µg protein extract based on the results from testing cold 1× trypsin (**chapter 4.2.6**). ERK 1/2 was phosphorylated by all stimuli but was markedly stimulated by A23187+PMA, indicating that ERK 1/2 may be abundantly expressed in MIA PaCa–2 cells (**Figure 24**). It was confirmed that the ERK 1/2 Ab functioned as intended. Although, SAPK/JNK was phosphorylated in the control only, it was confirmed that the Ab functioned as intended. However, Ponceau red staining of the membrane shows equal loading of proteins (**Figure 29 – Appendix**), thus, this deviation is unknown. p38 was phosphorylated by TNFα only, confirming that the Ab worked (**Figure 24**). eIF2α was phosphorylated in both the control and stimulated sample, indicating that this pathway is constitutively active in this cell line. Both epitopes of MYPT1 (Ser853/Ser696) were phosphorylated in both the control and stimulated sample (**Figure 24**). All tested antibodies worked, although p38 and SAPK/JNK Ab require the more sensitive SuperSignal™ West Femto Maximum Sensitivity Substrate for development of the membranes due to weak signal. For further WBs, including Abs not tested here, Femto Maximum Sensitivity Substrate was used only if detecting a signal with Pico Chemiluminescent Substrate was not successful.

5.3.10 Optimisation of incubation time following sonoporation

MIA PaCa–2 cells were sonoporated at High US (358 mW/cm^2) with Sonazoid MBs and cells were harvested after 5 min, 1h, 2h, and 4h incubation following sonoporation as a check of phosphorylation kinetics in a few relevant pathways. Cells treated with MBs only was the control. Unfortunately, the protein concentration of cells from 4h incubation was too low to

be included in the WB due to sampling error. Therefore, only the control and cells from 5 min, 1h and 2h incubation following sonoporated were included in the WB analysis. ERK 1/2 was increasingly phosphorylated until 1h, indicating that ERK 1/2 phosphorylation increases until a certain time–point, then the signal fades (**Figure 25**). The amount of total protein is a bit higher in this sample, and this may be due to variation in loading. MLC was not phosphorylated until the 2h. sampling point, where the signal was strong, indicating a delayed reaction. MLC is phosphorylated downstream of Rho/ROCK. eIF2α had a time–dependent steady increase in phosphorylation (**Figure 25**). Many signalling proteins are downstream in extensive signalling cascades such as ERK 1/2, MLC and eIF2α. It is therefore natural to have a delayed response to stimuli. Clearly, it is essential to check signalling at other time–points following treatment, however, 2h incubation is a good starting point based on these results. Thereby, based on these results it was determined to proceed with 2h incubation time for further sonoporation studies of MIA PaCa–2.

5.3.11 Sonoporated MIA PaCa–2 – viability

MIA PaCa–2 cells, cultured in Petaka 3G bioreactors, were sonoporated at Low (3 mW/cm^2), Medium (50mW/cm^2) and High (358mW/cm^2) US with and without Sonazoid MBs incubated for 2h following sonoporation. Cells were detached by ice–cold 1× trypsin and harvested for viability assays as described previously (**chapter 3.3.1.1 – 3.3.1.3**) Trypan blue counting was performed 2h after sonoporation. Cells for Hoechst 33342 and WST–1 were seeded 2h after sonoporation and then incubated for 24h further. The viability assays were started 2hours post sonoporation because cells were detached from the Petaka at this timepoint. Hoechst fixated cells were stored at 4^{o}C for imaging and the cells for WST–1 was incubated for 2h before reading the absorption, as per **chapter 3.3.1.2 and 3.3.1.3**, respectively.

The cells treated with US only differed in total cell count, of which the Low US sample had a higher cell count, and all of the samples had relatively few trypan blue stained cells (**Figure 26A**). Of the samples treated with US and MBs the total cell count was again higher for Low US compared the other samples, and here more cells were stained by trypan blue, compared to the sample without MBs (**Figure 26B**). There is a trend of decreasing trypan blue stained cells with increasing US intensity. The uneven cell number may be a sampling error, or simply variation in cell growth in each Petaka. The use of this test to check for cavitation after sonoporation seems unreliable due to variations in growth prior to sonoporation (cell concentration prior to sonoporation is not known).

The Hoechst assay showed ta decreasing trend of percentage apoptosis in across all samples with/without MBs, with the exception of High US with MBs, which was higher (**Figure 26C+D**), indicating that US and MBs is killing the cells at higher US intensities.

The WST–1 metabolic assay showed a decrease in metabolic activity with increasing US intensity without MBs in the treated samples (**Figure 26E**), suggesting that higher US intensities in fact influence cell viability. This correlates with the Hoechst assay. The absorbance of the samples treated with US and MBs was very similar between the samples, and no difference was observed in the control (**Figure 26F**). Hence, no apparent effect on the cells metabolic ability caused by sonoporation was observed with MBs. There results indicate that US alone has an effect on MIA PaCa-2 cells, however, this needs to me confirmed.

5.3.12 Sonoporated MIA PaCa–2 – western blot

5.3.12.1 MAPK pathway

ERK 1/2 was weakly phosphorylated without MBs and a stronger signal with increasing US intensity with MBs. No phosphorylation of p38 or SAPK/JNK was detected (**Figure 27**). ERK 1/2, p38 and JNK are all MAP kinases, however they are not activated by the same cellular stimuli. The UPR, which has cross–talk with MAPKs, can be activated by ER–stress (32), that has been shown to be induced by sonoporation in leukaemia cells (MOLM–13) (20). It is not given that sonoporation will have the same effect on ERK 1/2 in pancreatic cells (MIA PaCa–2), nevertheless, the results indicate that ERK 1/2 was activated. Recalling that ERK 1/2, p38 and JNK had some activation in sonoporated MOLM–13 cells with MBs at higher US intensities (**Figure 15**), suggesting that sonoporation can induce phosphorylation in MAPKs. However, in MIA PaCa–2 the results deviate from the assumption that sonoporation can induce p38 and JNK signalling in MIA PaCa–2 cells as well. Importantly, the US intensities, referred to as Low, Medium and High US in studies of MOLM-13 and pancreatic cell lines were not the same. For MOLM-13 the US intensities were 74, 501 and 2079 mW/cm^2. For pancreatic cell lines the US intensities were 3, 50 and 358 mW/cm^2. Consequently, High US (358 mW/cm^2) used for pancreatic cells is quite low, compared to High US (2079 mW/cm^2) used for MOLM-13. The US intensities used in diagnostic US range from 17 mW/cm^2 to 720 mW/cm^2, which is considered safe. For example for fetal imaging 94 mW/cm^2 is used (23). Comparative to the diagnostic US the intensities used for MIA PaCa-2 is quite low and it is possible that a higher intensity is necessary to induce phosphorylation. Alternatively, it is possible that more than 40 μg protein is necessary to

detect a signal in p38 and JNK. However, the optimisation of WB, where Abs were tested, (**Figure 26**) indicated that 40 µg was sufficient to detect phosphorylation of these proteins. Importantly, conformation of the results is crucial.

5.3.12.2 UPR pathway

eIF2α was phosphorylated in all samples, suggesting that this is constitutively active (**Figure 27**). However, there is no difference between the treated samples and the control, indicating activation by something else than sonoporation. Interestingly, in the optimisation of incubation time post sonoporation eIF2α was increasingly phosphorylated by high (358 mW/cm^2) and MBs, seen between 5 min and 2h after sonoporation (**Figure 25**), indication that phosphorylation of eIF2α is time–dependent. Here (**Figure 27**), samples for WB were only analysed after 2h. Together, these results prompt the need to investigate phosphorylation of eIF2α at multiple time–points following sonoporation to confirm

5.3.12.3 JAK-STAT pathway

STAT3 (Ser727) was phosphorylated in all samples (**Figure 27**). STAT3, which is a transcription factor, is constitutively active in many cancers, including pancreatic cancer (40). STAT3 promote angiogenesis, survival, immune evasion, cell proliferation and migration/invasion, all of which are actions that aid in tumour progression. The constant activation of STAT3 across all samples correlate with a constitutively active STAT3. Considering that STAT3 (Ser727) also was constitutively activated in MOLM-13 at both 5 min and 2h after sonoporation (**Figure 15**), suggests that sonoporation has little effect on this epitope of STAT3.

5.3.12.4 PI3K–mTOR pathway

S6 was increasingly phosphorylated at higher US intensities (**Figure 27**), indicating activation by sonoporation. S6 is downstream in the PI3K–mTOR pathway, which is normally activated by hormones, integrins and growth factors and mediates proliferation, growth, translation and survival (**Figure 7**) (42). Integrins are activated by mechanical stimuli (47), thus, it is possible that sonoporation induced a phosphorylation in S6 via integrins and the PI3K–mTOR pathway. However

5.3.12.5 Rho-ROCK pathway

MLC was phosphorylated to some extent without MBs and a clear increase at High US with MBs (**Figure 27**). MYPT1 (Ser853) was weakly phosphorylated, while no phosphorylation was detected for MYPT1 (Ser696). MLC and MYPT1 is part of the Rho/ROCK pathway, which mediates stress–fibre assembly and cell contraction (**Figure 7**) (43). MYPT1 is a part of MLCP (**Figure 8**), which inhibits the dephosphorylation of MLC, thereby increasing myosin II activity and stress–fibre formation (focal adhesions) and contractility (44). Since there was not detected any phosphorylation of either epitopes of MYPT1, one can assume that MLC was not de–phosphorylated in the MIA PaCa–2 cells (**Figure 27**), which correlated with the strong phosphorylation of MLC at High US with MBs (**Figure 27**). This indicates that MLC and MYPT1 is not very sensitive to mechanical treatment (sonoporation).

6.0 Concluding remarks and future directions

The overall aim of this project was to elucidate the pathways activated by sonoporation in pancreatic cell lines by analysing post–translational modifications (*i.e.*, phosphorylation). The long–term goal is to identify biomarkers for sonoporation that can be used to optimise sonoporation therapy.

The investigation of protein signalling pathways in the AML cell line MOLM–13 showed that sonoporation affects cell viability and can induce phosphorylation of multiple signalling pathways. The most apparent effect on viability was found in samples treated with US and MBs. The number of dead cells, treated with MBs, increased with increasing US intensity, which correlated with a decrease in cell proliferation ability with increasing US intensity. The effect of sonoporation with MBs was also reflected in increased phosphorylation in apoptosis related proteins.

The pancreatic cell lines were treated in the bioreactor Petaka G3 LOT, and in order to study cell signalling in adherent cells, they need to be detached. We used trypsin, which is a serine protease known to affect surface epitopes and intracellular signalling. It was confirmed that phosphorylation status differed when comparing cold and warm trypsinization with cell detachment by scraping. Phosphorylation of p38 was detected in cells detached with cold 1× trypsin, but not in cells detached with heated trypsin or by scaping. Non–enzymatic cell detachment should be further explored in signalling studies induced by sonoporation, since it eliminates the influence of enzymatic activation or de-activation of signalling proteins. In fact, Petakas are available with a built–in magnet used for cell detachment by scraping. A

more concentrated trypsin (10×) was also tested and, as expected, the cells detached faster, compared to 1×. However, it is not known whether cell detachment with 10× trypsin affects cell signalling or viability. We, therefore, used cold 1× trypsin from that point on. Faster cell detachment would be of great benefit when investigating multiple signalling pathways in several cell lines. Originally this project intended to investigate the sonoporation–induced signalling in the three pancreatic cell lines MIA PaCa–2, PANC–1 and BxPC3 to get a good representation of patient heterogeneity. However, since the test with 10× trypsin was inconclusive, and since detaching PANC–1 and BxPC3 with cold 1× trypsin took too long only MIA PaCa-2 was further investigated. Future studies should include all three cell lines.
We investigated change in phosphorylation status in MIA PaCa-2 cells 2h after sonoporation, however, considering that phosphorylation is a transient event further incubation times should be thoroughly tested. We found, for example that eIF2a had a time–dependent increase in phosphorylating. Although, a trend of decreasing metabolic activity, corresponding to an increase in number of apoptotic cells with increasing US intensity (without MBs) was identified in MIA PaCa-2 cells this needs to be further investigated to confirm the results.
We have successfully identified sonoporation–induced signalling in the MAPK pathway (ERK 1/2), PI3K/mTOR pathway (S6) and Rho/ROCK pathway (MLC), but it would be advisable to investigate this further, including other post sonoporation incubation times. The lack of phosphorylation in the MAPKs p38 and JNK, as well as in both epitopes of MYPT1 may be due to the fact that the phosphorylation occurs at other time–points. Additionally, it would be advisable to include higher US intensities in order to determine whether it affects the aforementioned pathways to a greater degree. Comparative studies should include non–cancerous cells, such as endothelial cells and fibroblasts to elucidate how sonoporation affects healthy cells.

Methodology for in vitro optimisation of sonoporation was developed. Using this methodology, we have identified several pathways activated by sonoporation that may have potential as biomarkers for PDAC that can be used to optimise sonoporation therapy. It was also found that higher US intensities and microbubbles may have an effect of cell viability, depending on the US intensity. However, these are preliminary results which needs to be confirmed.

7.0 Bibliography

1. J. J. Bass DJW, D. Rankin, B. E. Phillips, N. J. Szewczyk, K. Smith, P. J. Atherton. An overview of technical considerations for Western blotting applications to physiological research. Scand J Med Sci Sports 2017;27:4-25.
2. Organization WH. Cancer, Key Facts www.who.int: World Health Organization; 2018 [Available from: http://www.who.int/news-room/fact-sheets/detail/cancer.
3. Organization WH. World cancer factsheet, World cancer burden (2012) www.cancerresearchuk.org: Cancer Research UK; 2014 [Available from: http://www.cancerresearchuk.org/sites/default/files/cs_report_world.pdf.
4. G. Dimcevski SK, T. Bjanes, D. Hoem, J. Schjott, B. T. Gjertsen, M. Biermann, A. Molven, H. Sorbye, E. McCormack, M. Postema, O. H. Gilja,. A human clinical trial using ultrasound and microbubbles to enhance gemcitabine treatment of inoperable pancreatic cancer. J Control Release. 2016;243:172-81.
5. A. Adamska ADaMF. Pancreatic Ductal Adenocarcinoma: Current and Evolving Therapies. Int J Mol Sci. 2017;18(1338):1-43.
6. UK Cr. UK Pancreatic Cancer Prognosis and Survival Rates https://pancreaticcanceraction.org: Cancer research UK; 2018 [Available from: https://pancreaticcanceraction.org/about-pancreatic-cancer/medical-professionals/stats-facts/prognosis-survival/.
7. Society AC. Cancer Facts & Figures 2016. Atlanta: American Cancer Society: American Cancer Society; 2016.
8. J. C. Forster WMH-P, M. J. J. Douglass and E. Bezak. A review of the development of tumor vasculature and its effects on the tumor microenvironment. Hypoxia. 2017;5:21-32.
9. Jain PCaRK. Principles and mechanisms of vessel normalization for cancer and other angiogenic diseases. Nature Reviews, Drug Discovery. 2011;10:417-27.
10. G. Baronzio GPaMB. Overview of methods for overcoming hindrance to drug delivery to tumors, with special attention to tumor interstitial fluid. Front Oncol 2015;5(165).
11. T. Ojha VP, Y. Shi, W. Hennink, C. Moonen, G. Storm, F. Kiessling, and T. Lammers. Pharmacological and Physical Vessel Modulation Strategies to Improve EPR-mediated Drug Targeting to Tumors. Adv Drug Deliv Rev. 2017;119:44-60.
12. D. M. Gilkes GLSaDW. Hypoxia and the extracellular matrix: drivers of tumour metastasis. Nat Rev Cancer. 2014;14(6):430-9.
13. Mousa CMSaSA. Status and future directions in the management of pancreatic cancer: potential impact of nanotechnology. J Cancer Res Clin Oncol. 2018.
14. J. Taieb A-LP, J. L. Van Laethem, B. Laquente, S. Pernot, F. Lordick and M. Reni. What treatment in 2017 for inoperable pancreatic cancers? Annals of Oncology 2017;28:1473-83.
15. T. Conroy FD, M. Ychou, O. Bouché, R. Guimbaud, Y. Bécouarn, A. Adenis, J-L. Raoul, S. Gourgou-Bourgade, C. de la Fouchardière, J. Bennouna, J-B. Bachet. FOLFIRINOX versus Gemcitabine for Metastatic Pancreatic Cancer. N Engl J Med. 2011;364:1817-25.
16. D. D. Von Hoff RKR, M. J. Borad, D. A. Laheru, L. S. Smith, T. E. Wood, R. L. Korn, N. Desai, V. Trieu, J. L. Iglesias, H. Zhang, P. Soon-Shiong, T. Shi, N.V. Rajeshkumar, A. Maitra, and M. Hidalgo. Gemcitabine Plus nab-Paclitaxel Is an Active Regimen in Patients With Advanced Pancreatic Cancer: A Phase I/II Trial. J Clin Oncol 2011 Dec. 1;29(34):4548–54.

17. K. K. Frese AN, N. Cook, T. E. Bapiro, M. P. Lolkema, D. I. Jodrell and D. A. Tuveson. nab-paclitaxel potentiates gemcitabine activity by reducing cytidine deaminase levels in a mouse model of pancreatic cancer. Cancer Discov 2012;2(3):260–9.
18. A. Portal SP, D. Tougeron, C. Arbaud, A. Thirot Bidault, C. de la Fouchardière, P. Hammel, T. Lecomte, J. Dréanic, R. Coriat, J-B. Bachet, O. Dubreuil, L. Marthey, L. Dahan, B. Tchoundjeu, C. Locher, C. Lepère, F. Bonnetain, and J. Taieb. Nab-paclitaxel plus gemcitabine for metastatic pancreatic adenocarcinoma after Folfirinox failure: an AGEO prospective multicentre cohort. Br J Cancer. 2015;113(7):989-95.
19. V. Kunzmann RKR, D.Goldstein, H.Liu, S. Ferrara, B. Lu, M.F. Renschler and D. D. Von Hoff. Tumor Reduction in Primary and Metastatic Pancreatic Cancer Lesions With nab-Paclitaxel and Gemcitabine, An Exploratory Analysis From a Phase 3 Study. Pancreas 2017;46(2):203–8.
20. S. Kotopoulis RH, M. Mujic, A. Sulen, S-E. Gullaksen, E. McCormack, O. H. Gilja, M. Postema and B. T. Gjertsen. Evaluation of the effects of clinical diagnostic ultrasound in combination with ultrasound contrast agents on cell stress: Single cell analysis of intracellular phospho-signaling pathways in blood cancer cells and normal blood leukocytes. 2014.
21. SonoCURE. SonoCURE, Ultrasound Mediated Therapy https://sonocure.w.uib.no2018 [Available from: https://sonocure.w.uib.no/aboutsonocure/.
22. Hwang HCaJH. Ultrasound-targeted microbubble destruction for chemotherapeutic drug delivery to solid tumors. J Ther Ultrasound. 2013;1(10).
23. Administration UFaD. Guidance for Industry and FDA Staff Information for Manufacturers Seeking Marketing Clearance of Diagnostic Ultrasound Systems and Transducers. In: Services USDoHaH, Administration FaD, Health CfDaR, Branch RD, Division of Reproductive A, and Radiological Devices, Evaluation OoD, et al., editors.: US Food and Drug Administration; 2008.
24. S. Kotopoulis AD, M. Popa, V. Mamaeva, G. Dimcevski, O. H. Gilja, M. Postema, B. T. Gjertsen and E. McCormack. Sonoporation-enhanced chemotherapy significantly reduces primary tumour burden in an orthotopic pancreatic cancer xenograft. Mol Imaging Biol. 2014;16(1):53-62.
25. Borden SSaM. Microbubble Compositions, Properties and Biomedical Applications. Bubble Sci Eng Technol. 2009;1(1-2):3-17.
26. V. Paefgen DDaFK. Evolution of contrast agents for ultrasound imaging and ultrasound-mediated drug delivery. Front Pharmacol. 2015;6(197).
27. I. Lentacker IDC, R. Deckers, S.C. De Smedt, C. T. W. Moonen. Understanding ultrasound induced sonoporation: Definitions and underlying mechanisms. Advanced Drug Delivery Reviews. 2014;72: 49–64.
28. P. Qina TH, A. C.H. Yub and L. Xuc. Mechanistic understanding the bioeffects of ultrasound-driven microbubbles to enhance macromolecule delivery. Journal of Controlled Release. 2018;272:169-81.
29. Xu HYaL. Cell experimental studies on sonoporation: state of the art and remaining problems. J Control Release. 2014;174:151-60.
30. W. Zhong WHS, J. M. F. Wan and A. C. H.Yu. Sonoporation Induces Apoptosis and Cell Cycle Arrest in Human Promyelocytic Leukemia Cells. Ultrasound in Medicine & Biology. 2011;37(12).
31. W. Zhong XC, P. Jiang, J. M. Wan, P. Qin and A. C. Yu. Induction of endoplasmic reticulum stress by sonoporation: linkage to mitochondria-mediated apoptosis initiation. Ultrasound Med Biol. 2013;39(12):2382-92.
32. R. K. Yadav S-WC, H-R. Kim and H. J. Chae. Endoplasmic Reticulum Stress and Cancer. J Cancer Prev. 2014;19:75-88.

33. E. Dufey DS, D. Rojas-Rivera, and C. Hetz. Cellular Mechanisms of Endoplasmic Reticulum Stress Signaling in Health and Disease. 1. An overview. Am J Physiol Cell Physiol. 2014;307:C852-C594.
34. H. P. Harding YZ, A. Bertolotti, H. Zeng, and D. Ron. Perk Is Essential for Translational Regulation and Cell Survival during the Unfolded Protein Response. Mol Cell. 2000;5(5):897-904.
35. Cook NJDaSJ. The role of MAPK signalling pathways in the response to endoplasmic reticulum stress. Biochimica et Biophysica Acta. 2014;1843(10):2150-63.
36. C. J. Sheebaa GM, A. M. Revina and G. Franklin. Signaling pathways influencing tumor
microenvironment and their exploitation for
targeted drug delivery. Nanotechnol Rev. 2014;3(2):123-51.
37. Yamori D-XKaT. ZSTK474, a novel phosphatidylinositol 3-kinase
inhibitor identified using the JFCR39 drug discovery
system. Acta Pharmacologica Sinica. 2010;31:1189-97.
38. D. L. Knowlton KT, P. V. Henstock, R. R. Subramanian. miRNA Alterations Modify Kinase Activation In The IGF-1 Pathway And
Correlate With Colorectal Cancer Stage And Progression In Patients. Jouranal of Cancer. 2011;2:490-502.
39. J. A. Hutchinson NPS, H. Chang, R. S. Tibbetts. Regulation of Ribosomal Protein S6 Phosphorylation by
Casein Kinase 1 and Protein Phosphatase 1. J Biol Chem. 2011;286(10):8688-96.
40. J. A. Kopechek ARC, C. F. McTiernan, X. Chen, B. Hasjim, L. Lavery, M. Sen, J. R. Grandis, F. S. Villanueva. Ultrasound Targeted Microbubble Destruction-Mediated Delivery of a Transcription Factor Decoy Inhibits STAT3 Signaling and Tumor Growth Theranostics. 2015;5(12):1378-287.
41. A. L. A. Wong JLH, S. Pervaiz, J-Q. Eu, G. Sethi and B-C. Goh. Do STAT3 inhibitors have potential in the future for cancer therapy? Expert Opinion on Investigational Drugs. 2017;26(8):883-7.
42. M. C. Mendoza EEEaJB. The Ras-ERK and PI3K-mTOR Pathways: Cross-talk and Compensation. Trends Biochem Sci. 2011;36(6):320-8.
43. Sahai MFOaE. The actin cytoskeleton in cancer cell motility. Clin Exp Metastasis. 2009;26:273-87.
44. Ridley KRaAJ. ROCKs: Multifunctional kinases in cell behaviour. Nature Reviews, Drug Discovery. 2003;4(6):446-56.
45. X. Chen RSL, Y. Hu, J. M. F. Wan and A. C. H. Yu. Single-site sonoporation disrupts actin cytoskeleton organization. J R Soc Interface. 2014;11(95).
46. M. Wang YZ, C. Cai, J. Tu, X. Guo and D. Zhang. Sonoporation-induced cell membrane permeabilization and cytoskeleton disassembly at varied acoustic and microbubble-cell parameters. Scientific Reports. 2018;8.
47. B. D. Matthews DRO, R. Mannix and D. E. Ingber. Cellular adaptation to mechanical stress: role of
integrins, Rho, cytoskeletal tension and
mechanosensitive ion channels. Journal of Cell Science. 2006;119:508-18.
48. D. M. Gilkesa LX, S. J. Leea S, P. Chaturvedia, M. E. Hubbia, D. Wirtzc and G. L. Semenzaa. Hypoxia-inducible factors mediate coordinated RhoA-ROCK1
expression and signaling in breast cancer cells. Proceedings of the National Academy of Sciences (PNAS). 2014;111(3):E384-E93.

49. V. Longo OB, A. Gnoni, S. Cascinu, G. Gasparini, V. Lorusso, D. Ribatti and N. Silvestris. Angiogenesis in pancreatic ductal adenocarcinoma: A controversial issue. Oncotarget. 2016;7(36).
50. B. H. A. Lammertink CB, R. Deckers, G. Storm, C. T. W. Moonen and J-M. Escoffre. Sonochemotherapy: from bench to bedside. Front Pharmacol 2015;6:138.
51. R. Ishida DK, T. Kusaba, Y. Kirita, T. Kishida, O. Mazda, T. Adachi and S. Gojo. Kidney-specific Sonoporation-mediated Gene Transfer. Mol Ther 2016;24(1): 125–34.
52. H-X. Li J-HZ, L. Ji, G.-Y. Liu, Y-K. Lv, D. Yang, Z. Hu, H. Chen, F-M. Zhang and W. Cao. Effects of low-intensity ultrasound combined with low-dose carboplatin in an orthotopic hamster model of tongue cancer: A preclinical study. Oncol Rep 2018;39(4):1609–18.
53. S. Tinkov CC, S. Serba, N. A. Geis, H. A. Katus, G. Winter, R. Bekeredjian. New doxorubicin-loaded phospholipid microbubbles for targeted tumor therapy: In-vivo characterization. Journal of Controlled Release. 2010;148(3).
54. E. S. Lee JYL, H. Kim, Y. S. Choi, J. Park, J. K. Han and b. i. Choi. Pulsed High-Intensity Focused Ultrasound Enhances Apoptosis of Pancreatic Cancer Xenograft with Gemcitabine. Ultrasound in Medicine & Biology. 2013;39(11):1991-2000.
55. A. Carpentier MC, A. Vignot, V Reina, K. Beccaria, C. Horodyckid, C. Karachi, D. Leclercq, C. Lafon, J-Y. Chapelon, L. Capelle, P. Cornu, M. Sanson, K. Hoang-Xuan, J-Y. Delattre, A. Idbaih. Clinical trial of blood-brain barrier disruption by pulsed ultrasound. Science Translational Medicine. 2016;8(343):343.
56. L. B. Feril Jr. TK, Z-G. Cui, Y. Tabuchi, Q-L. Zhao, H. Ando, T. Misaki, H. Yoshikawa and S-I. Umemura. Apoptosis induced by the sonomechanical effects of low intensity
pulsed ultrasound in a human leukemia cell line. Cancer Letters. 2005;221:145-52.
57. R. Gradiz HCS, L. Carvalho, M. F. Botelho and A. Mota-Pinto. MIA PaCa-2 and PANC-1 – pancreas ductal adenocarcinoma cell lines with neuroendocrine differentiation and somatostatin receptors. Sci Rep. 2016;6(21648).
58. E. L. Deer JG-H, J. D. Coursen, J. E. Shea, J. Ngatia, C. L. Scaife, M. A. Firpo and S. J. Mulvihill. Phenotype and Genotype of Pancreatic Cancer Cell Lines. Pancreas. 2010;39(4):425-35.
59. Lorens IAaJB. Evaluating Extracellular Matrix influence on
adherent cell signaling by Cold Trypsin
Phosphorylation-specific Flow Cytometry. BMC Cell Biology 2013;14(36).
60. Sigma-Aldrich. Cell Dissociation with Trypsin www.sigmaaldrich.com: Sigma-Aldrich; [09/04/18]. Available from: https://www.sigmaaldrich.com/technical-documents/articles/biology/cell-dissociation-with-trypsin.html.
61. E. K. Paluch CMN, N. Biais, B. Fabry, J. Moeller, B. L. Pruitt, C. Wollnik, G. Kudryasheva, F. Rehfeldt and W. Federle. Mechanotransduction: use the force(s). BMC Biol 2015;13(47).
62. Celartia. PetakaG3™ ET™ (Easy Transfer) www.celartia.com: Celertia; 2018 [Available from: http://www.celartia.com/petakag3-et.
63. Sigma-Aldrich. Trypsin-EDTA solution (1x), T3924 Sigma www.sigmaaldrich.com: Sigma-Aldrich; [09/04/18]. Available from: https://www.sigmaaldrich.com/catalog/product/sigma/t3924?lang=en&region=NO.
64. D. L. Greenberg GJM, and T. K. Takayama. Protease-Activated Receptor Mediated RhoA Signaling and Cytoskeletal
Reorganization in LNCaP Cells. Biochemistry. 2003;42:702-9.

65. Sigma-Aldrich. BRAND® counting chamber BLAUBRAND® Fuchs-Rosenthal with clips, double ruled www.sigmaaldrich.com: Sigma-Aldrich; 2018 [Available from: https://www.sigmaaldrich.com/catalog/product/aldrich/br719820?lang=en&region=NO.
66. Sigma-Aldrich. Cell Proliferation Reagent WST-1 www.sigmaaldrich.com: Sigma-Aldrich; [Available from: https://www.sigmaaldrich.com/catalog/product/roche/cellproro?lang=en&region=NO.
67. Sigma-Aldrich. Cell Proliferation Reagent WST-1 www.sigmaaldrich.com: Sigma-Aldrich; 2018 [Available from: https://www.sigmaaldrich.com/content/dam/sigma-aldrich/docs/Roche/Bulletin/1/cellprorobul.pdf.
68. T. Yddal SC, O. H. Gilja, M. Postema and S. Kotopoulis. Open-source, high-throughput ultrasound treatment chamber. Biomed Tech. 2014.
69. Sigma-Aldrich. TPP® tissue culture plates www.sigmaaldrich.com: Sigma-Aldrich; 2018 [Available from: https://www.sigmaaldrich.com/catalog/product/sigma/z707910?lang=en&region=NO.
70. H. Ogi MH, and T.Honda Absolute Measurement Of Ultrasonic Attenuation By Electromagnetic
Acoustic Resonance Review of Progress in Quanlitative Nondestructive Evaluation, . 1995;14.
71. Bio-Rad. DC Protein Assay Instruction
Manual www.bio-rad.com: Bio-Rad Laboratories; [Available from: https://www.bio-rad.com/webroot/web/pdf/lsr/literature/LIT448.pdf.
72. Sigma-Aldrich. Trypan Blue solution, 0.4%, liquid, sterile-filtered, suitable for cell culture www.sigmaaldrich.com: Sigma-Aldrich; [Available from: https://www.sigmaaldrich.com/catalog/product/sigma/t8154?lang=en&region=NO.
73. H. B. Forrester CHV, N. Albright, C. C. Ling and W. C. Dewey. Using Computerized Video Time Lapse for Quantifying Cell Death of X-irradiated Rat Embryo Cells Transfected with c-myc or c-Ha-ras. Cancer Research. 1999;59:931-9.
74. Ihle JN. Cytokine receptor signalling. Nature. 1995;377(6550):591-4.
75. M. Sakaguchi MO, T. Iwasaki, Y. Fukami and C. Nishigori. Role and Regulation of STAT3 Phosphorylation at Ser727 in Melanocytes and Melanoma Cells. Journal of Investigative Dermatology. 2012;132(7):1877-85.
76. T. Bowman RG, J. Turkson and R. Jove. STATs in oncogenesis. Oncogene. 2000;19:2474-88.
77. H-L. Huang H-WH, T-C. Lai, Y-W. Chen, T-R. Lee, H-T. Chan, P-C. Lyu, C-L. Wu, Y-C. Lu, S-T. Lin, C-W. Lin, C-H. Lai, H-T. Chang, H-C. Chou and H-L. Chan. Trypsin-induced proteome alteration during cell subculture in mammalian cells. J Biomed Sci. 2010;17(1):36.
78. R. T. Tavaluc LSH, D. T. Dicker, W. S. El-Deiry. Effects of Low Confluency, Serum Starvation and
Hypoxia on the Side Population of Cancer Cell
Lines. Cell Cycle. 2007;6(20):2554-62.
79. Sköld AZaO. The effect of serum starvation on DNA, RNA and protein synthesis during interphase in L-cells. Experimental Cell Research. 1969;57(1):114-8.
80. M. Aghababazadeh MAK. Cell Fasting: Cellular Response and Application of Serum Starvation J Fasting and Health. 2014;2(4):147-50.
81. Celartia. PetakaG3™ LOT (Low Oxygen Transfer) Celartia.com: Celartia; [Available from: http://www.celartia.com/petakag3-lot.
82. M. A. Brown CSW, C. C. Anamelechi, E. Clermont, W. M. Reichert and G. A. Truskey. The Use of Mild Trypsinization Conditions in the Detachment of Endothelial Cells

to Promote Subsequent Endothelialization on Synthetic Surfaces. Biomaterials. 2007;28(27):3928-35.
83. Z. Pei GZ, X. Huo, L. G. S. Liao, J. He,, Y. Long HY, S. Xiao, W. Y. P. Chen,, X. Li GLaYZ. CD24 promotes the proliferation and inhibits the apoptosis of cervical cancer cells in vitro. Oncology Reports. 2016;35:1593-601.
84. C. M. Belham RJT, P. H. Scott, A. D. Pemberton, H. R. P. Miller, R. M. Wadsworth, G. W. Gould, R. Plevin. Trypsin stimulates proteinase-activated receptor-2-dependent and -independent activation of mitogen-activated protein kinases. Biochem J. 1996;320:939-46.
85. Abcam. A23187 (Calcimycin) (ab120287) www.abcam.com2018 [Available from: http://www.abcam.com/a23187-calcimycin-ab120287.html.
86. Technologies S. Phorbol 12-myristate 13-acetate www.stemcell.com: Stemcell Technologies; 2018 [Available from: https://www.stemcell.com/phorbol-12-myristate-13-acetate.html.
87. F. Mohideen JAP, A. Ordureau, S. P. Gygi and J. W. Harper. Quantitative Phospho-proteomic Analysis of TNFα/NFκB Signaling Reveals a Role for RIPK1 Phosphorylation in Suppressing Necrotic Cell Death In: Biology ASfBaM, editor. Molecular and Cellular Proteomics. www.mcponline.org2017.

8.0 Appendixes

Appendix A Antibodies

Table 7: List of primary antibodies

Antibody	Epitope	Molecular weight (kDa)	Clone	Isotype	Product number*	Dilution
Phospho–eIF2α pAb	Ser^{51}	38		Rabbit	9721	1:5000
eIF2α mAb		38		Mouse	2103	1:5000
Phospo–p44/42 MAPK (ERK 1/2) XP® mAb	Thr^{202} Tyr^{204}	44/42	D13.14.4E	Rabbit	4370	1:2000
p44/42 MAP Kinase (ERK 1/2) mAb		44/42	L34F12	Mouse	4696	1:2000
Phospho–p38 MAPK	Thr^{180} Tyr^{182}	43	28B10	Mouse	9216	1:2000
p38 MAPK XP® mAb		43	D13E1	Rabbit	8090	1:2000
Phospho–MYPT1 pAb	Ser^{853} Ser^{696}	140		Rabbit	4563 5163	1:1000 1:1000
MYPT1 mAb		140	D6C1	Rabbit	8574	
Phospho–SAPK/JNK mAb	Thr^{183} Tyr^{185}	46/54	G9	Mouse	9255	1:2000
SAPK/JNK Ab		46/54		Rabbit	9252	1:2000
Phospho–S6 Ribosomal Protein XP® mAb	Ser^{235} Ser^{236}	32	D57.2.2E	Rabbit	4858	1:2000
S6 Ribosomal Protein mAb		32	54D2	Mouse	2317	1:1000
Phospho–Stat3 α/β mAb	Tyr^{705}	79/86	D3A7	Rabbit	9145	1:2000
Phospho–Stat3 α/β pAb	Ser^{727}	79/86		Rabbit	9134	1:1000
Stat3 α/β mAb		79/86	124H6	Mouse	9139	1:1000
Phospho–MLC mAb	Ser^{19}	18		Mouse	3675	1:1000
MLC Ab		18		Rabbit	3675	1:1000
COX IV		17		Rabbit	**ab16056	1:2000

*Cell Signalling Technology
** Abcam

Table 8: Secondary antibodies

Target	Host	Antibody format	Specificity	Conjugate	Clonality	Product number*
Mouse	Goat	Whole IgG	IgG (H+L)	Horseradish peroxidase	Polyclonal	115/035–003
Rabbit	Goat	Whole IgG	IgG (H+L)	Horseradish peroxidase	Polyclonal	111–035–003

*Jackson Immuno Research Laboratories Inc., West Grove, PA, USA

Appendix B Positive controls

Table 9: Function of positive controls

Chemical	Function
A23187 (Calcimycin)	Calcium Ionophore, highly selective for Ca^{2+} (85)
Phorbol 12–myristate 13–acetate (PMA)	A phorbol ester that activates protein kinase C (PKC), ERK1/2 and p38 (86)
TNFα	Activates NF-κB pathway (including c-Jun, STATs, and nuclear hormone receptors) (87)

Appendix C Optimisation of growth rate MIA PaCa-2

Recipe for semi-automated identification of Hoechst 33342 stained cells.

The contrast was adjusted, and the background was flattened to correct for illumination inhomogeneity. A dark texture filter was used to highlight dark components of the image via a grayscale closing method. A standard deviation filter was used to accentuate the cell edges by brightening pixels which have dissimilar neighbours. A range threshold was applied, holes were filled, and areas of 800 pixels or less were rejected to remove false positives. The percentage of selected pixels as a ratio of the original image size was considered the percentage surface area covered by cells

Table 10: Recipe for Cell surface area.

1- Adjust Contrast: Auto
2- Flatten Background: 299
3- Dark Texture: 83
4- Standard deviation Filter: 15
5- Range Threshold: 50 255
6- Fill all holes
7- Reject Features: Area <800pixel

Appendix D Ponceau red images from western blots

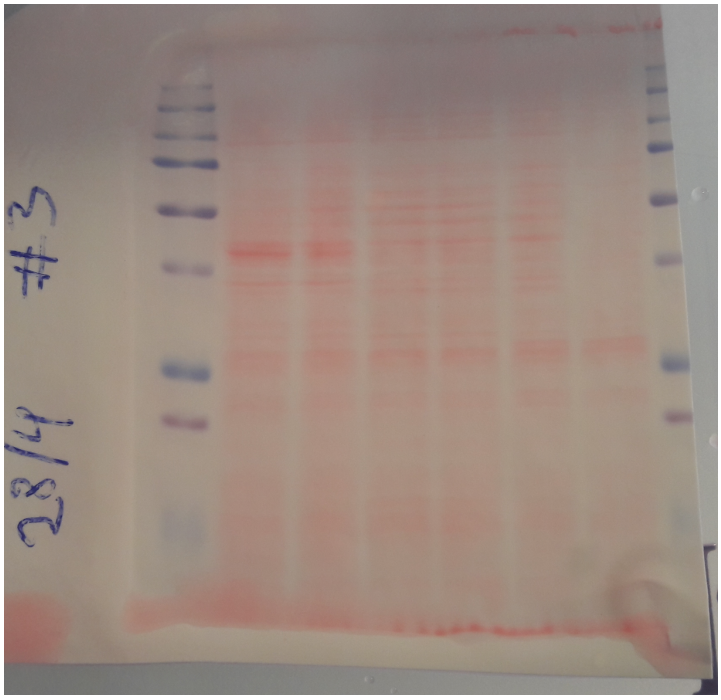

Figure 28: Ponceau red stained membrane for 10×trypsin test (MLC).

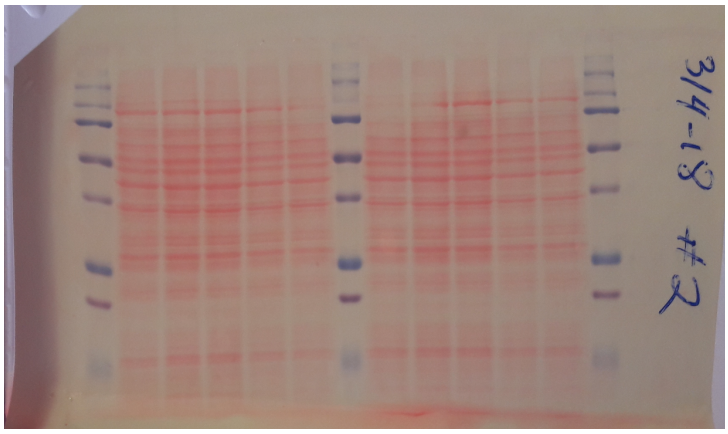

Figure 29: Ponceau red stained membrane (JNK)